

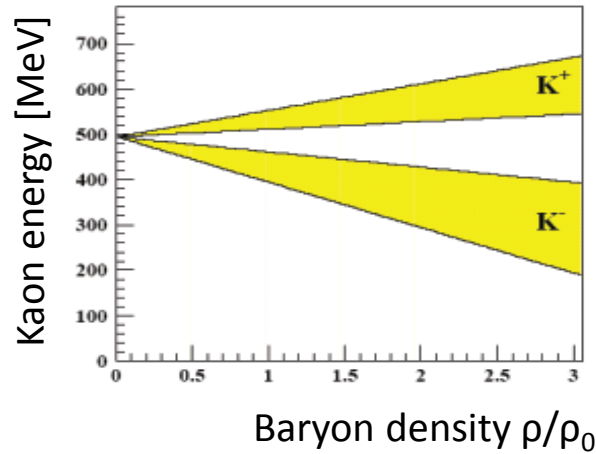
Is there a Kaonic bound state?

Outline

- Introduction
 - Interaction between K^- and Nucleon
 - The $\Lambda(1405)$
 - The Kaonic Bound state in theory and experiment
- Results for exclusive measurement in $p + p$
 - $\Lambda(1405)$ at HADES
 - KNN with FOPI and HADES
- Summary
- Outlook

K–N Interaction

Kaons in Medium



K^+ : Repulsive Interaction

K^- : Attractive Interaction

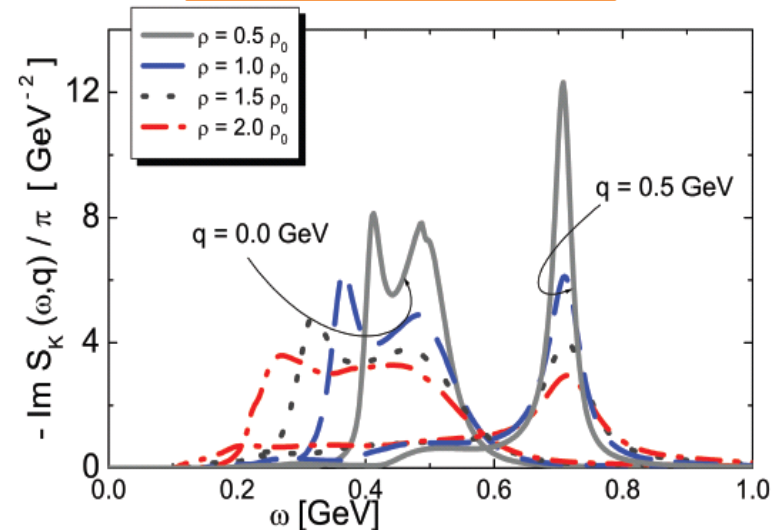
C. Sturm, Diss. TUD 2001

Coupling of \bar{K} to Resonances

$$\Sigma + \pi \leftrightarrow \Lambda(1405) \leftrightarrow \bar{K} + N$$

$$\Lambda + \pi \leftrightarrow \Sigma(1385) \leftrightarrow \bar{K} + N$$

\bar{K} Spectral Function



Lutz, Prog.Part.Nucl.Phys, 53 125-136

Resonances close to $\bar{K}N$ threshold
 \rightarrow Chiral Perturbation cannot be applied

Coupled Channel Calculation

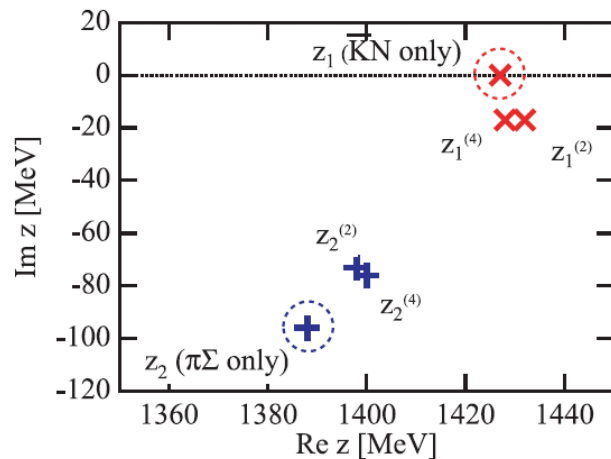
Self Consistent Bethe-Salpeter Equation

$$T_{ij}(\sqrt{s}) = V_{ij}(\sqrt{s}) + V_{il}(\sqrt{s})G_l(\sqrt{s})T_{lj}(\sqrt{s})$$



T.Hyodo, W.Weise, Phys.Rev.C77 (2008)

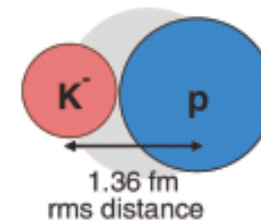
Chiral Potential



T.Hyodo, W.Weise, Phys.Rev.C77 (2008)

Phenomenological Potential

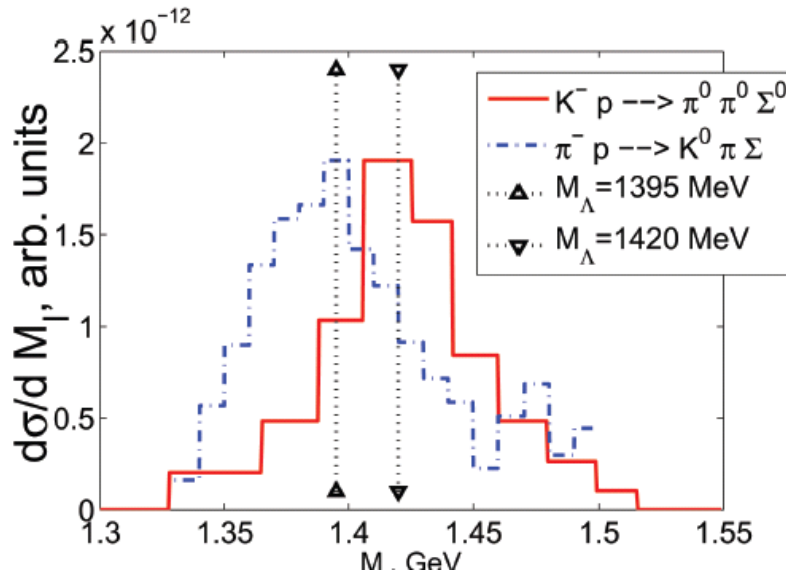
Quasi bound state of K^-p
via attractive $l=0$ interaction



J. Esmaili, Y.Akaishi, T. Yamazaki Phys.Lett. B 686,23
J. Esmaili, Y.Akaishi, T. Yamazaki Phys.Rev. C 83

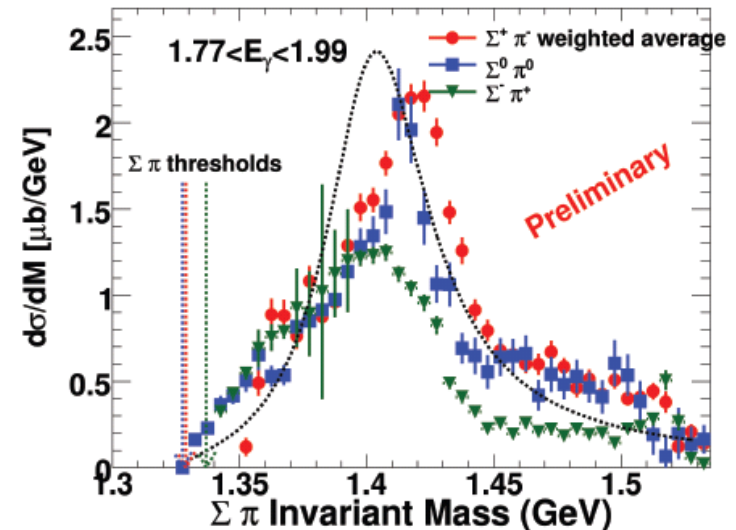
$\Lambda(1405)$ Measurements

π^- / K^- induced production



Thomas et. al., Nucl.Phys. B56:15-45,1973
 S.Prakhov, Phys.Rev. C79:034605,2004

γ induced production



K.Moriya R.Schumacher
 Nucl.Phys. A 835:325-328,2010

Different initial reactions may couple different to poles of $\Lambda(1405)$

Kaonic Cluster



Theoretical Predictions

Chiral, energy dependent

	var. [DHW09, DHW08]	Fad. [BO12b, BO12a]	var. [BGL12]	Fad. [IKS10]	Fad. [RS14]
BE	17–23	26–35	16	9–16	32
Γ_m	40–70	50	41	34–46	49
Γ_{nm}	4–12	30			

Non-chiral, static calculations

	var. [YA02, AY02]	Fad. [SGM07, SGMR07]	Fad. [IS07, IS09]	var. [WG09]	var. [FIK ⁺ 11]
BE	48	50–70	60–95	40–80	40
Γ_m	61	90–110	45–80	40–85	64–86
Γ_{nm}	12			~20	~21

Binding Energy (BE):

10–100 MeV

Mesonic Decay (Γ_m)

30–110 MeV

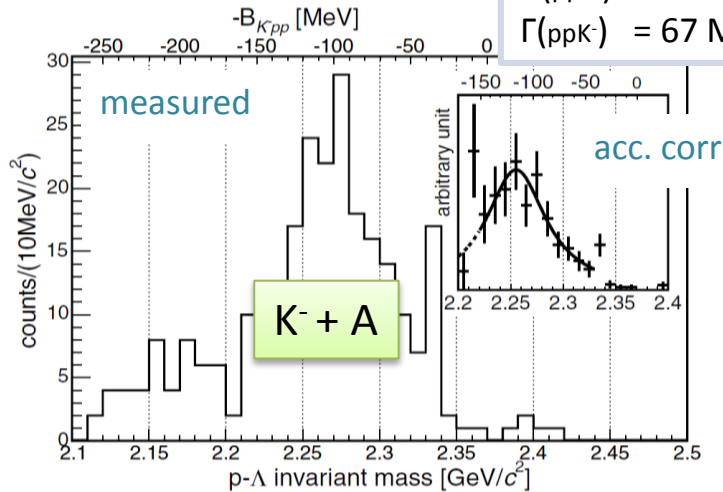
Non-Mesonic Decay (Γ_{nm})

4–30 MeV

Experimental Results on ppK^-

FINUDA

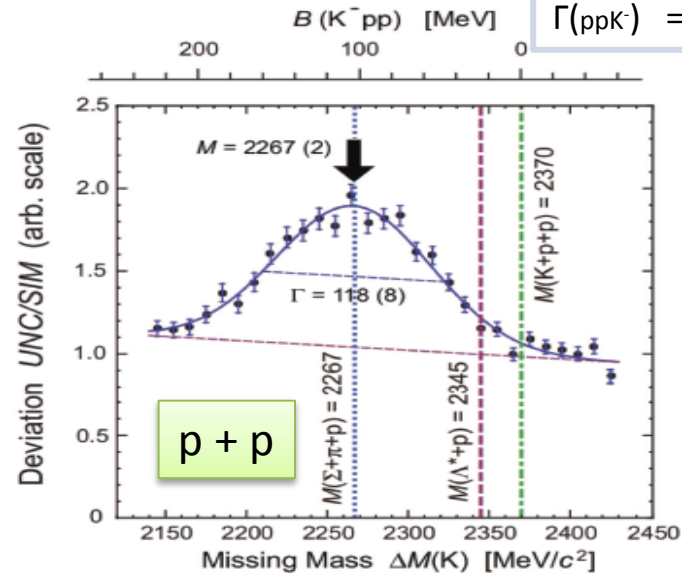
$$\begin{aligned} M(ppK^-) &= 2.255 \text{ GeV}c^{-2} \\ B(ppK^-) &= 115 \text{ MeV} \\ \Gamma(ppK^-) &= 67 \text{ MeV}c^{-2} \end{aligned}$$



M. Agnello et al.
Phys.Rev.Lett.**94** (2005)

DISTO

$$\begin{aligned} M(ppK^-) &= 2.267 \text{ GeV}c^{-2} \\ B(ppK^-) &= 103 \text{ MeV} \\ \Gamma(ppK^-) &= 118 \text{ MeV}c^{-2} \end{aligned}$$

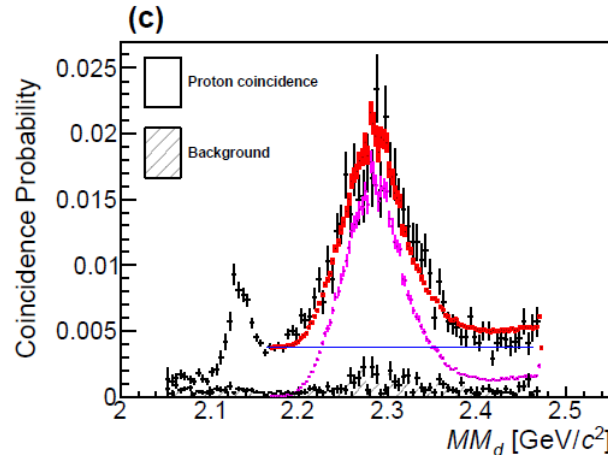


T. Yamazaki et al.
Phys.Rev.Lett.**104**, (2010)

Newest J-Parc Results

E-15 JParc

$\pi^- + d$



$$M(ppK^-) = 2.27 \text{ GeV}c^{-2}$$

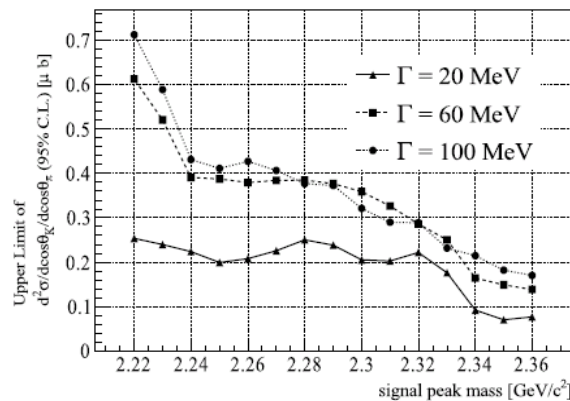
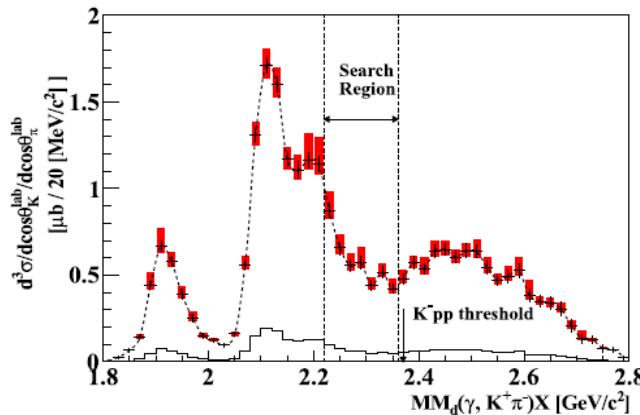
$$B(ppK^-) = 95 \text{ MeV}$$

$$\Gamma(ppK^-) = 162 \text{ MeV}c^{-2}$$

Y. Ichikawa et al.
Prog. Theor. Exp. Phys. 2013

LEPS/ SPRING8

$\gamma + d$



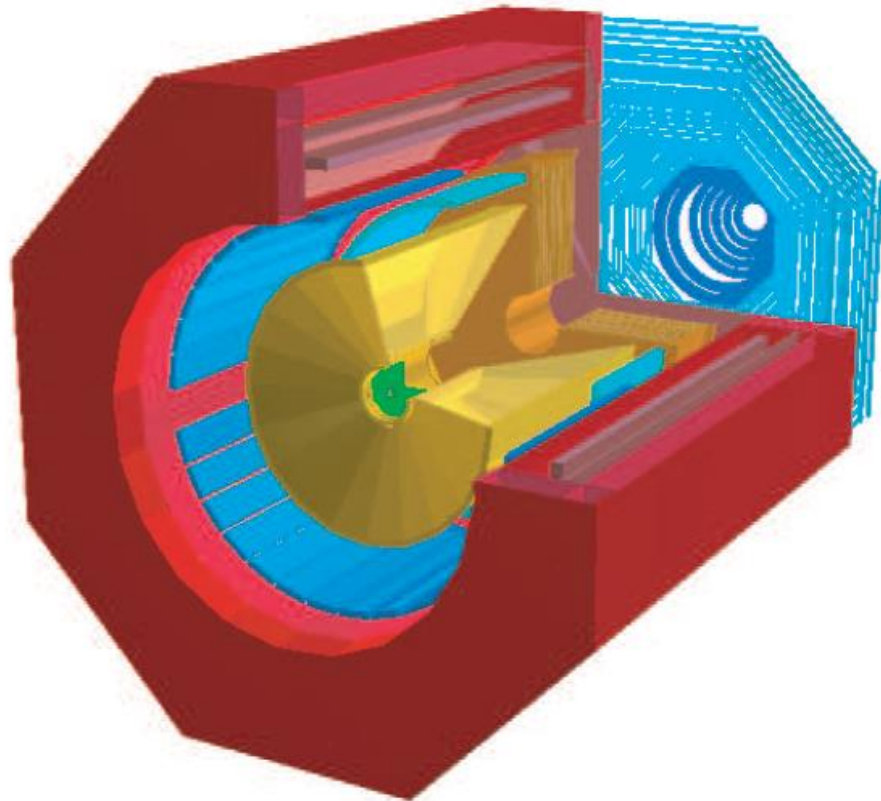
A.O. Tokayasu et al.
Phys.Lett. B728, (2014)

Experimental Data

The FOPI Experiment

SIS18 GSI Darmstadt

Beam Energy: 3.1 GeV



- Fixed-target Setup
- Full azimuthal coverage, 5° - 110° in polar angle
- Momentum resolution $\approx 7\%$ - 15%
- Particle identification via dE/dx & ToF

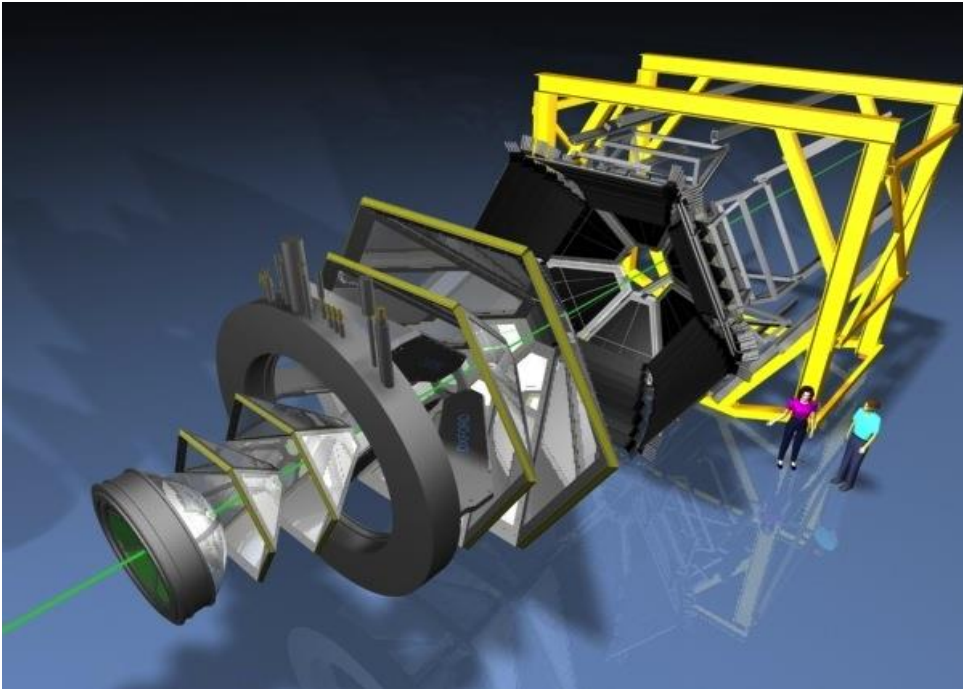
Trigger Detector – Si/AlO:

Λ – Enhancement: $14.1 \pm 7.9(stat)^{+4.3}_{-0.6}$

The HADES experiment

High Acceptance Di-electron Spectrometer
GSI, Darmstadt

Beam Energy: 3.5 GeV



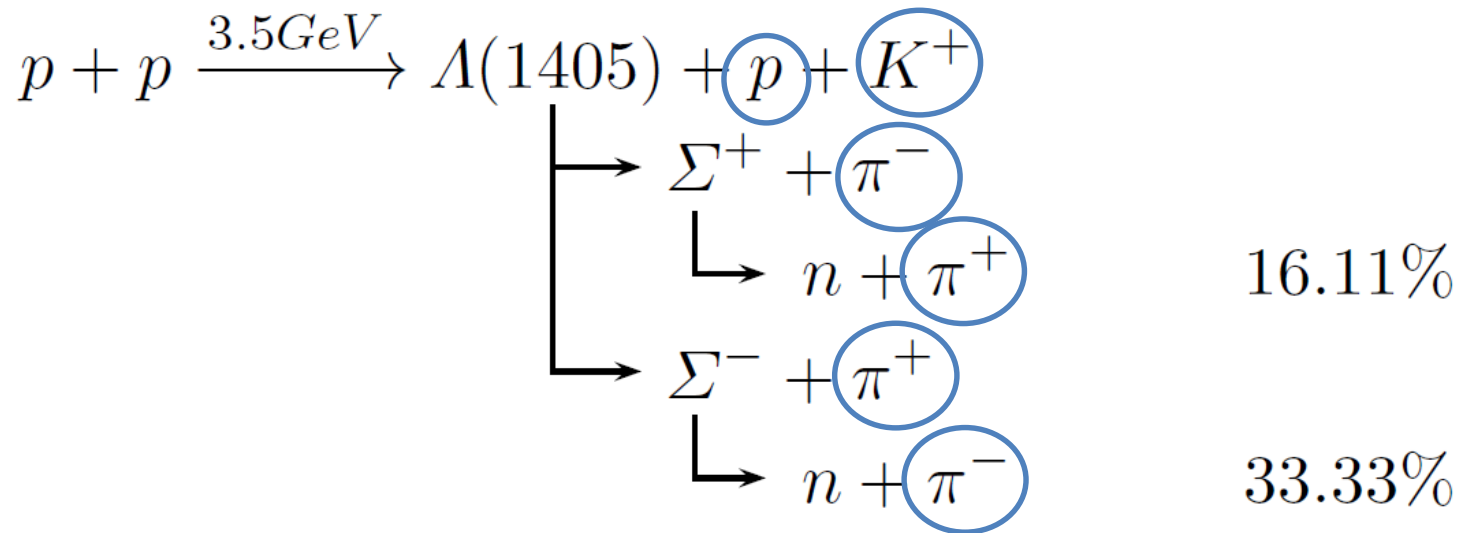
- Fixed-target Setup
- Full azimuthal coverage, 15° - 185° in polar angle
- Momentum resolution $\approx 1\%$ - 5%
- Particle identification via dE/dx & ToF

HADES Coll. (G. Agakishiev et al.),
Eur. Phys. J. **A41** (2009)

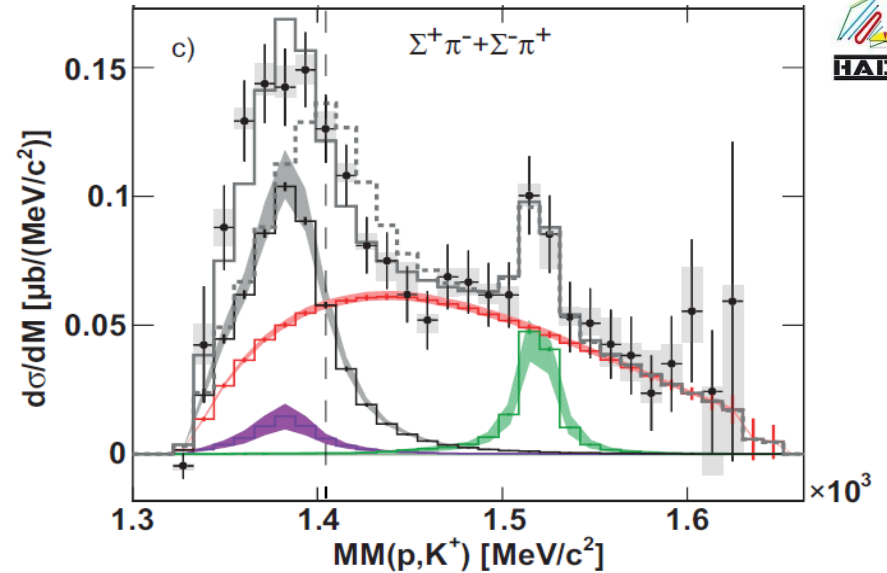
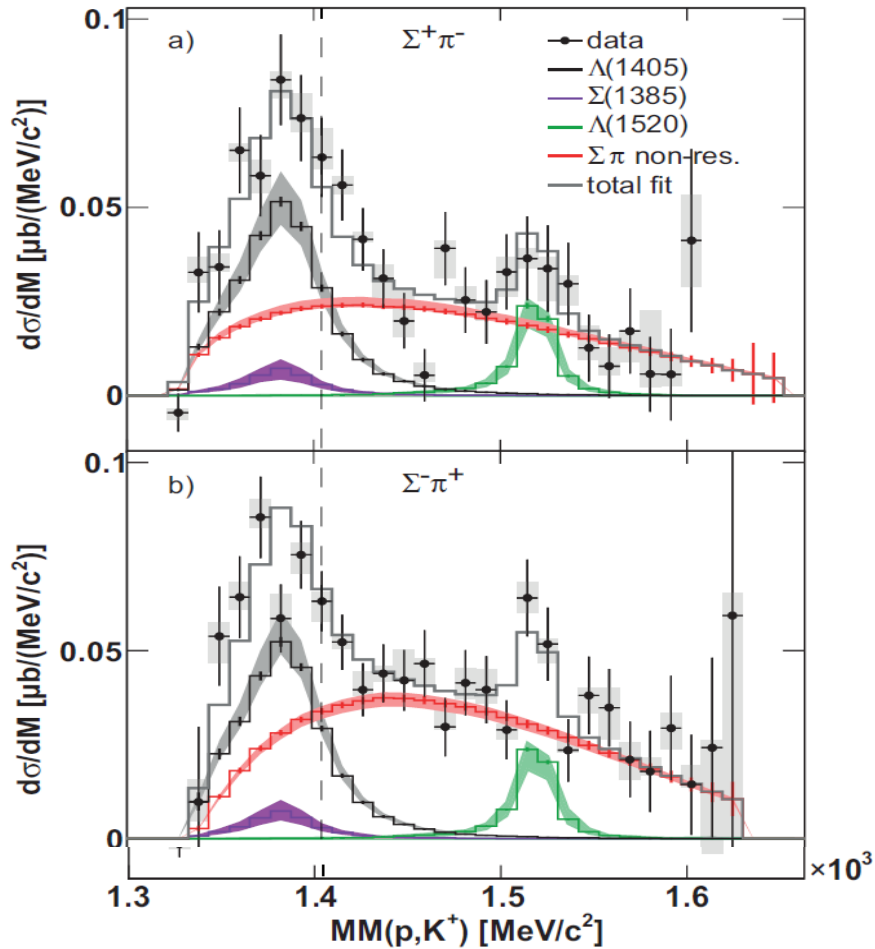
$\Lambda(1405)$

Hades reconstruction

Reaction



Results



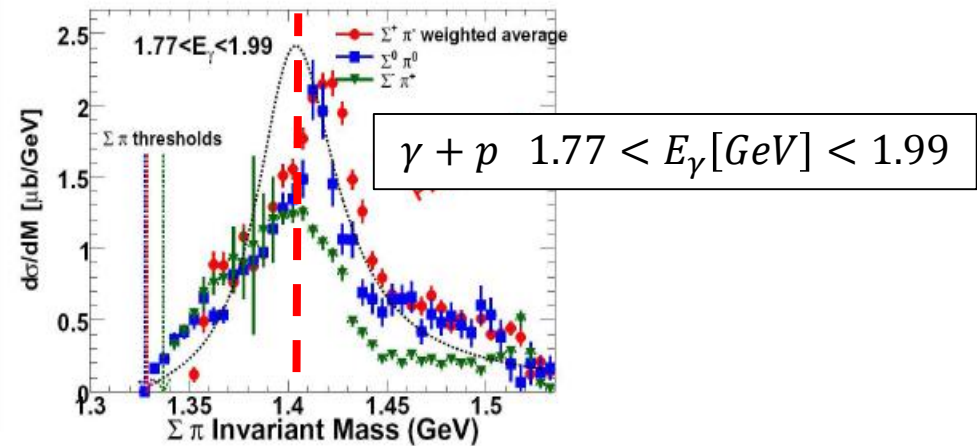
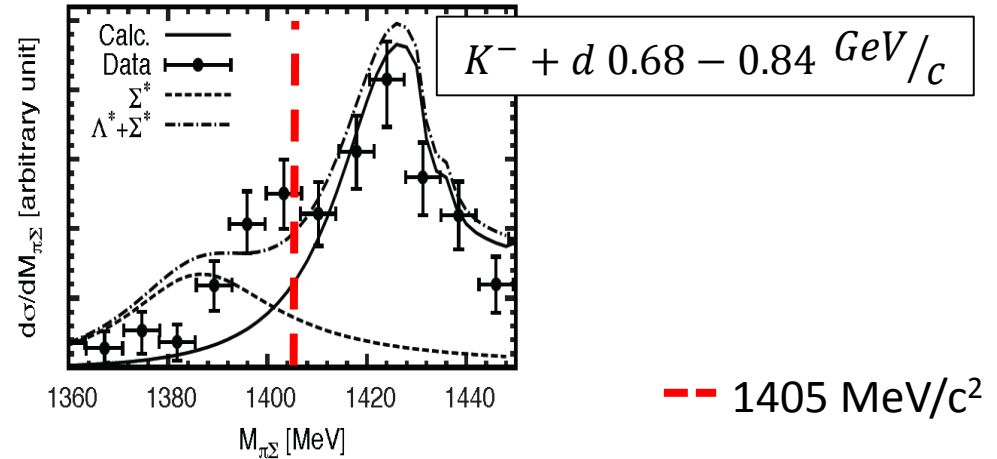
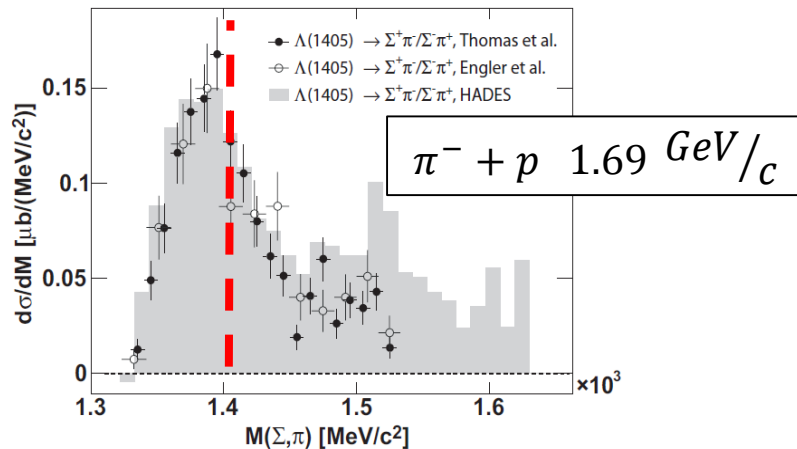
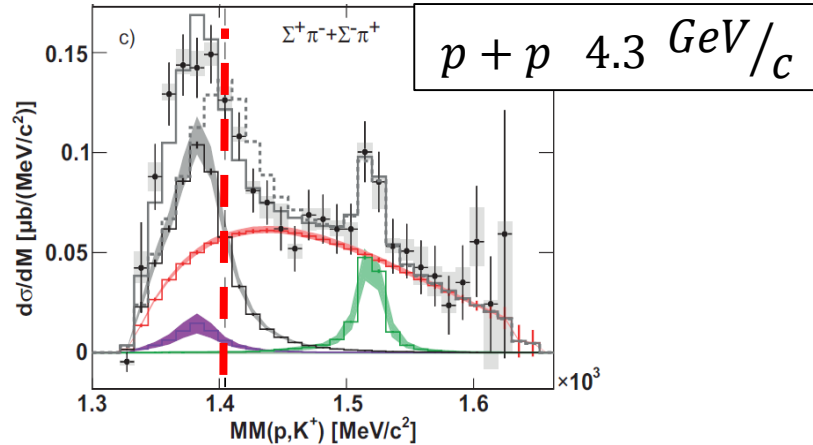
Reaction:

Cross section

$p + p \rightarrow \Lambda(1405) + p + K^+$	$9.2 \pm 0.9 \pm 0.7^{+3.3}_{-1.0} \mu b$
$p + p \rightarrow \Sigma(1385)^0 + p + K^+$	$5.56 \pm 0.48^{+1.94}_{-1.06} \mu b$
$p + p \rightarrow \Lambda(1520) + p + K^+$	$5.6 \pm 1.1 \pm 0.4^{+1.1}_{-1.6} \mu b$
$p + p \rightarrow \Sigma^+ + \pi^- + p + K^+$	$5.4 \pm 0.5 \pm 0.4^{+1.0}_{-2.1} \mu b$
$p + p \rightarrow \Delta^{++}(1232) + \Sigma^- + K^+$	$7.7 \pm 0.9 \pm 0.5^{+0.3}_{-0.9} \mu b$

HADES coll. (G. Agakishiev et al.) Phys. Rev. **C 87**, 025201 (2013)

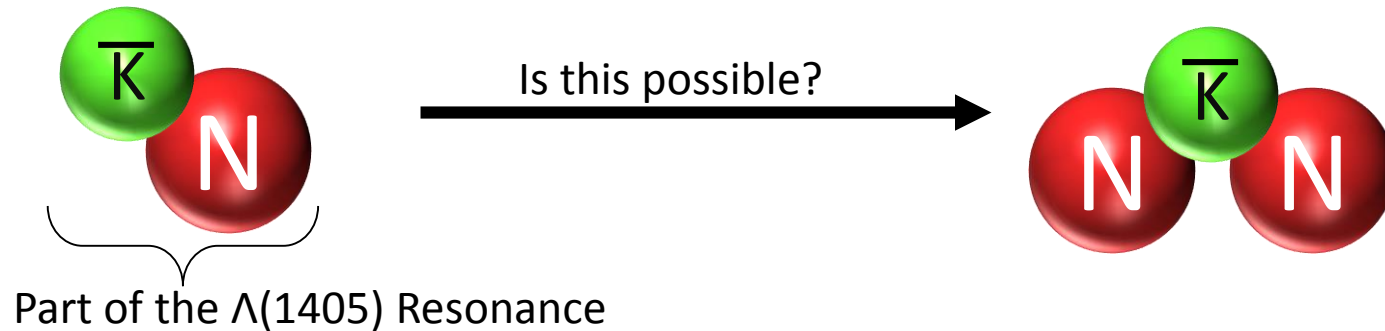
HADES Signal in the Context



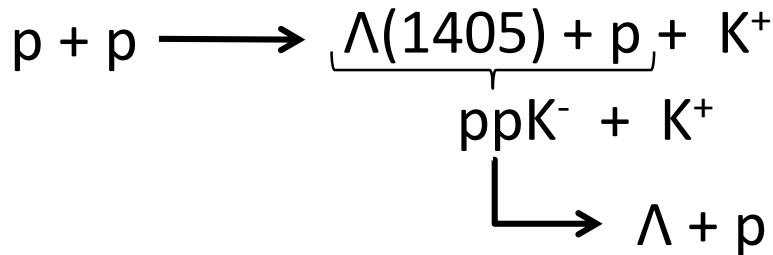
D.W. Thomas et al. Nuclear Physics **B56** (1973)
 A. Engler et al. Phys. Rev. Lett. **15**, 5 (1965)

O. Braun et al. Nuclear Physics **B129** (1977)
 R. Schumacher Nucl. Phys. **A835** (2010)

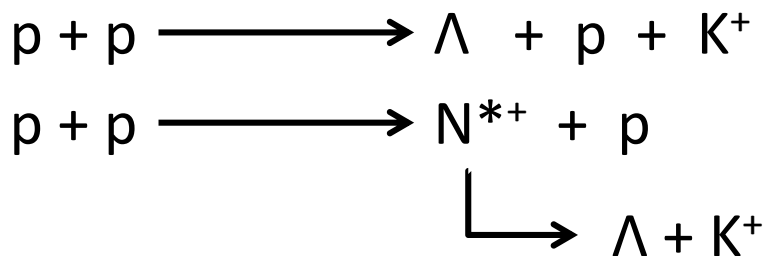
Kaonic Cluster



Kaonic Cluster



Physical Background:



N^{*+} - Resonances

	Mass [GeV/c ²]	Width [GeV/c ²]	$\Gamma_{\Lambda K}/\Gamma_{All}$ %
N(1650)S ₁₁	1.655	0.150	3-11
N(1710)P ₁₁	1.710	0.200	5-25
N(1720)D ₁₃	1.720	0.250	1-15
N(1875)D ₁₃	1.875	0.220	4 \pm 2
N(1880)P ₁₁	1.870	0.235	2 \pm 1
N(1895)S ₁₁	1.895	0.090	18 \pm 5
N(1900)P ₁₃	1.900	0.250	0-10

J. Beringer
Phys.Rev. D86 (2012)

Total Data Set

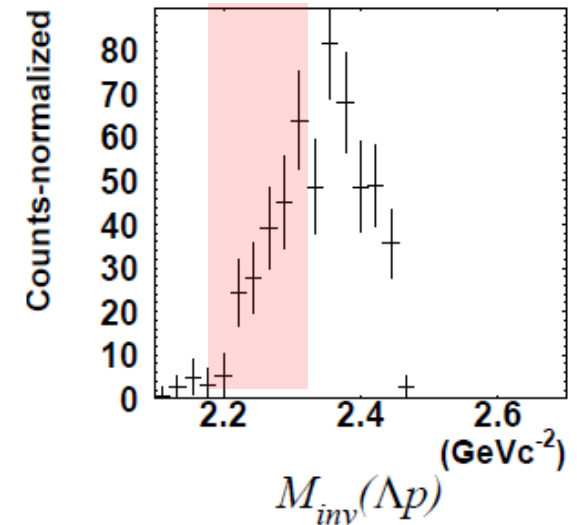
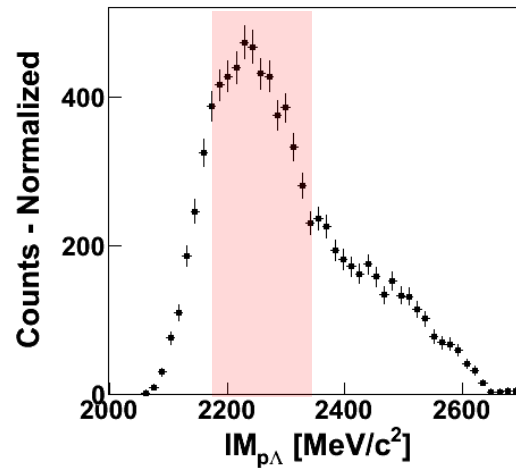
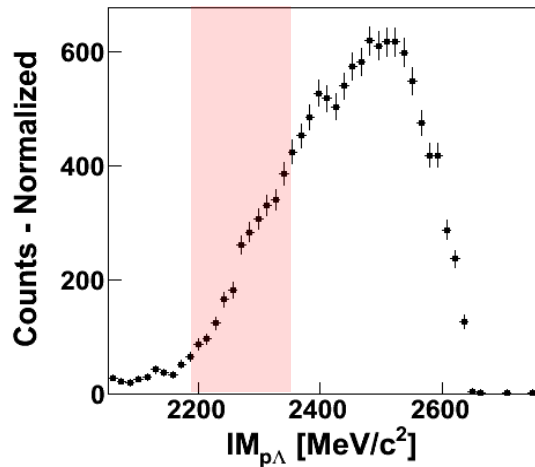
Hades Data $E_{\text{beam}}=3.5$ GeV

Had. Wall Data $E_{\text{beam}}=3.5$ GeV

FOPI Data $E_{\text{beam}}=3.1$ GeV

Total Number of exclusive Events: 21000

Total Number of exclusive Events: 903



No Peak Visible
No Signal?

R. Münzer, Hyperfine Interaction, in print
G. Agakishiev, Phys. Lett. B 742 (2015) 242-248

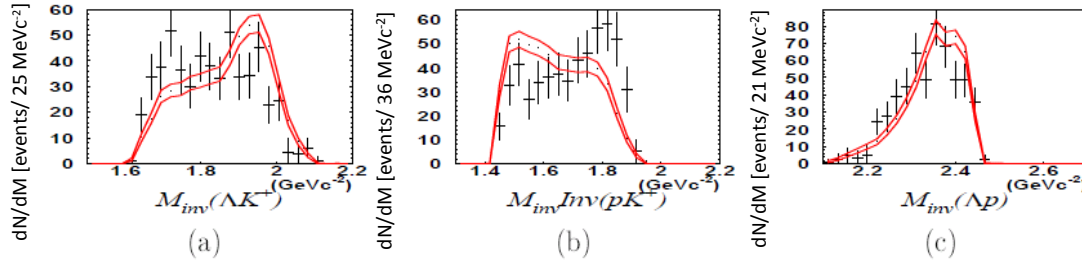
Model Comparison

Phase Space Simulation

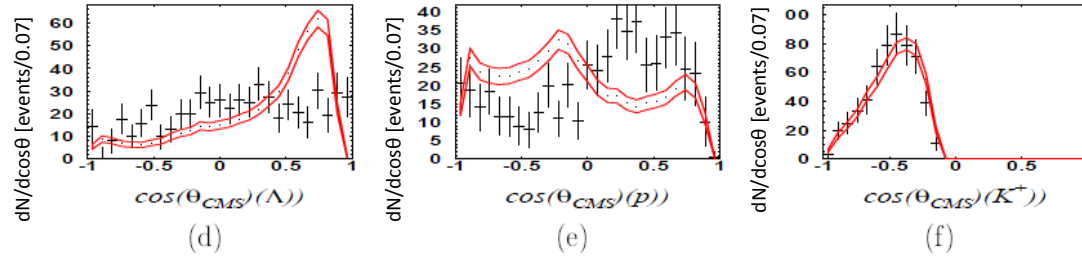
Partial Wave Analysis

Phase Space Simulation

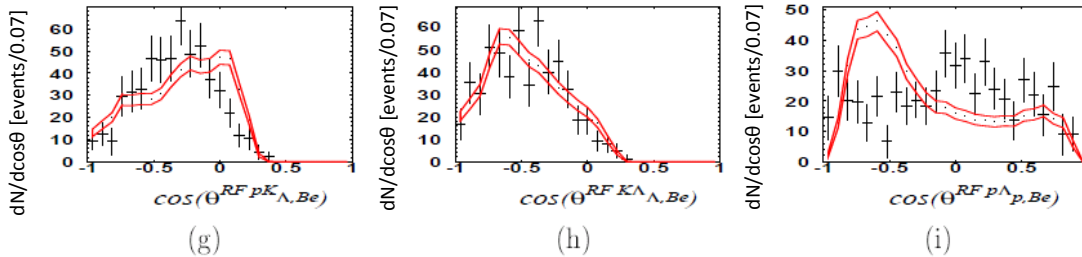
Masses



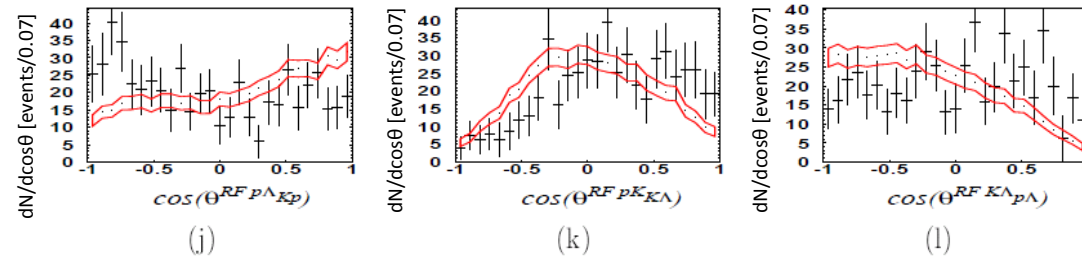
CMS Angle



G.-J.-Angle



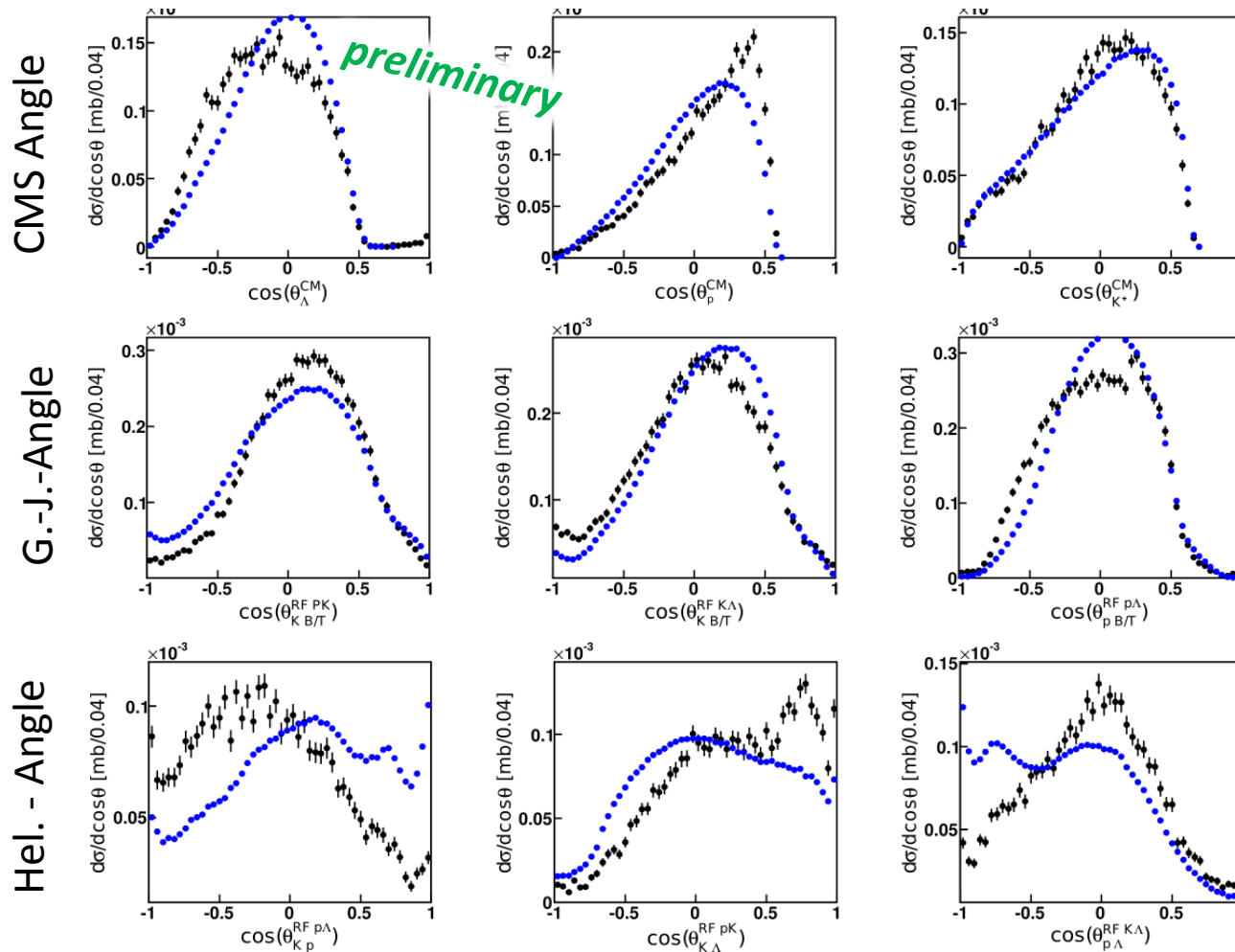
Hel. - Angle



✚ Experimental Data

— $pp \rightarrow p K^+ \Lambda$ Phase Space

Phase Space Model



Inside HADES acceptance

- Experimental Data
- $pp \rightarrow p K^+ \Lambda$ Phase Space

Partial Wave Analysis

Bonn-Gatchina PWA Framework

A. Sarantsev et.al., Eur.Phys J A 25 2005

Cross-section Decomposition

$$d\sigma = \frac{(2\pi)^4 |A|^2}{4|k|\sqrt{s}} d\phi(P, q_1, q_2, q_3), \quad P = k_1 + k_2$$

A : reaction amplitude $A \propto A_{tr}^\alpha(s)$ (Transition amplitude of wave α)

k : 3-momentum of the initial particle in the CM

$s - P^2 : (k_1 + k_2)^2$

$d\phi(P, q_1, q_2, q_3)$: invariant three-particle phase space

Parameterization of the Transition

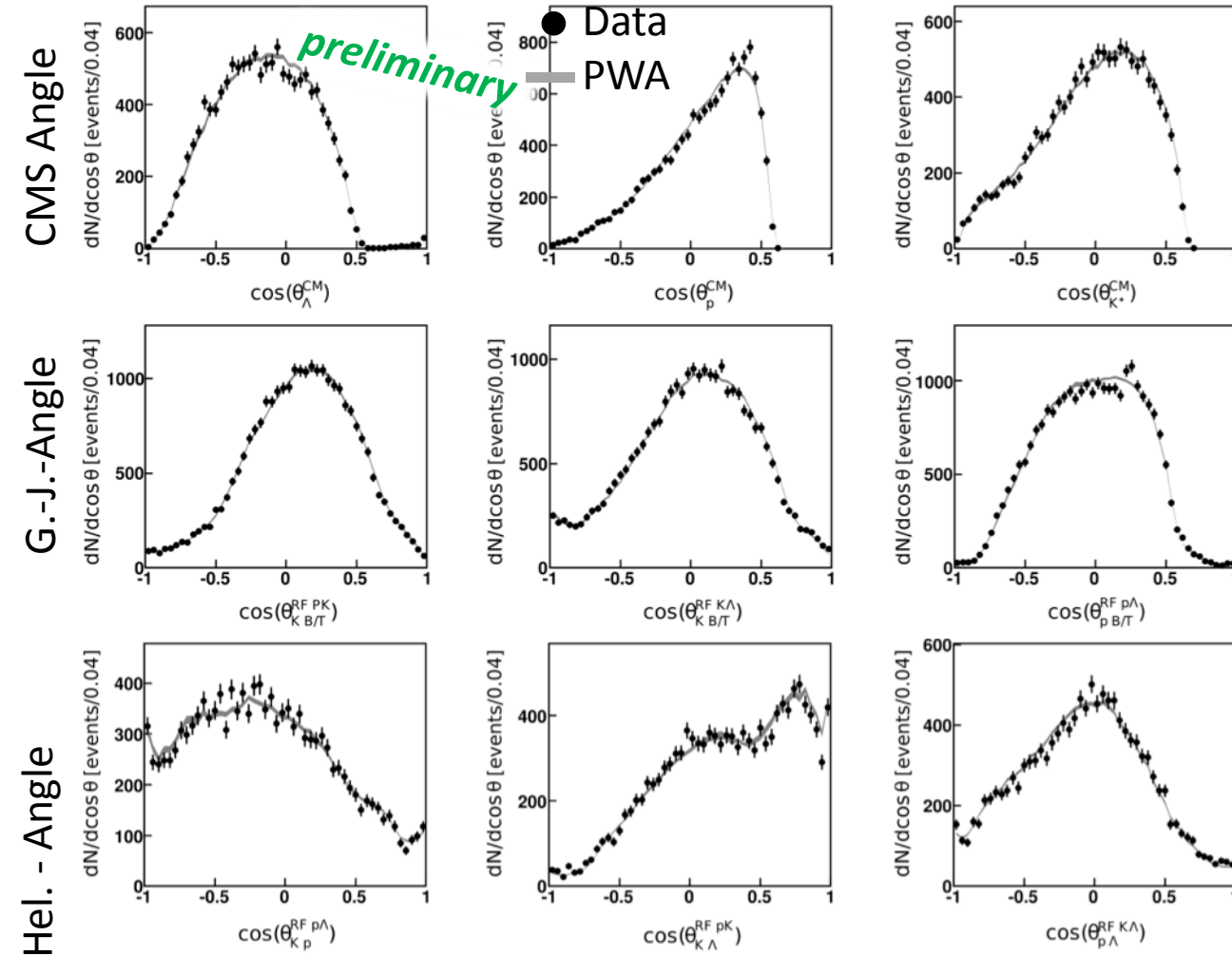
$$A_{tr}^\alpha(s) = (a_1^\alpha + a_3^\alpha \sqrt{s}) e^{a_2^\alpha}$$

a_1^α Constant amplitude

a_2^α Phase

a_3^α Energy dependent amp.

Four Best PWA Solutions



Inside HADES acceptance

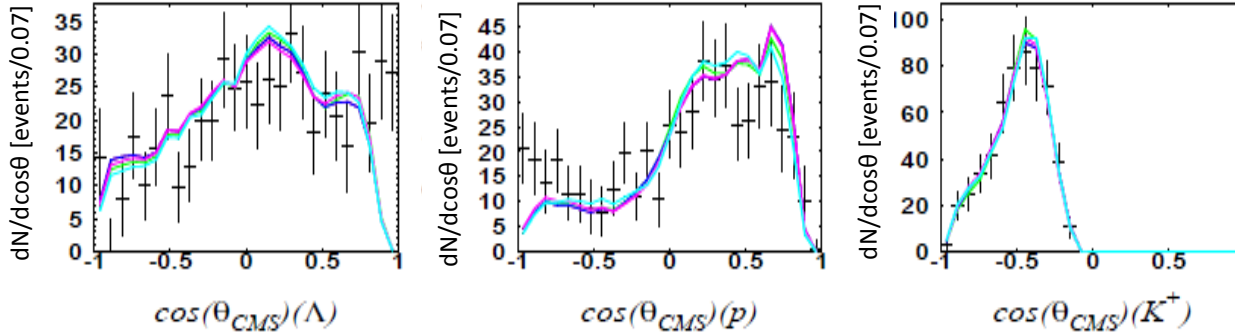
Measured Data
PWA solutions

PWA Results

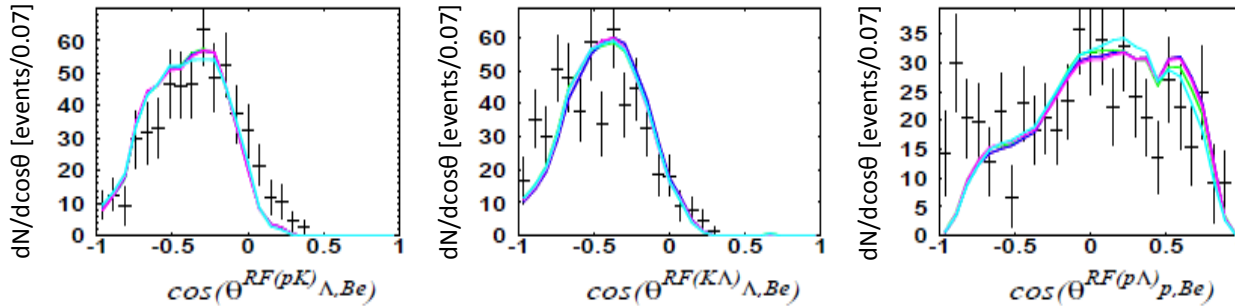
✚ Experimental Data

— Solution A
— Solution B
— Solution C
— Solution D
— Solution E

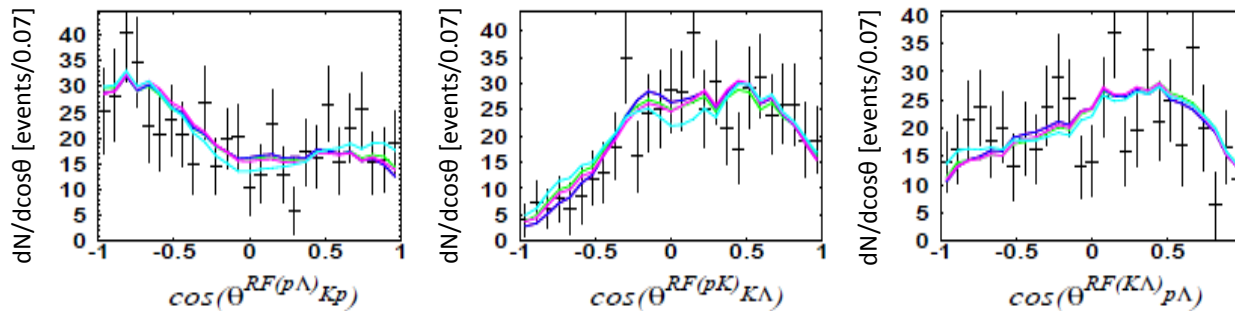
CMS Angle



G.-J.-Angle

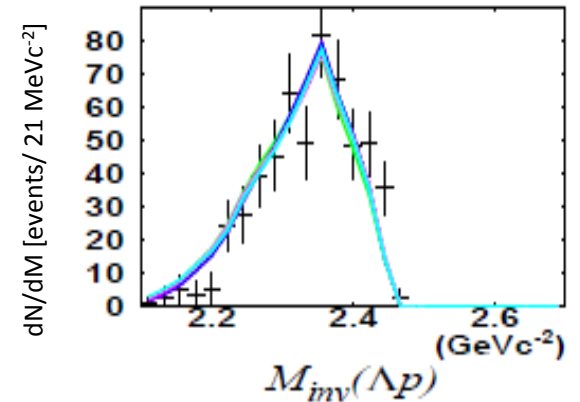
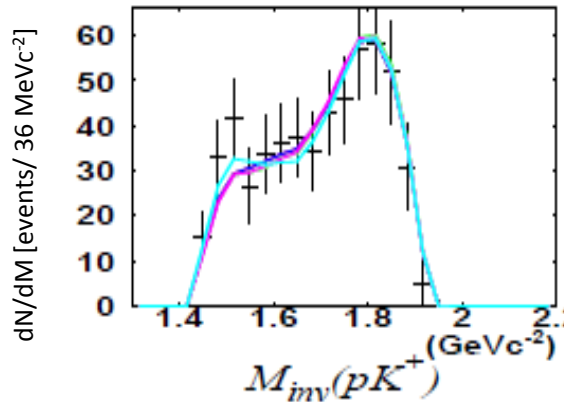
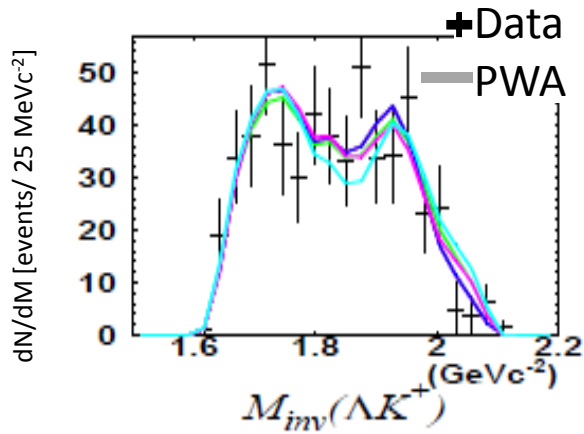


Hel. - Angle

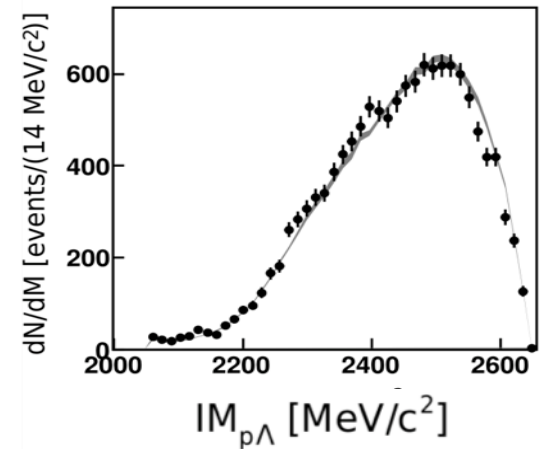
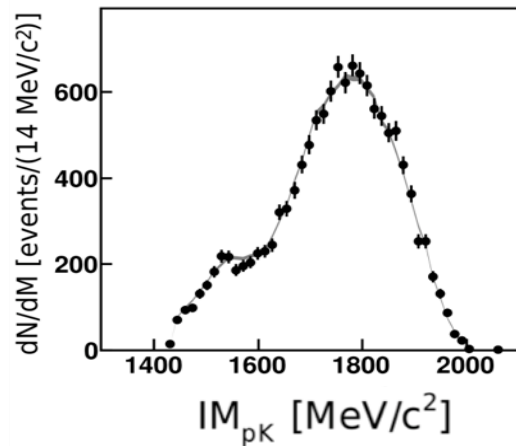
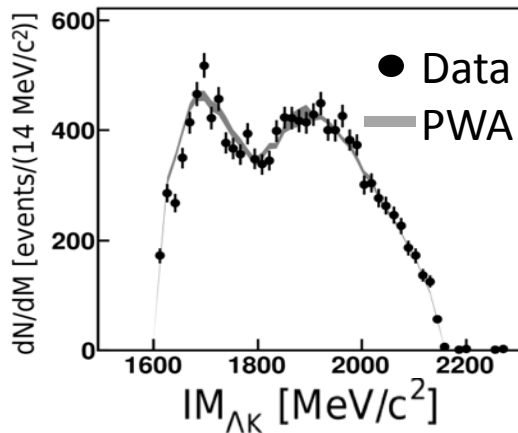


Four Best PWA Solutions

FOPI



HADES

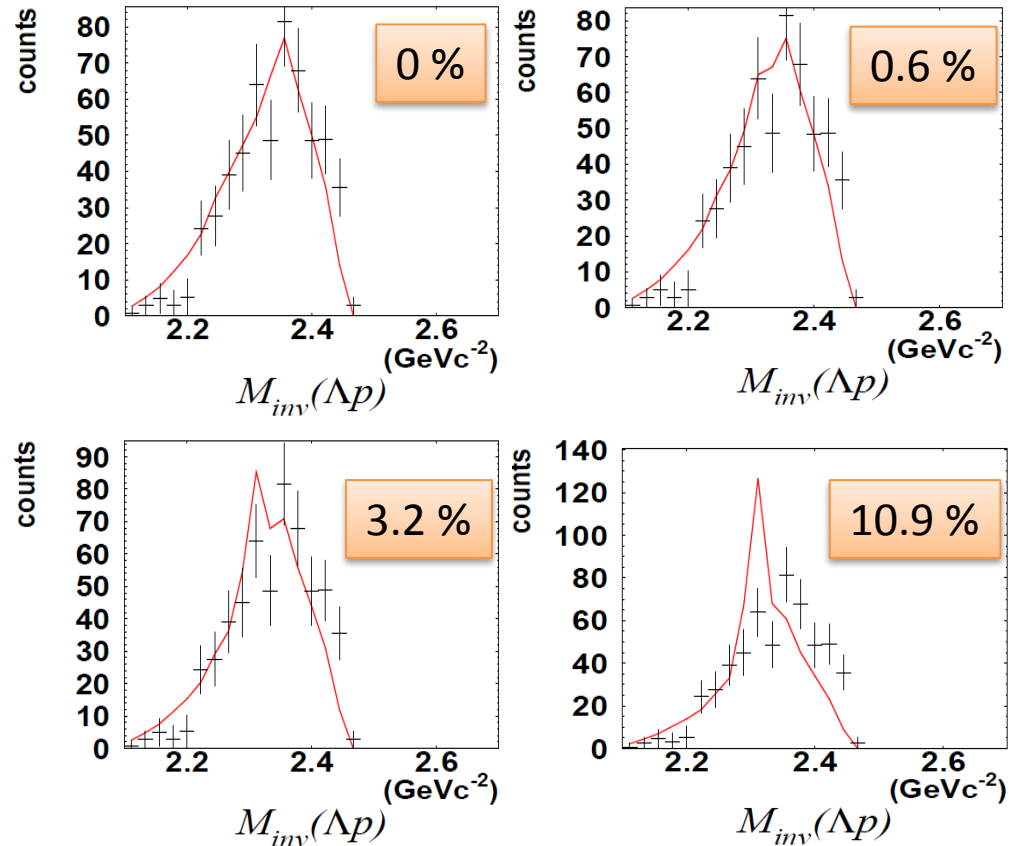


Upper Limit of ppK^- Contribution

ppK⁻ Upper Limit Determination

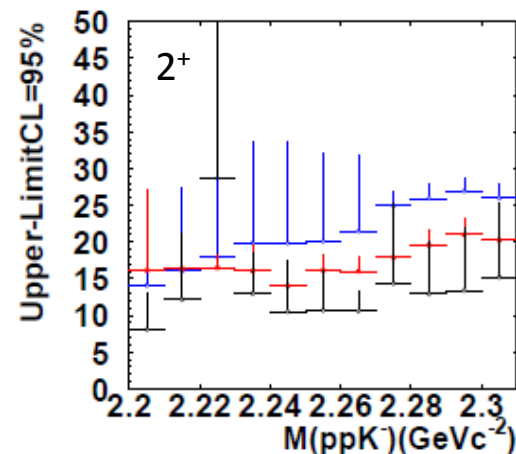
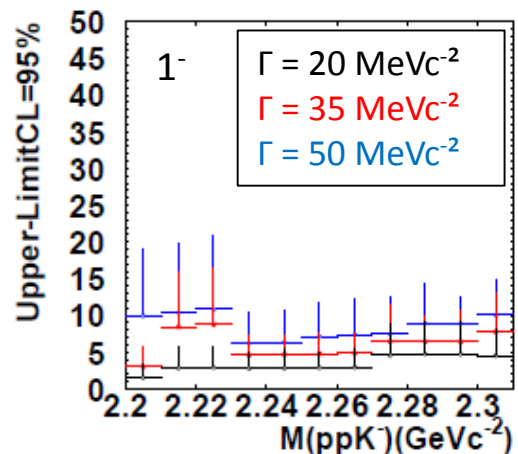
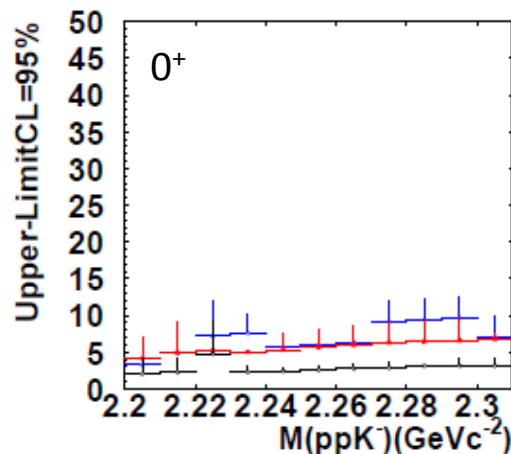
- > ppK⁻ Waves include in BG-PWA
- > Mass and Width fixed
- > Background for 5 best solution without ppK⁻
- > Stepwise increase of Amplitude (a_1)
- > Phase Parameter free (a_2)
=> Optimal amount of Interference

Exclusion limit:
Confidence Level (95%) (CL_s)



$$M(\text{ppK}^-) = 2.305 \text{ GeV}c^{-2} \quad \Gamma(\text{ppK}^-) = 20 \text{ MeV}c^{-2}$$

ppK⁻ Upper Limit Determination



$p + p \rightarrow p + K^+ + \Lambda$
Total Cross Section

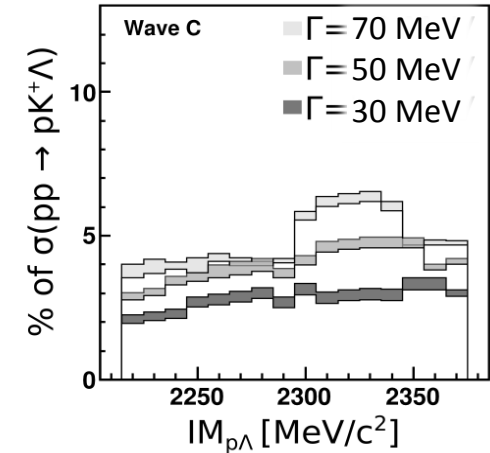
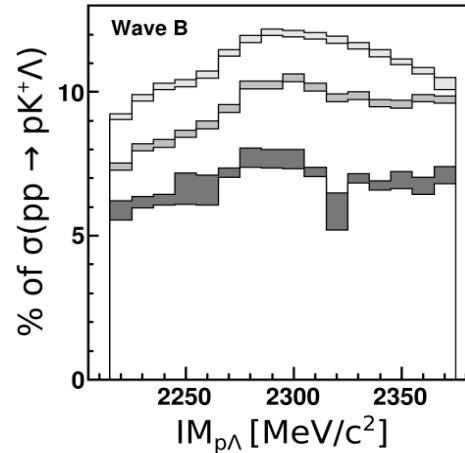
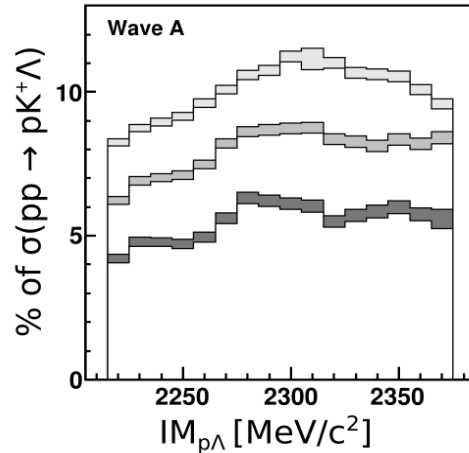
$$\sigma_{pK+\Lambda} = 41.0 \pm 12.8 \mu b$$

Interpolated from literature

Upper Limit Cross Section

Γ (MeVc ⁻²)	Cross Section (μb)
20	$7.6 \pm 1.2^{-3.5} - 22.4 \pm 3.6^{-10.7}$
35	$6.3 \pm 1.7^{-0.6} - 9.5 \pm 2.6^{-0.9}$
50	$10.2 \pm 1.8^{-4.5} - 11.6 \pm 3.4^{-0.6}$
60	$11.2 \pm 1.9^{-5.0} - 33.8 \pm 5.2^{-16.9}$
80	$11.4 \pm 2.7^{-3.8} - 35.9 \pm 5.7^{-17.4}$

Upper Limit



Measured total cross-section: $\sigma_{pK^+\Lambda} = 38.12 \pm 0.43^{+3.55}_{-2.83} \pm 2.67(p+p\text{-error}) - 2.9(\text{background}) \mu\text{b}$

Upper limit of ppK^- Cross Section:

$\Gamma \text{ (MeVc}^{-2}\text{)}$	Cross Section (μb)
0^+	1.9 – 3.9
1^-	2.1 – 4.2
2^+	0.7 – 2.1

Production Cross Section $\Lambda(1405)$

$$9.2 \pm 0.9 \pm 0.7^{+3.3}_{-1.0} \mu\text{b}$$

HADES coll. (G. Agakishiev et al.)
 Phys. Rev. **C 87**, 025201 (2013)

Summary $\Lambda(1405)$

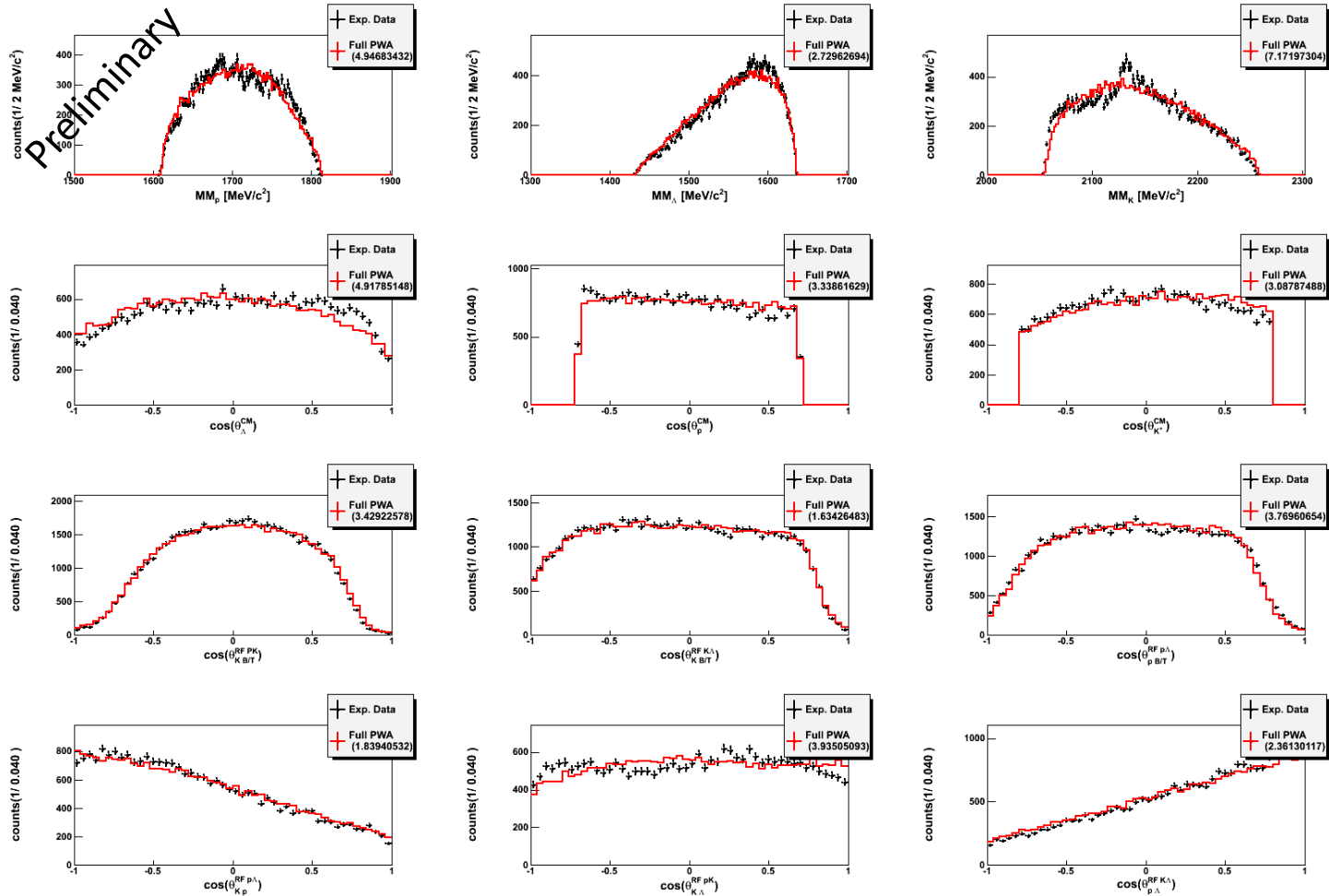
- $\Lambda(1405)$
 - Coupling between $\Sigma\pi$ and K^-p : Different Coupling to final state.
 - First reconstruction of charged decay channel of $\Lambda(1405)$ in $p + p$ with HADES
 - Peak position at $1385 \text{ GeV}/c^2$ (Best description by according simulation input)
 - Position comparable to π production, different to K^-/γ production
- Kaonic Bound State
 - Kaon Nucleon Bound States -> Predicted by Theory but not conclusive Properties
 - Experimental Results show different behavior
 - No Signal Visible in $p + p$ Reaction data measured at FOPI and HADES
 - Production Mechanism has to be described by Partial Wave Analysis including Interference
 - Extraction of Upper Limit: $0.7 - 4.1 \text{ } \mu\text{b}$ (HADES) $7.1 - 35.7 \text{ } \mu\text{b}$ (FOPI)

Outlook

- Improvement of description Background description
- Combined Analysis

Experiment	E_B [GeV]	$pK^+\Lambda$ Statistics	ϵ_{ppK^-} [MeV]	Status
COSY-TOF	1.96	~160k	-104	In Preparation
DISTO	2.15	120 k	-114	Available
COSY-TOF	2.16	3.6 k	-104	Available
COSY-TOF	2.16	40 k	-104	Available
COSY-TOF	2.16	~90k	-104	In Preparation
COSY-TOF	2.25	36 k	-83	Available
COSY-TOF	2.40	1.6 k	-24	Available
DISTO	2.5	304 k	26	Available
DISTO	2.85	424 k	116	Available
FOPI	3.1	0.9 k	196	Single PWA
HADES	3.5	21 k	315	Single PWA

PWA Results – COSY@2.16 GeV

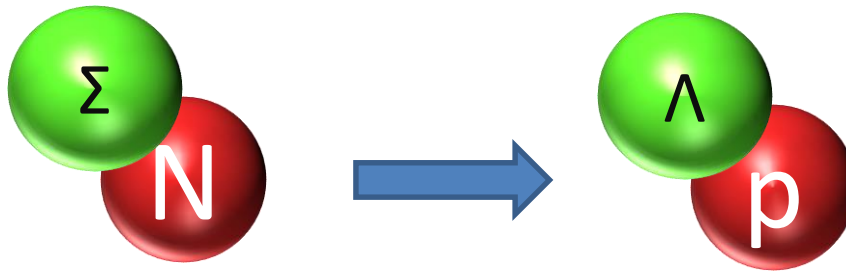


M. Roeder et al., Eur. Phys. J. A49, 157 (2013)



The ΣN Cusp Effect

Coupled Channel:



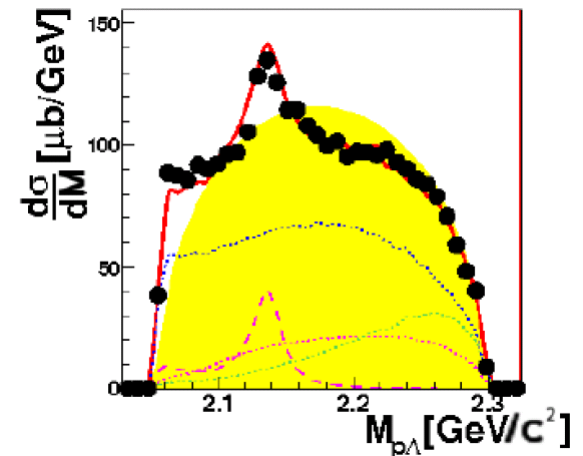
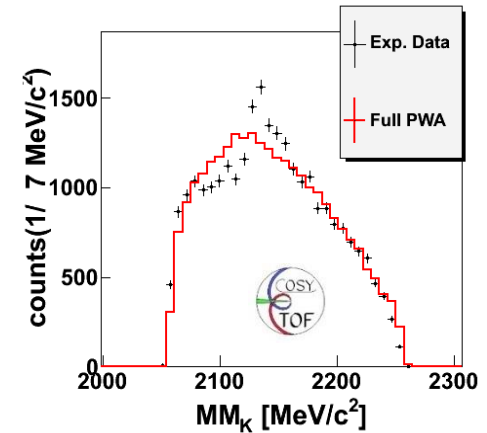
At Threshold : 2130 MeVc^{-2}

Quantum Number of Cusp: $0^+ / 1^+ (L=0,2)$

Spectral Function:

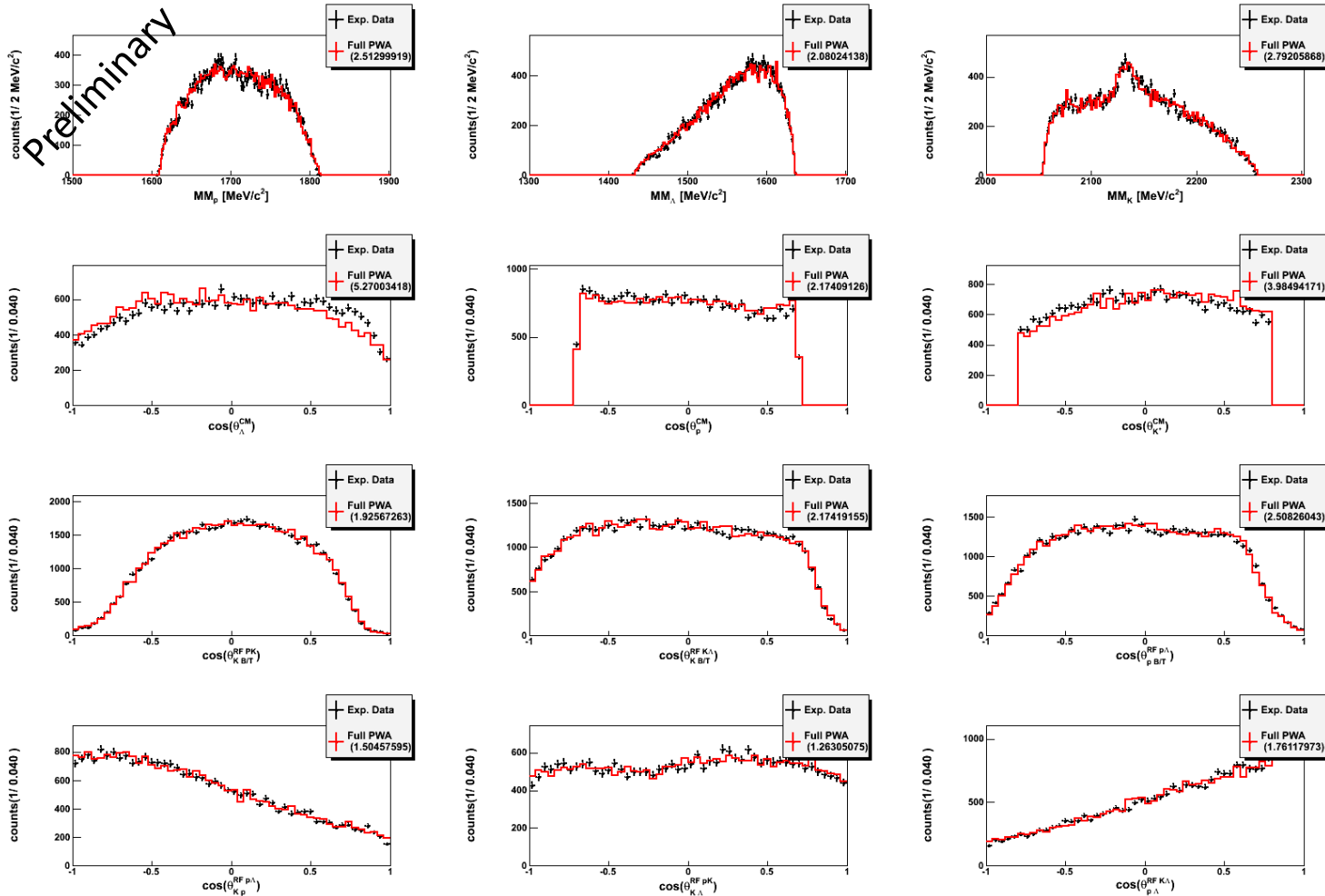
Breit Wigner

Flatté



S.Abd El-Samad, Eur.Phys.J A49(2013)

PWA Results with Cusp – COSY@2.16 GeV



M. Roeder et al., Eur. Phys. J. A49, 157 (2013)



Data Sets

Experiment	E_b [GeV]	pK ⁺ Λ Statistics	ϵ_{ppK^-} [MeV]	Status
COSY-TOF	1.96	~160k	-104	In Preparation
DISTO	2.15	120 k	-114	Combined PWA
COSY-TOF	2.16	3.6 k	-104	Combined PWA
COSY-TOF	2.16	40 k	-104	Combined PWA
COSY-TOF	2.16	~90k	-104	In Preparation
COSY-TOF	2.25	36 k	-83	Combined PWA
COSY-TOF	2.40	1.6 k	-24	Combined PWA
DISTO	2.5	304 k	26	Combined PWA
DISTO	2.85	424 k	116	Combined PWA
FOPI	3.1	0.9 k	196	Combined PWA
HADES	3.5	21 k	315	Combined PWA

Thank You



HADES Collaboration



FOPI Collaboration



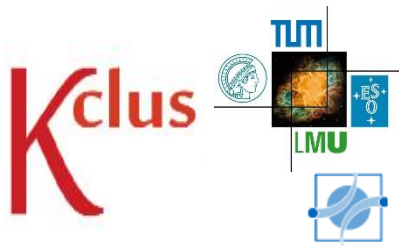
DISTO Collaboration
M. Maggiora



COSY-TOF Collaboration
J. Ritman, E. Roderburg
F. Hauenstein, D. Gronzka



Bonn Gatchina Group
A. Sarantsev



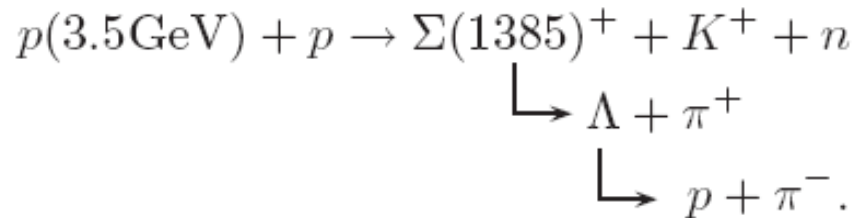
K-Cluster – Excellence Cluster Universe – TU Munich
L. Fabbietti, E. Eppe, P. Klose, S.Lu, J. Siebenson, D. Soliman

Backup

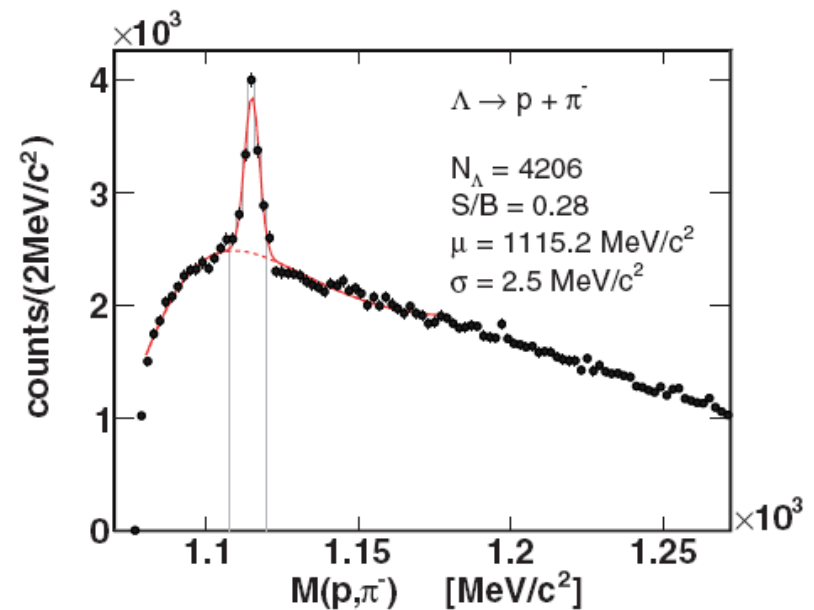
$$\Sigma(1385)^+$$

Hades reconstruction

Reconstruction

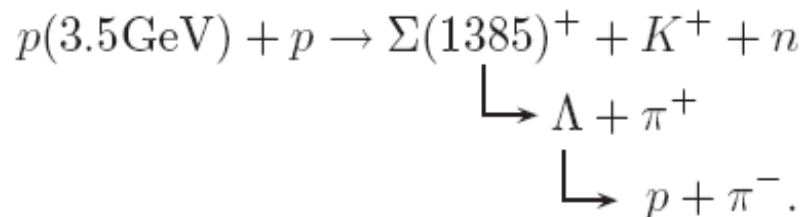


1. Reconstruct charge Particles
2. Reconstruct Lambda Signal
3. Identify Neutron Signal via Missing Mass
4. Precise Kaon Selection



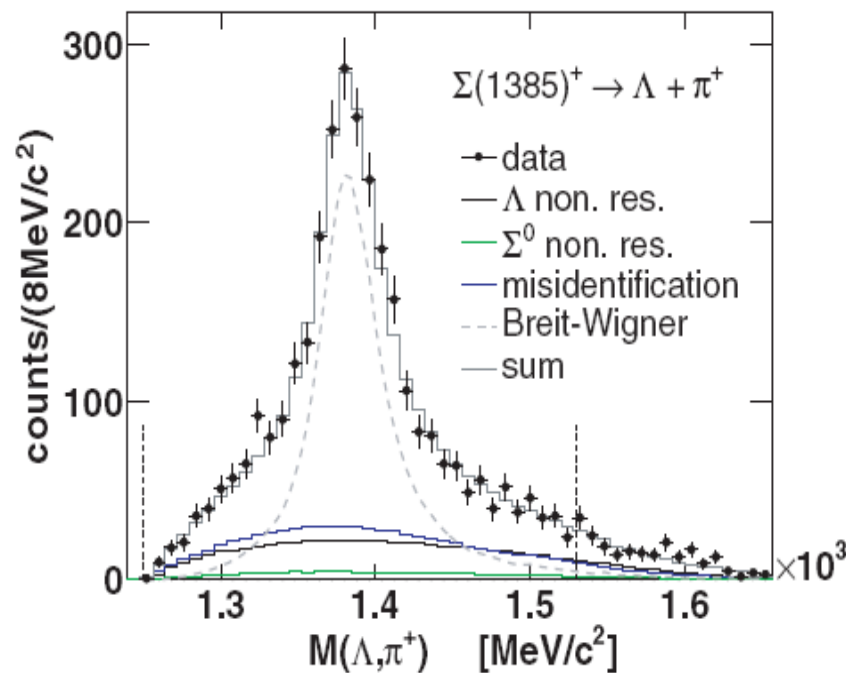
$\Sigma(1385)^+$ Signal

Reaction



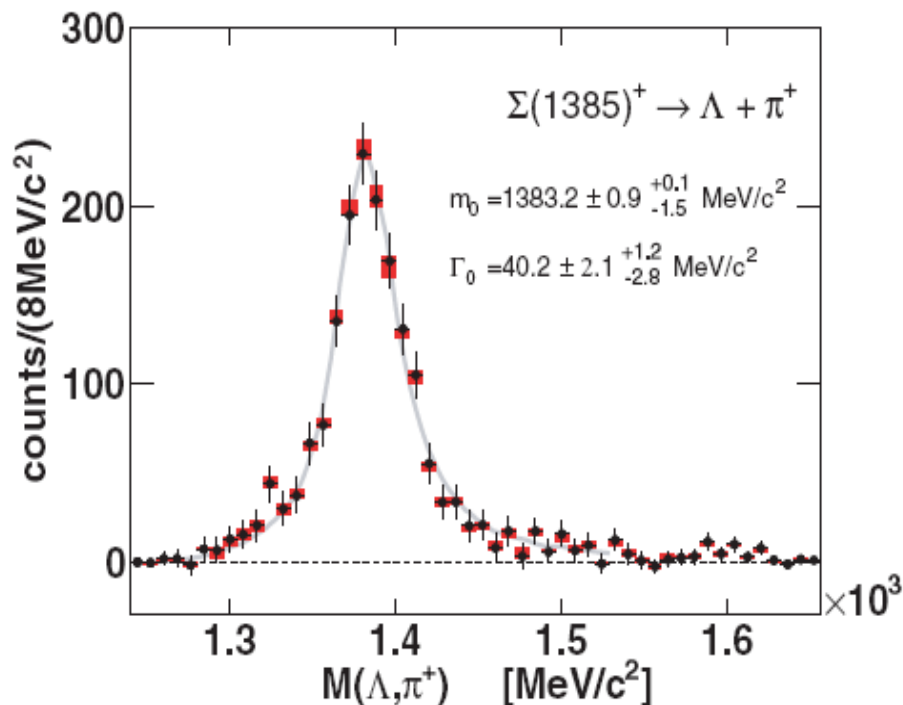
Background Contribution

- Misidentification
Fixed by K^+ sideband analysis
- Non resonant background
simultaneous fit



G. Agakishiev et al., Phys. Rev. C 85, 2013

$\Sigma(1385)^+$ Signal



Relativistic p-wave
Breit – Wigner

$$\text{Breit-Wigner} \propto \frac{q^2}{q_0^2} \frac{m_0^2 \Gamma_0^2}{(m_0^2 - m^2)^2 + m_0^2 \Gamma^2},$$

$$\Gamma = \Gamma_0 \frac{m_0 q^3}{m q_0^3} F_1(q),$$

$$F_1(q) = \frac{1 + (q_0 R)^2}{1 + (q R)^2},$$

$$\sigma_{\Sigma(1385)^+} = 22.42 \pm 0.99 \pm 1.57^{+3.04}_{-2.23} \mu b$$

G. Agakishiev et al., Phys. Rev. C 85, 2013

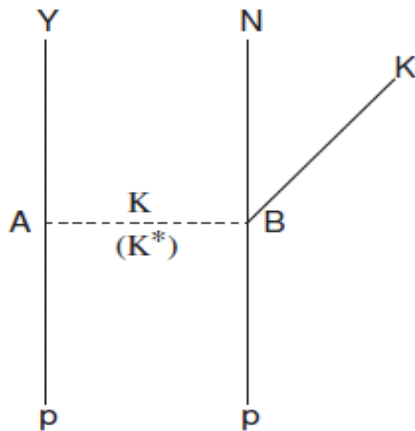


PDG Entry

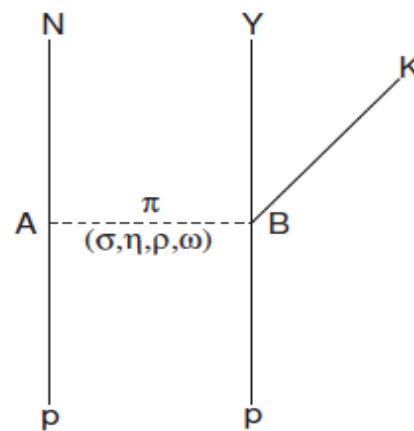
Production Mechanism



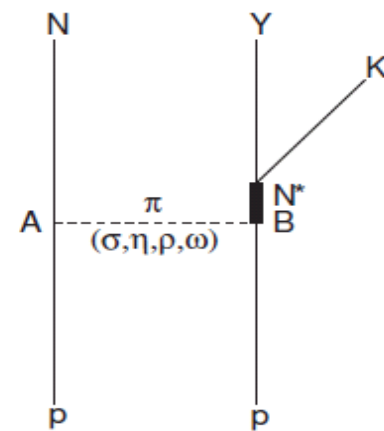
One Boson Exchange (OBE) Model



Strange boson
exchange



Non strange boson
exchange

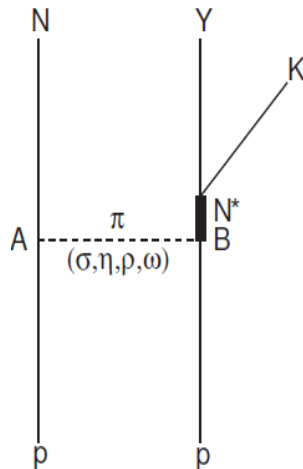
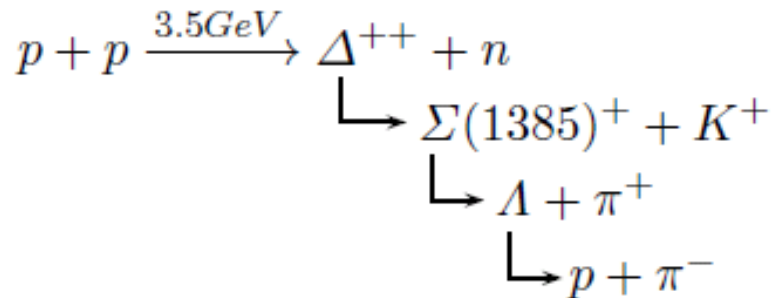


Non strange boson
resonance production

E.Ferrari, S.Serio Phys.Rev. 167:1298-1308

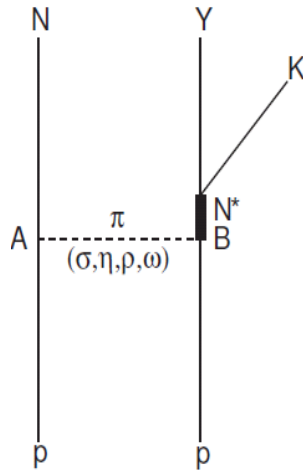
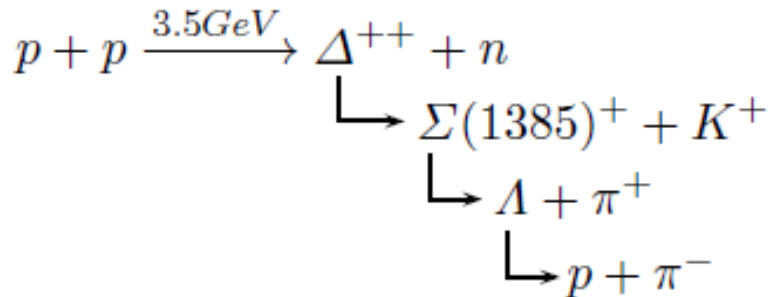
Production Mechanism

Intermediate Resonance

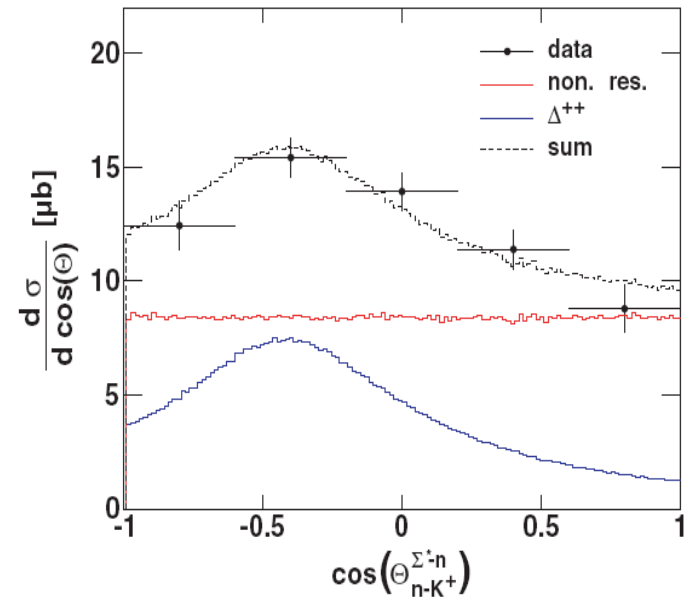


Production Mechanism

Intermediate Resonance



Helicity Angle



66% free production

33% resonant production via $\Delta(2050)^{*++}$

G. Agakishiev et al., Phys. Rev. C 85, 2013

Summary $\Sigma(1385)^+$



- Reconstructed $\Sigma(1385)^+$ signal
 - $m = 1383.2 \pm 0.9_{-1.5}^{+0.1} \text{ MeV}/c^2$
 - $\Gamma = 40.2 \pm 2.1_{-2.8}^{+1.2} \text{ MeV}/c^2$
 - $\sigma_{\Sigma(1385)^+} = 22.42 \pm 0.99 \pm 1.57_{-2.23}^{+3.04} \mu\text{b}$
- Important role of resonances: 33% from $\Delta(2050)^{++}$
- Angular distribution extracted
 - Input for transport model
- Benchmark for $\Lambda(1405)$ analysis

Spectral Function

Relativistic BW distribution $\frac{d\sigma}{dm} \approx \frac{1}{(M^2 - s - i\Gamma M)}$

$\Sigma N CUSP: \Lambda N, \Sigma N$ coupled channel interaction

Flatté approach: $\frac{d\sigma}{dm} \approx \frac{\sqrt{(\Gamma_{p\Lambda})}}{(M^2 - s - i(\Gamma_{p\Lambda} + \Gamma_{p\Sigma}) M)}$

$$\Gamma_{p\Lambda} = g_{p\Lambda} * q_{p\Lambda}$$

$$\Gamma_{p\Sigma} = g_{p\Sigma} * q_{p\Sigma}$$

⇒ Separate Analysis
By Shuna Lu

$$q_{p\Lambda} = \frac{\sqrt{((s + (m_\Lambda^2 + m_p^2)) * (s - (m_p - m_\Lambda)^2))}}{2\sqrt{s}} \quad q_{p\Sigma} = i \frac{\sqrt{((s + (m_\Lambda^2 + m_p^2)) * (s - (m_p - m_\Lambda)^2))}}{2\sqrt{s}}$$

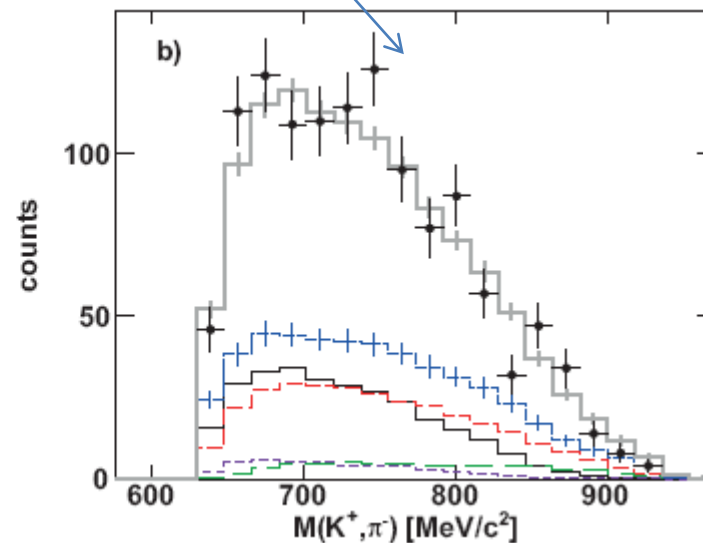
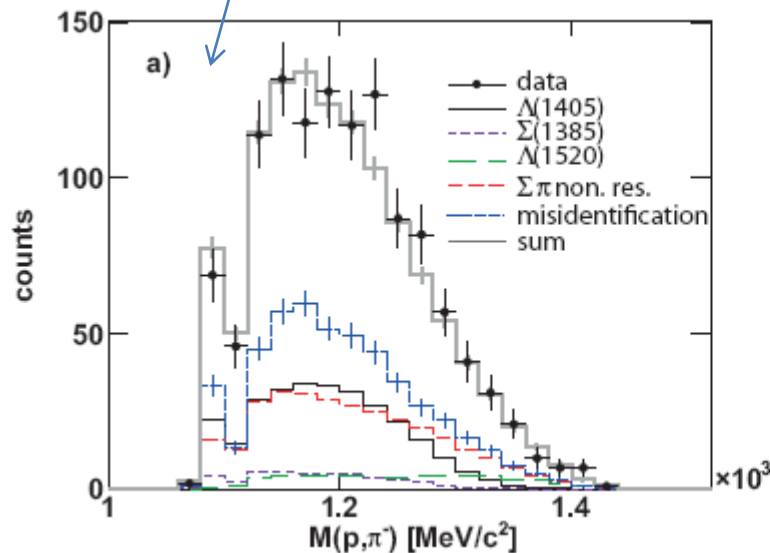
$g_{p\Lambda}, g_{p\Sigma}$ is coupling constant squared . $q_{p\Lambda}, q_{p\Sigma}$ is c.m. momentum

Background Discussion Sigma-

$$\Sigma^+ + \pi^- + p + K^+$$

$$\Sigma^+ + K^+ + \Delta^0(1232)/N(1440) \rightarrow \Sigma^+ + K^+ + (p\pi^-)$$

$$\Sigma^+ + p + K^{*0} \rightarrow \Sigma^+ + p + (K^+\pi^-)$$



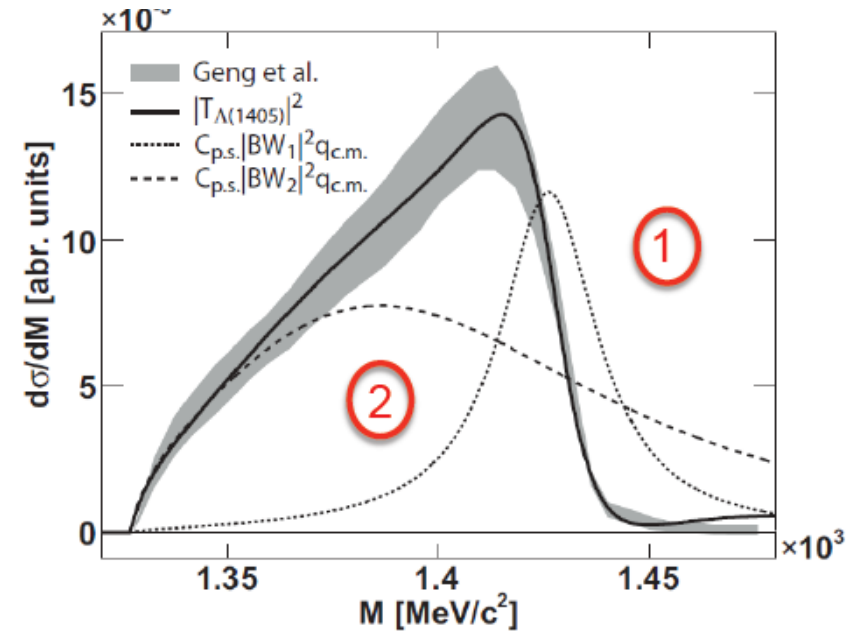
No Signature of Intermediate Resonance Visible
 => Background can be described by Free production

Interference

Double pole nature of $\Lambda(1405)$ and include interference effects with non-resonant channels

Assumption:

- Parameterize $\Lambda(1405)$ as coherent sum of two Breit-Wigner functions with
 - $C_{p.s.}$ the available phase space
 - $q_{c.m.}$ the decay momentum for $\pi\Sigma$
- Constrain $m_{0,i}$ and $\Gamma_{0,i}$ from latest Weise calculations
(Nucl.Phys. A881 (2012) 98-114)



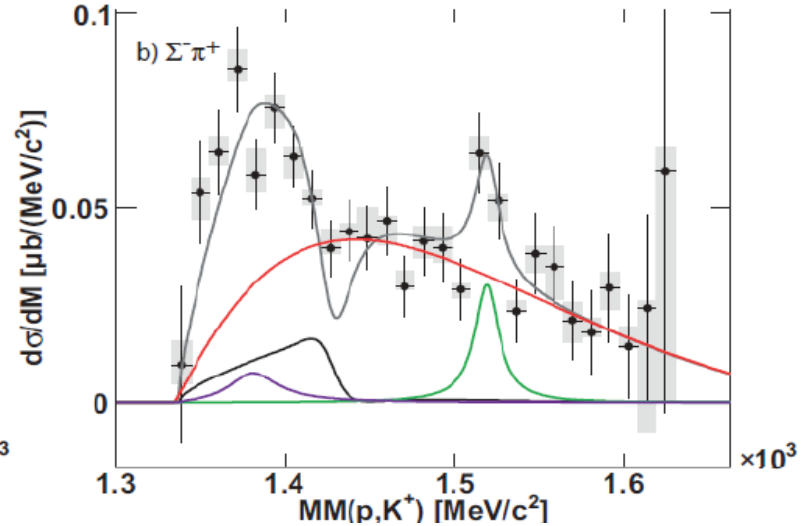
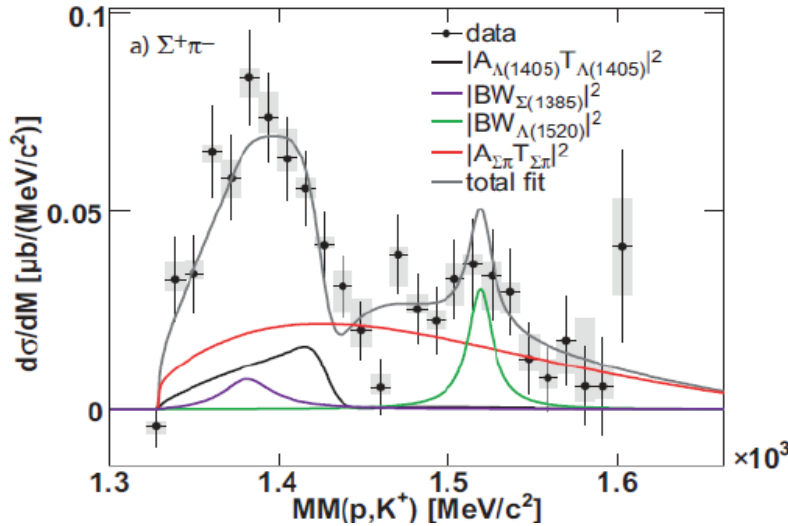
m_1	Γ_1	m_2	Γ_2	A_1/A_2	φ_1
1426	28	1375	147	0.23	206

Nucl.Phys. A881 (2012) 98-114

Interference with Background

$$\left(\frac{d\sigma}{dm}\right)_{\Sigma^+\pi^-} = |A_{\Lambda(1405)}T_{\Lambda(1405)} + e^{i\alpha}A_{\Sigma^+\pi^-}T_{\Sigma^+\pi^-}|^2 + |BW_{\Sigma(1385)^0}|^2 + |BW_{\Lambda(1520)}|^2$$

$$\left(\frac{d\sigma}{dm}\right)_{\Sigma^-\pi^+} = |A_{\Lambda(1405)}T_{\Lambda(1405)} + e^{i\beta}A_{\Sigma^-\pi^+}T_{\Sigma^-\pi^+}|^2 + |BW_{\Sigma(1385)^0}|^2 + |BW_{\Lambda(1520)}|^2$$



$A_{\Lambda(1405)}$	$A_{\Sigma^+\pi^-}$	$A_{\Sigma^-\pi^+}$	α	β
1.06	0.93	1.04	67°	109°

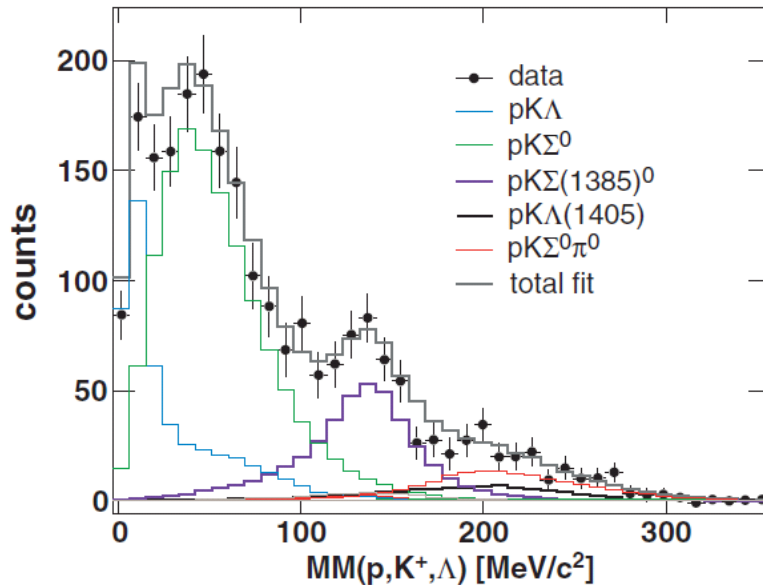
arXive - Referene

Could the Signal be Sigma (1385)

$\Sigma(1385)^0 \rightarrow \Lambda\pi^0$

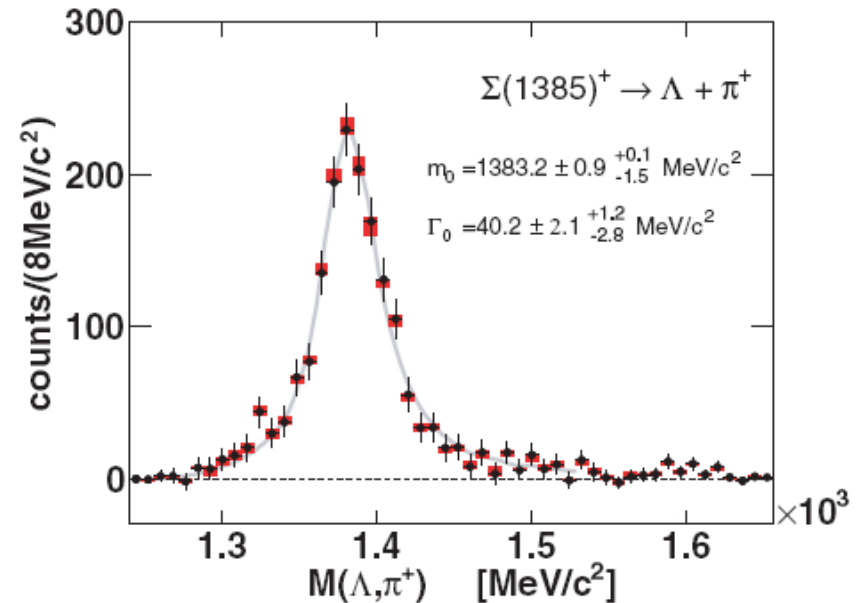
Slides => backup

$\Sigma(1385)^+$



$$\sigma_{\Sigma(1385)^0} = 5.56 \pm 0.48^{+1.94}_{-1.06} \mu b$$

G. Agakishiev et al., Phys Rev C 87, 2013



$$\sigma_{\Sigma(1385)^+} = 22.42 \pm 0.99 \pm 1.57^{+3.04}_{-2.23} \mu b$$

G. Agakishiev et al., Phys Rev C 85, 2013

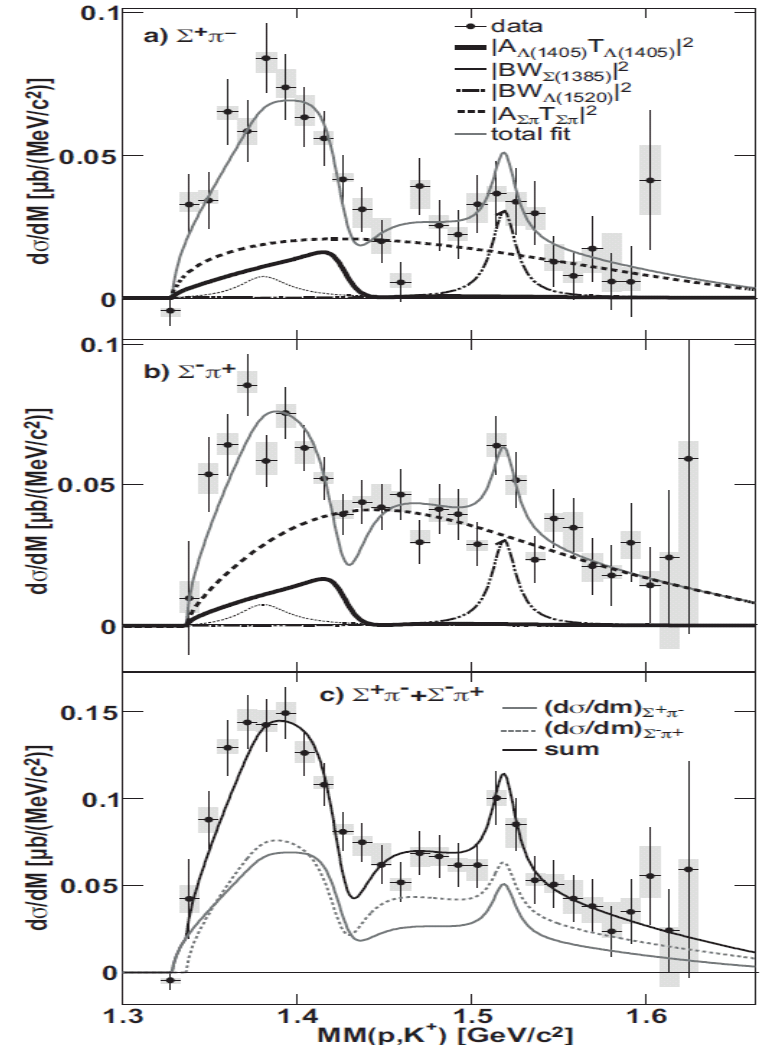
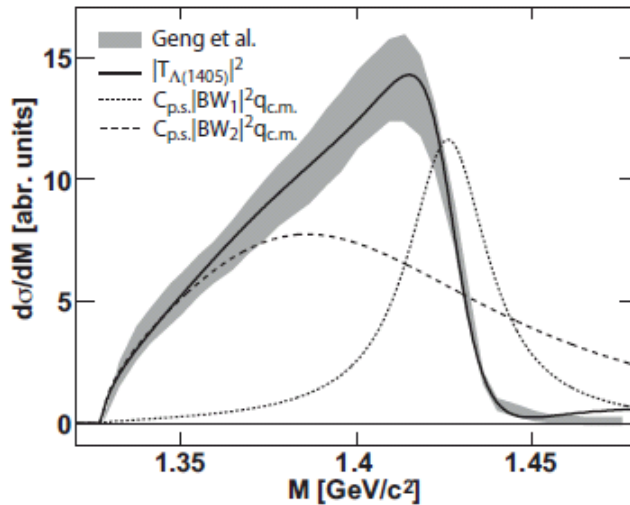
Assumption: Peak Dominated by $\Sigma(1385)^0 \rightarrow \sigma_{\Sigma(1385)^0} \cong 50 \mu b$

Interference with Background

$$\left(\frac{d\sigma}{dm}\right)_{\Sigma^+\pi^-} = |A_{\Lambda(1405)}T_{\Lambda(1405)} + e^{i\alpha}A_{\Sigma^+\pi^-}T_{\Sigma^+\pi^-}|^2 + |BW_{\Sigma(1385)^0}|^2 + |BW_{\Lambda(1520)}|^2$$

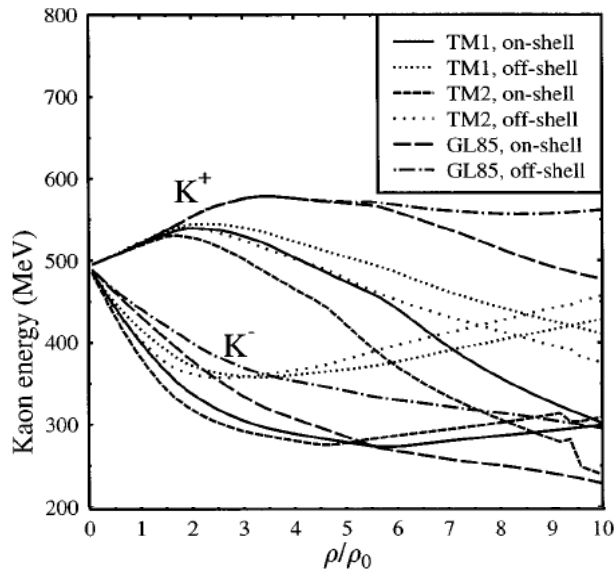
$$\left(\frac{d\sigma}{dm}\right)_{\Sigma^-\pi^+} = |A_{\Lambda(1405)}T_{\Lambda(1405)} + e^{i\beta}A_{\Sigma^-\pi^+}T_{\Sigma^-\pi^+}|^2 + |BW_{\Sigma(1385)^0}|^2 + |BW_{\Lambda(1520)}|^2$$

$A_{\Lambda(1405)}$	$A_{\Sigma^+\pi^-}$	$A_{\Sigma^-\pi^+}$	α	β
1.06	0.93	1.04	67°	109°

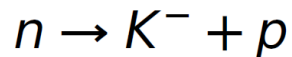


Strangeness in Matter

J. Schaffner and I. N. Mishustin
Phys. Rev. C **53**, 3 (1996)

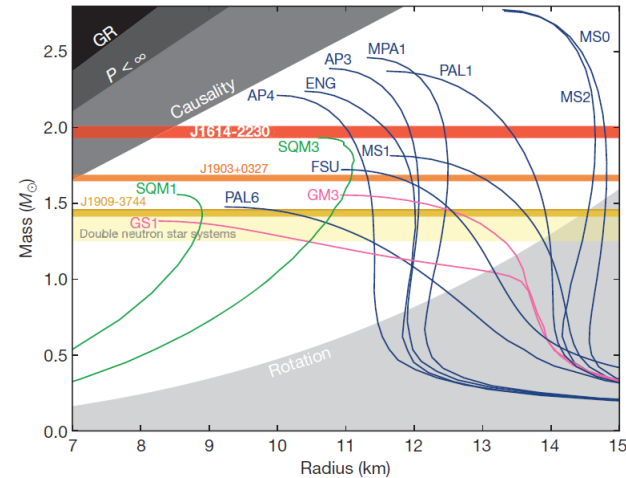


In case $m_{K^-}^* < \mu_e$

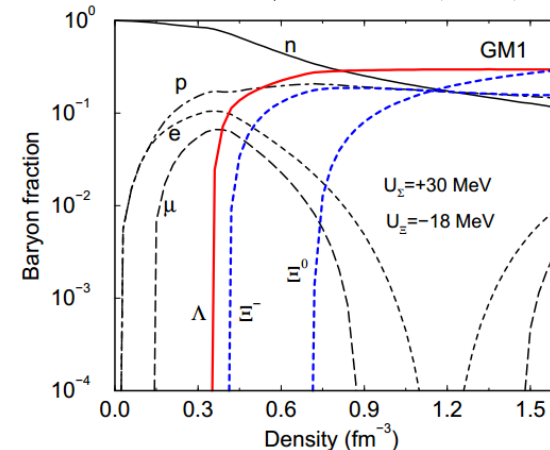


reduces Fermi pressure and softens EOS

P. B. Demorest et al., Nature **467** (2010)



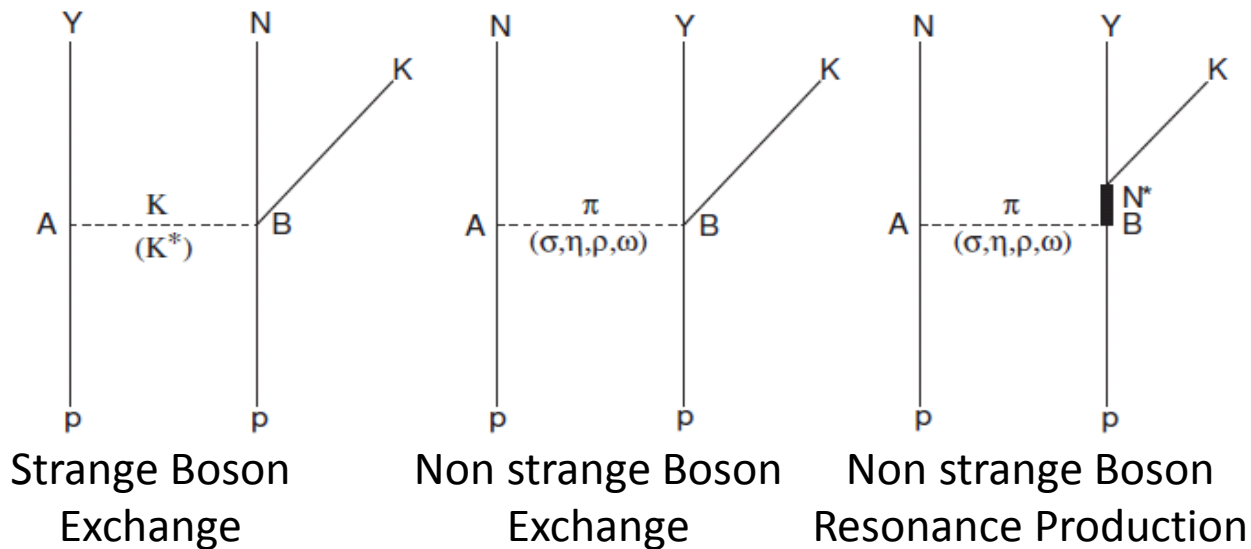
J. Schaffner-Bielich, NPA **804** (2008)



Current Data Set

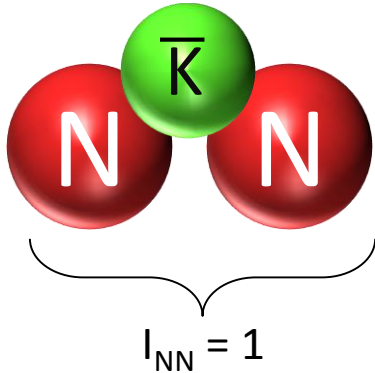
- Photoproduction D.Keller (CLAS) Phys.Rev. D78
- K^-p Baubillier - Z.Phys.C (1984) / Agulier Benitz - Ann.Fis A 77 (1981)
- pp S.Klein Phys. Rec D1

Production Mechanismus in p-p One Boson Exchange Model



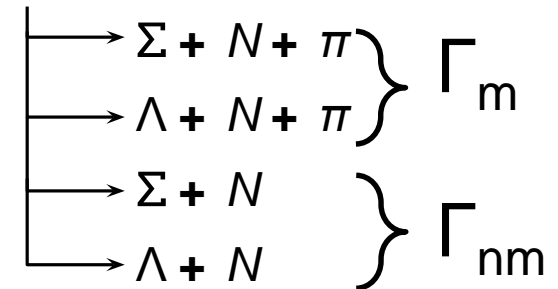
E.Ferrari, S.Serio Phys.Rev. 167:1298-1308

The Smallest Cluster



Property	Value
charge	+ 1
strangeness	-1
participants	ppK^- , $pn\bar{K}^0$
\mathcal{P}	0^-

$\bar{K}NN$



Chiral, energy dependent

	var. [DHW09, DHW08]	Fad. [BO12b, BO12a]	var. [BGL12]	Fad. [IKS10]	Fad. [RS14]
BE	17–23	26–35	16	9–16	32
Γ_m	40–70	50	41	34–46	49
Γ_{nm}	4–12	30			

Non-chiral, static calculations

	var. [YA02, AY02]	Fad. [SGM07, SGMR07]	Fad. [IS07, IS09]	var. [WG09]	var. [FIK ⁺ 11]
BE	48	50–70	60–95	40–80	40
Γ_m	61	90–110	45–80	40–85	64–86
Γ_{nm}	12			~20	~21

Binding Energy (BE):

10-100 MeV

Mesonic Decay (Γ_m)

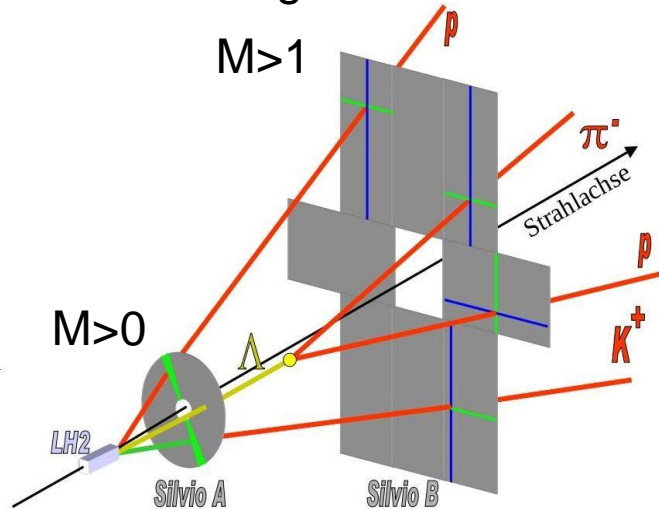
30-110 MeV

Non-Mesonic Decay (Γ_{nm})

4-30 MeV

Trigger Detector - SiΛViO

Silicon Λ -Vertexing and Identification Online

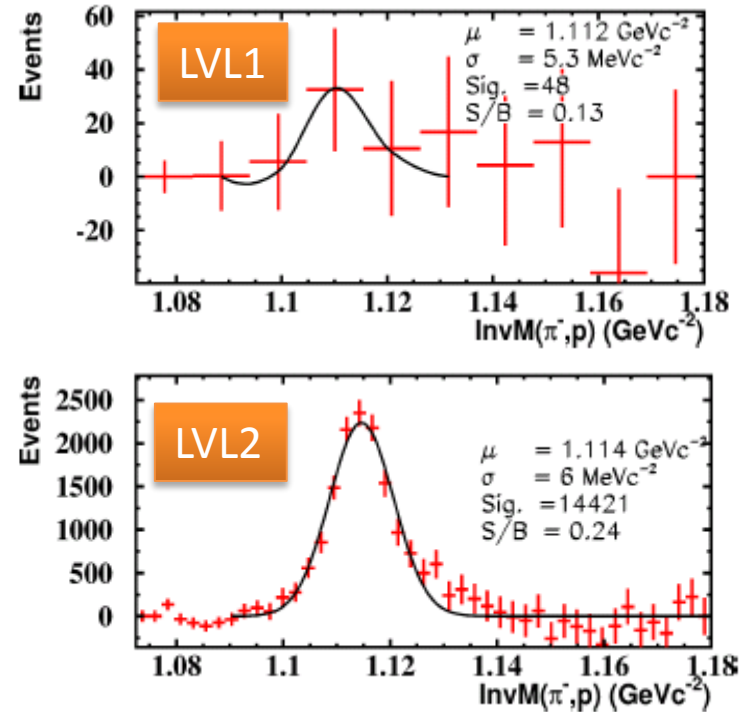


Trigger conditions:

LVL1 : Multiplicity(ToF) > 1

LVL2 : LVL1 + SiΛViO

Inclusive Λ Reconstruction



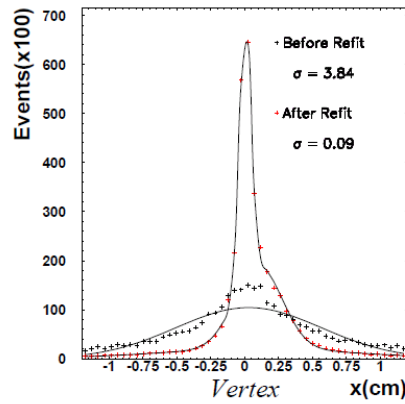
Λ – Enhancement: $14.1 \pm 7.9(\text{stat})_{-0.6}^{+4.3}$

R. Münzer et. al. NIM A 745 (2014) 38-49

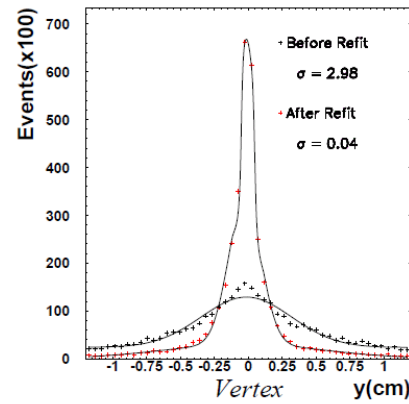
Reconstruction of exclusive Reactions

$$p + p \rightarrow p + K^+ + \Lambda$$

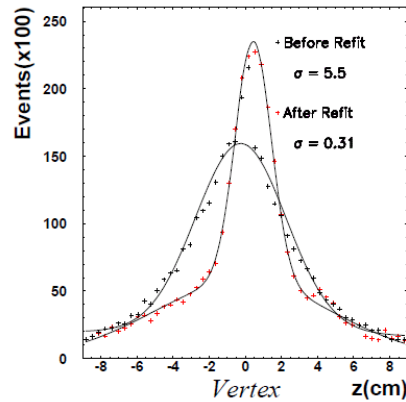
Inclusive Reconstruction



(a)



(b)

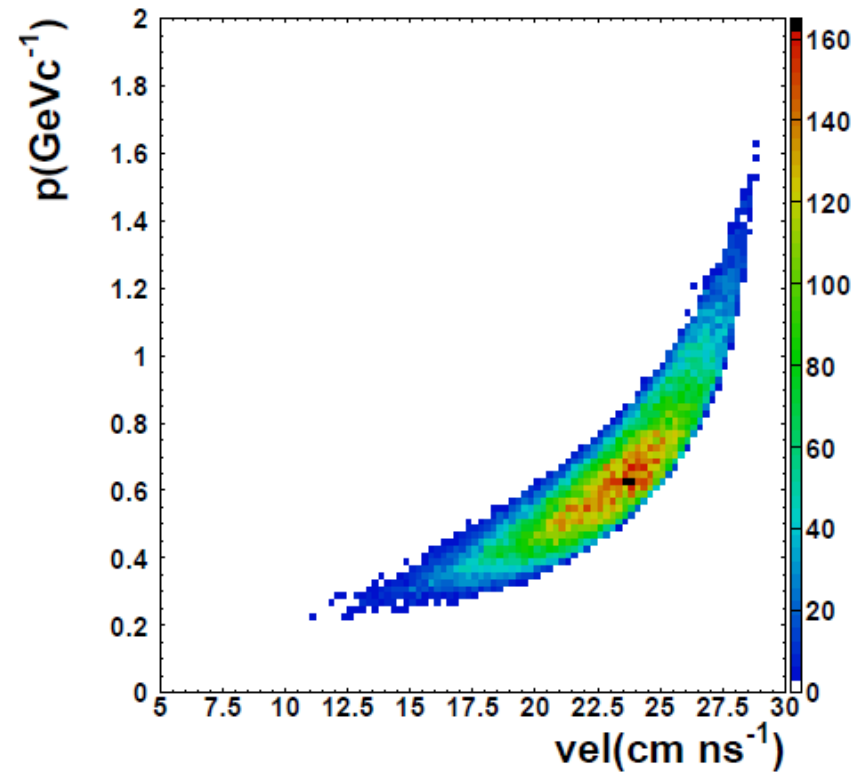


	Before Refit [cm]	After Refit [cm]
σ_x	3.84	0.09
σ_y	2.98	0.04
σ_z	5.50	0.31

Exclusive Data Sample

Primary K^+ Selection

Kaon Candidates in RPC and CDC



Exclusive Data Sample

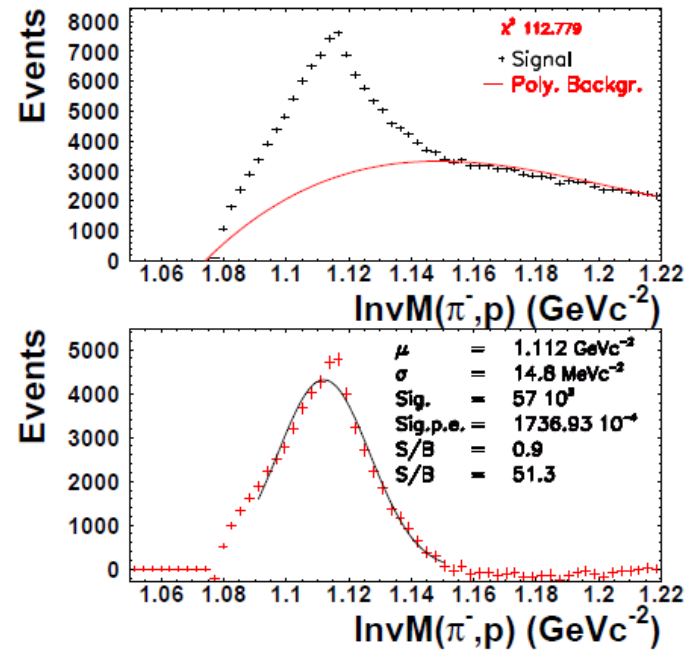
Primary K^+ Selection



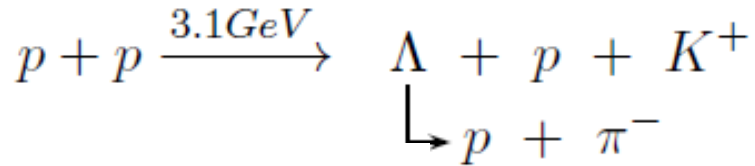
Λ Selection

Λ Candidates in all sub detector Combinations

$\Lambda \rightarrow p + \pi^-$



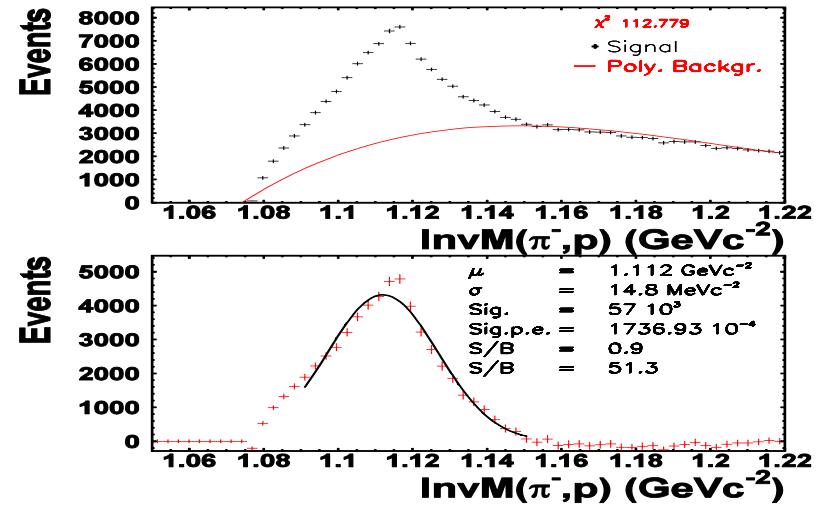
Exclusive Reconstruction



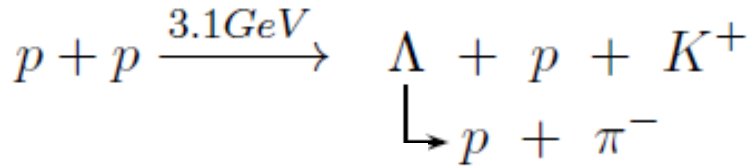
Primary K^+ Selection



Λ Identification



Exclusive Reconstruction



Primary K^+ Selection



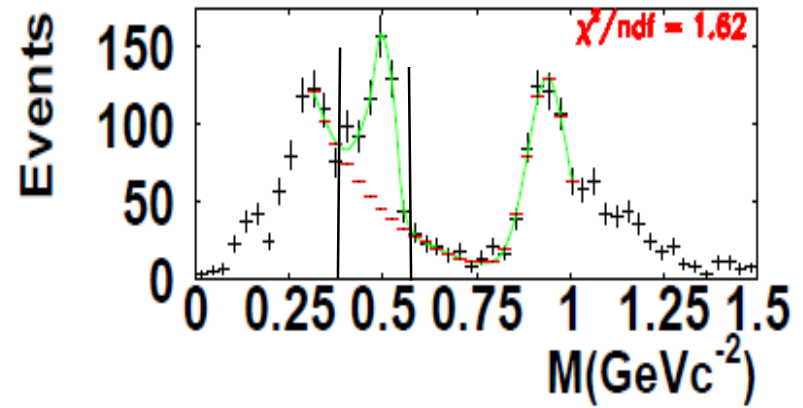
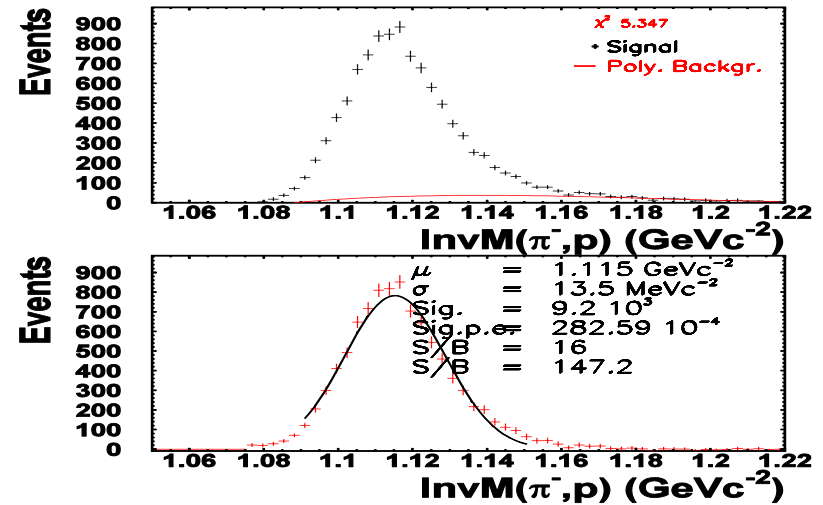
Λ Identification



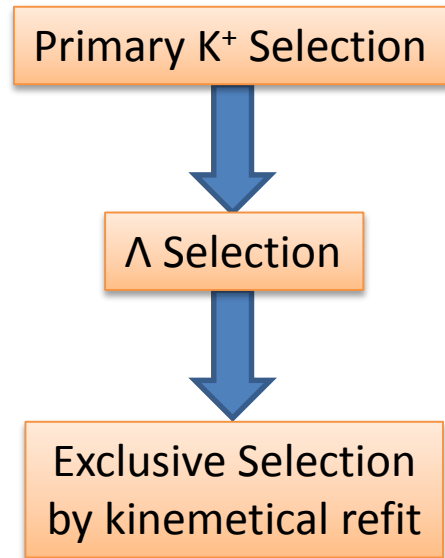
Exclusive Selection
by Kinematical Refit



Secondary K^+ Selection
Sideband Analysis



Exclusive Data Sample

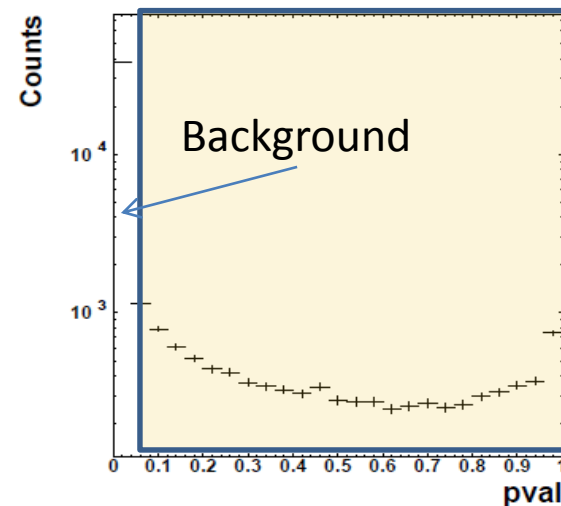


Kinematical Refit

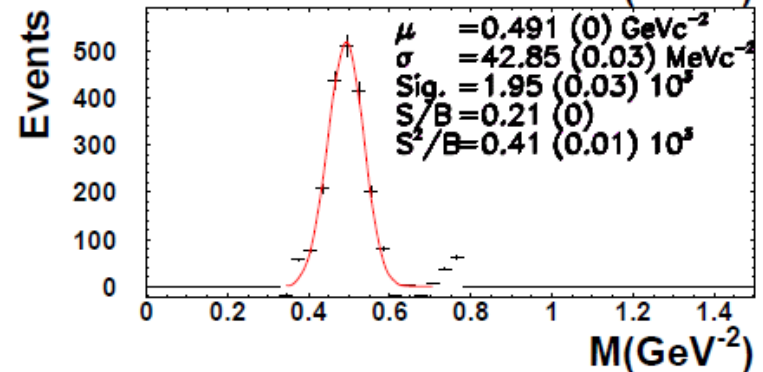
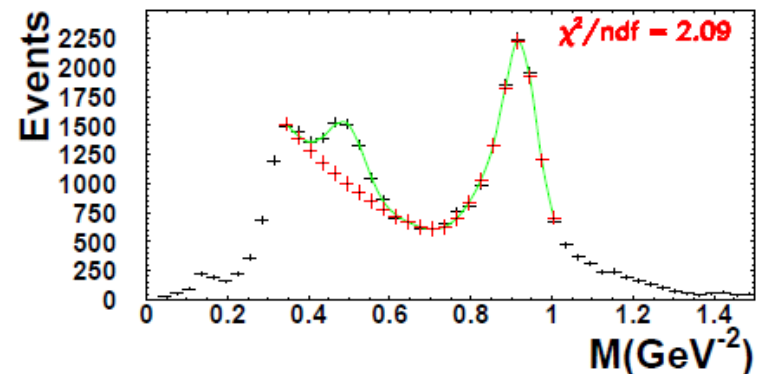
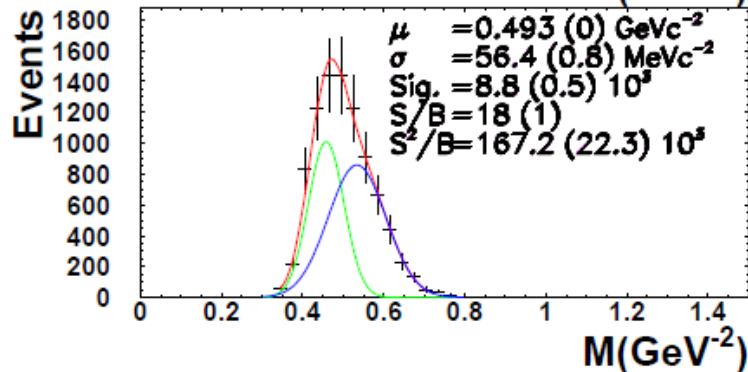
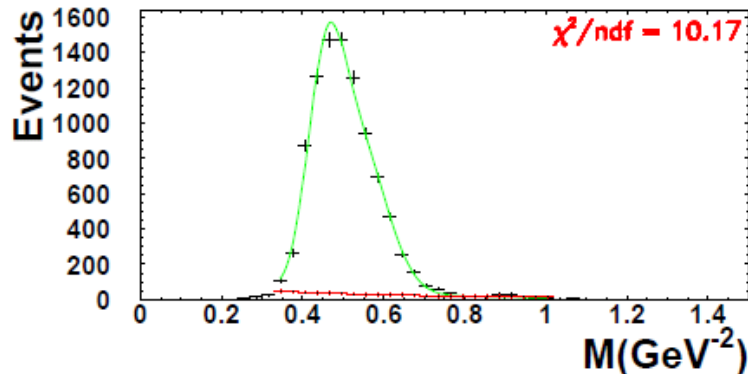
Variation of Track parameters with error

$$\chi^2 = (\vec{\alpha} - \vec{\alpha}_0)^T V_{\vec{\alpha}_0}^{-1} (\vec{\alpha} - \vec{\alpha}_0)$$

$$pvalue = \int_{\chi_{fit}^2}^{\infty} f_{\nu}(\chi^2) d\chi^2.$$



Different Kaon selection

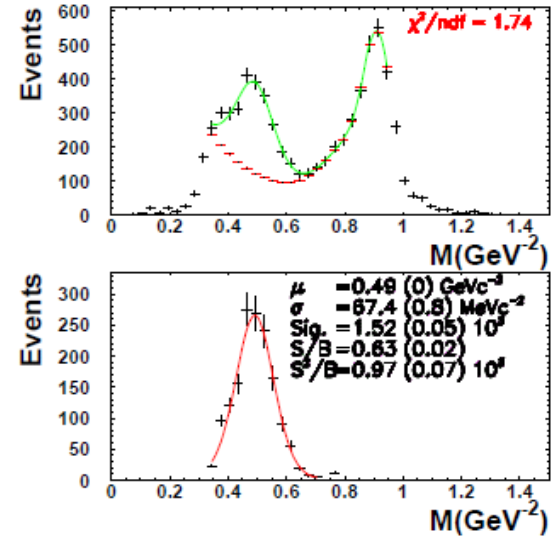
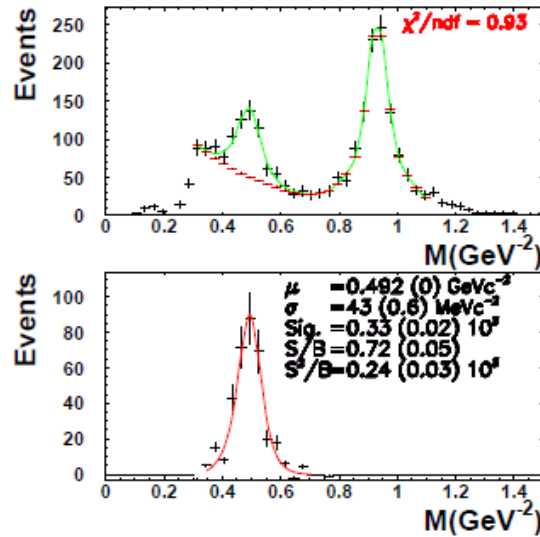
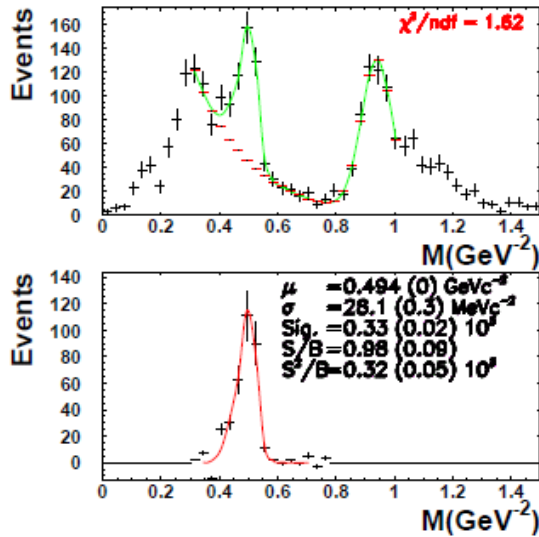


Backup

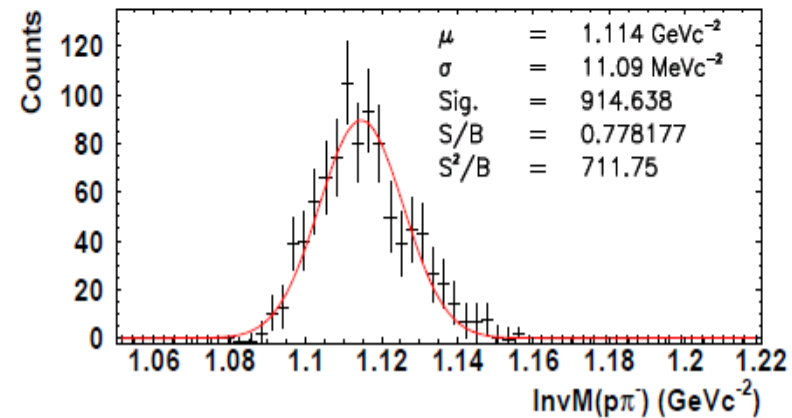
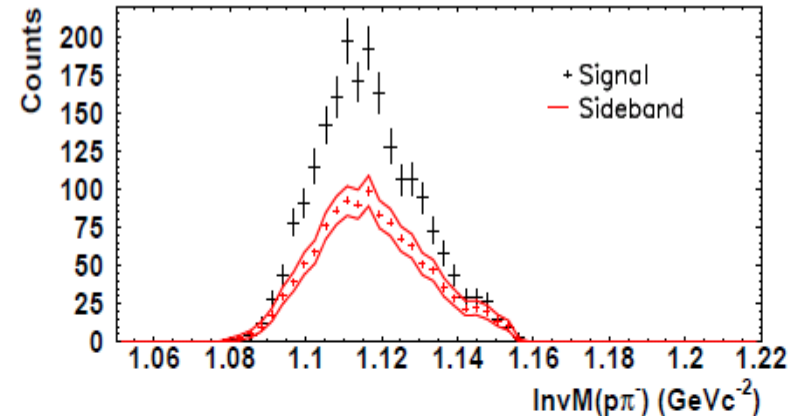
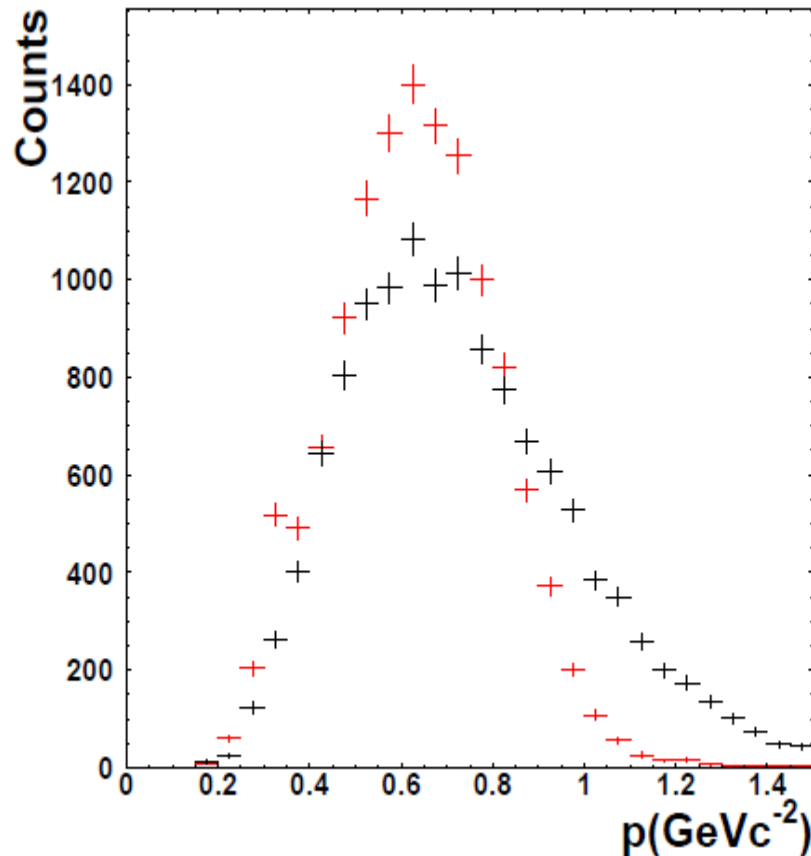
$p < 0.5 \text{ GeV}/c$

$0.5 \text{ GeV}/c < p < 0.6 \text{ GeV}/c$

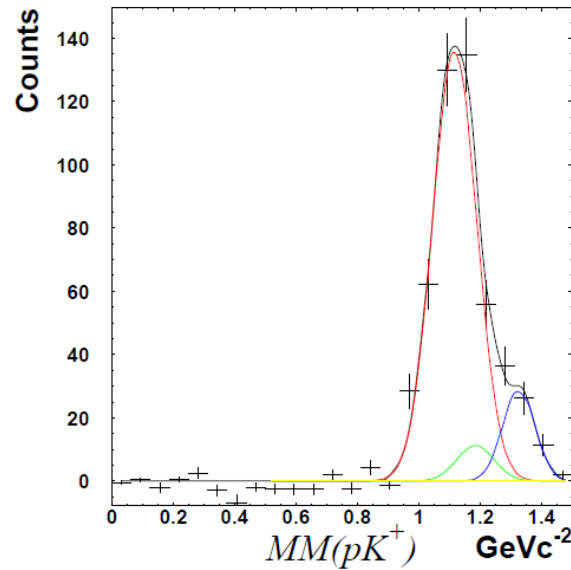
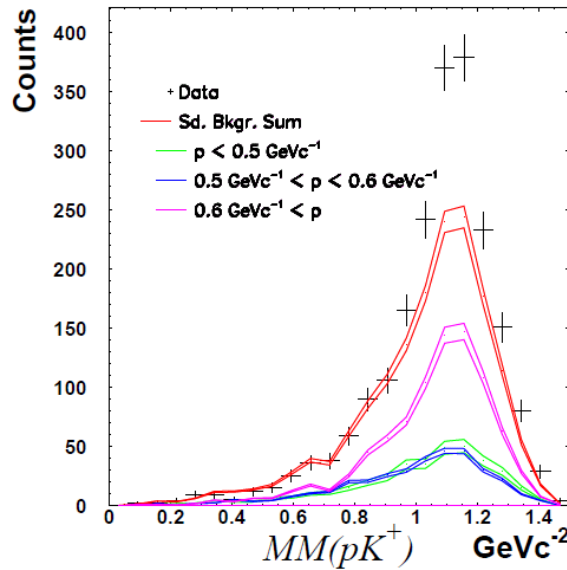
$p > 0.6 \text{ GeV}/c$



Sideband Analysis



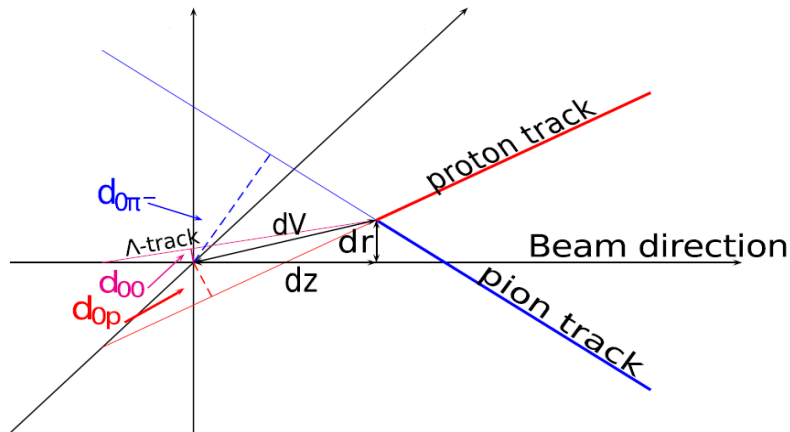
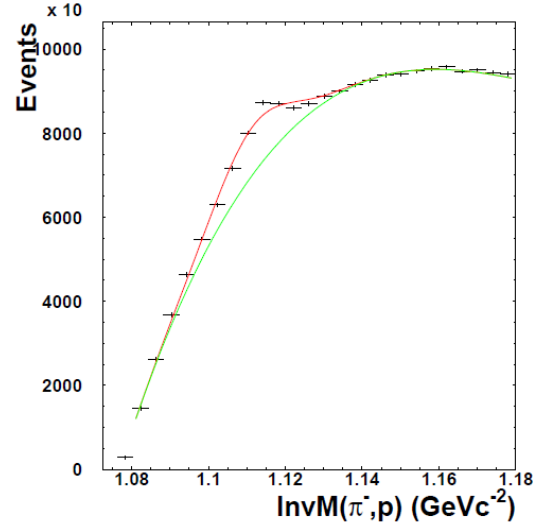
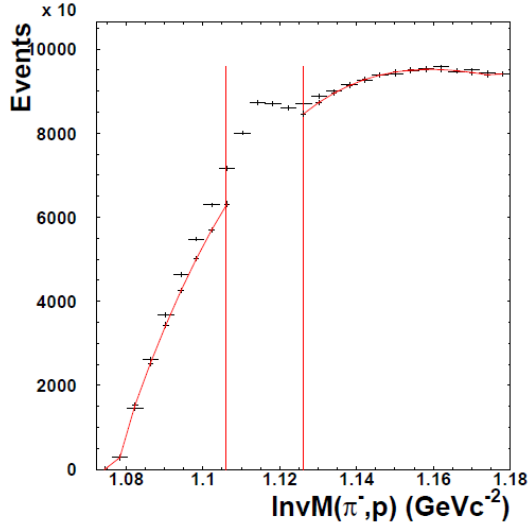
Λ / Σ Separation



Remaining Background

1/14.8.

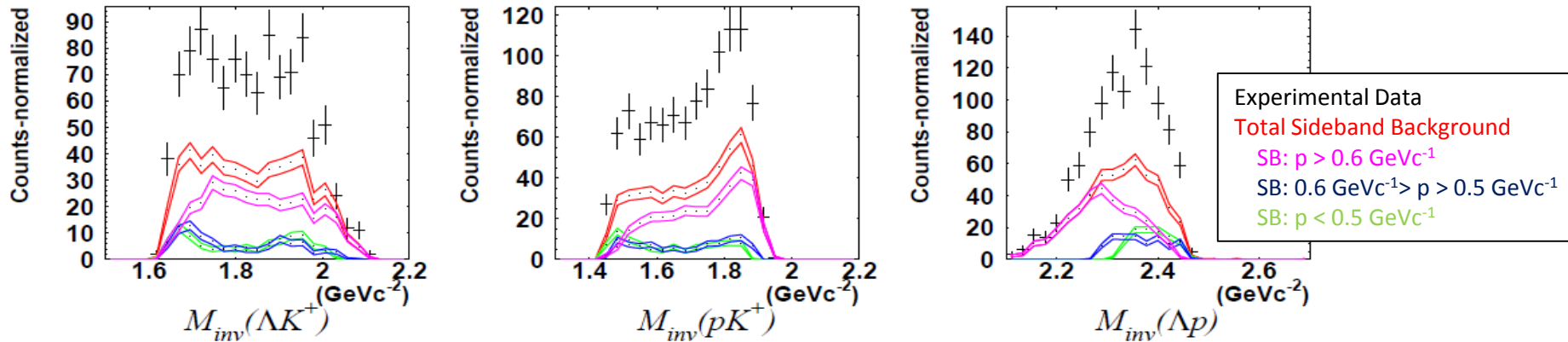
Particle	Mass	Fit μ	Fit σ	Fit Amplitude
Λ	1115.8	1.1171	0.07	136.35
Σ^0	1192.1	1.185	0.06	11.277
higher Resonance contribution		1.32	0.05	28.8



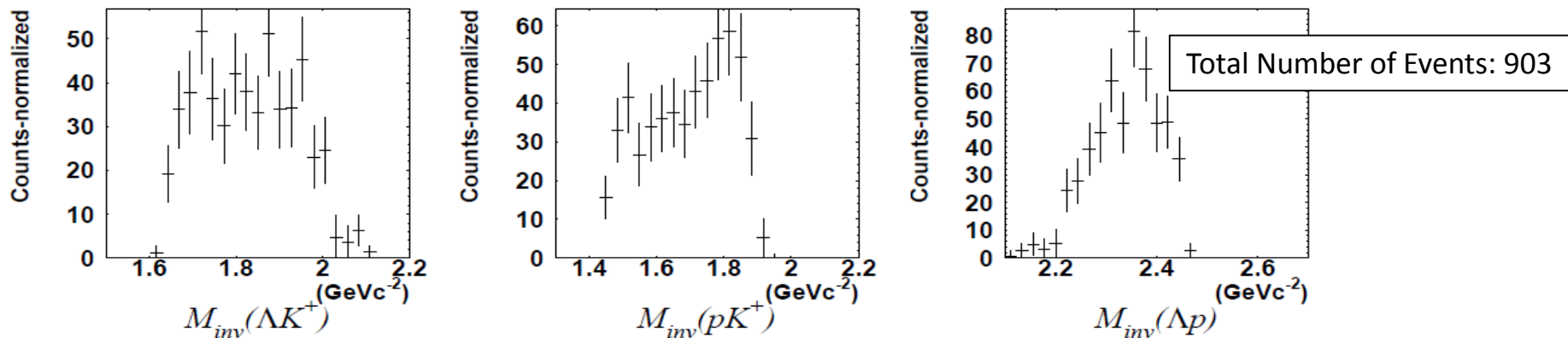
value	minimal value [cm]	maximal value [cm]
$primvertex_x$	-1.0	1.0
$primvertex_y$	-1.0	1.0
$primvertex_z$	-2.0	2.0
d_r	3.0	∞

Exclusive Data Sample

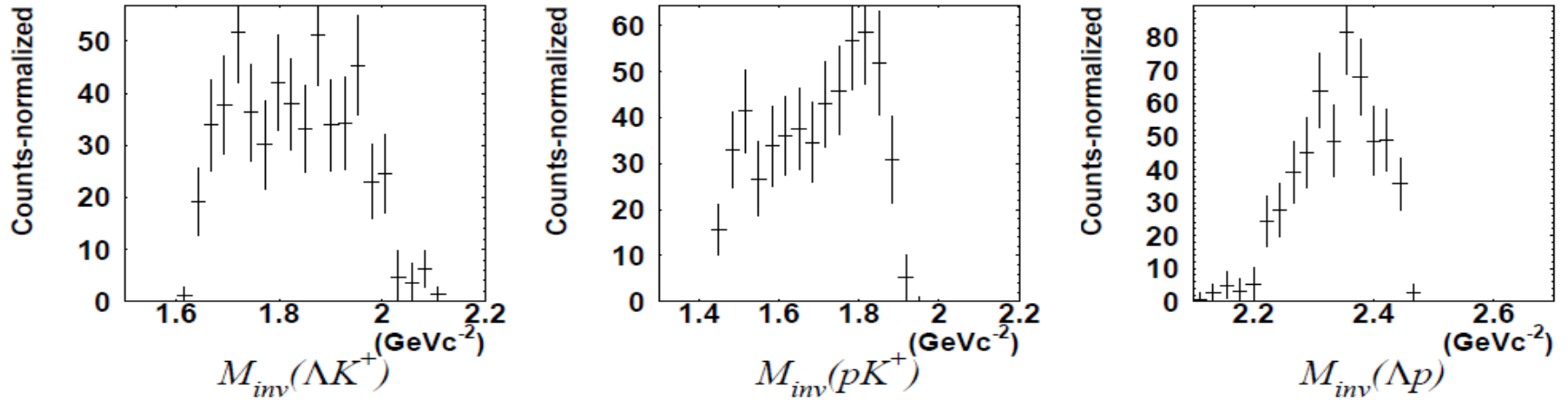
Sideband Background



Background Subtracted



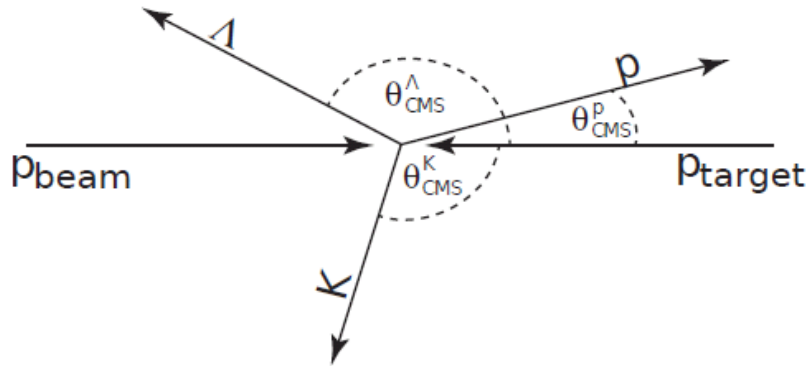
Exclusive Data Sample



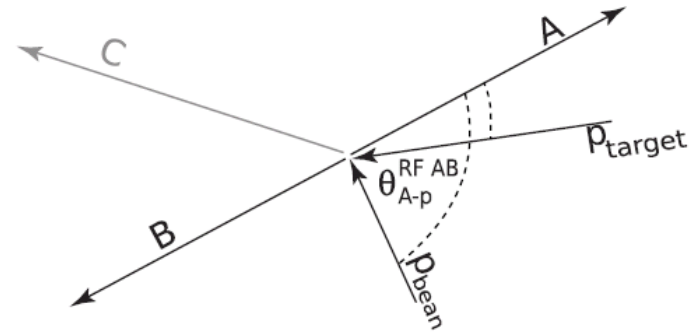
Momentum Region	Signal Events	Background Events
0.0 - 0.5 GeV/c	177	146
0.5 - 0.6 GeV/c	150	136
0.6 - GeV/c	577	577
Total	903	859

Angular Distributions

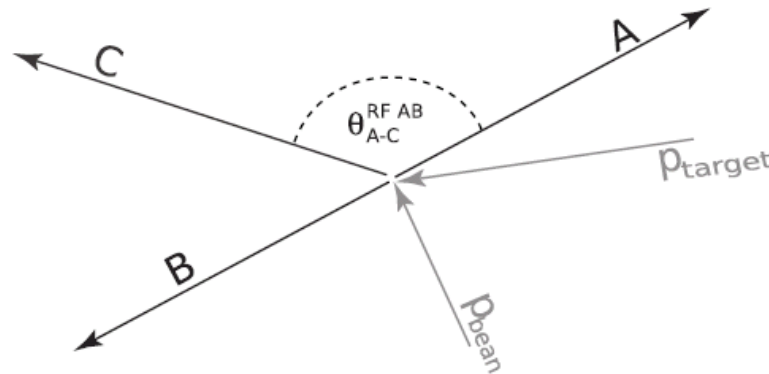
Center-of-mass angle



Gottfried-Jackson Angle



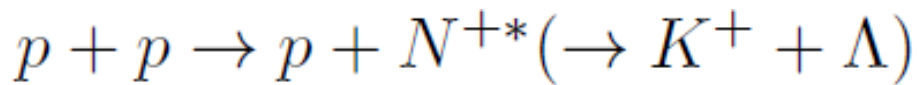
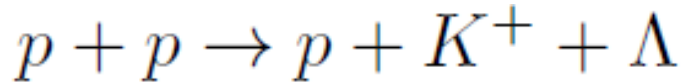
Helicity Angle



Simulation Packages

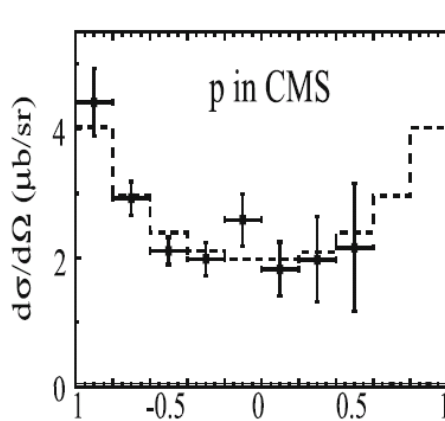
Phase Space Simulation

Incoherent Cocktail

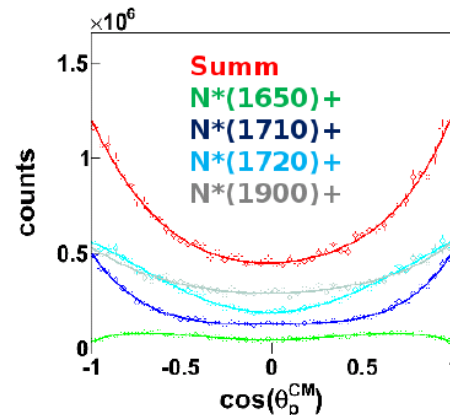


Angular Distribution

Fröhlich et al.
PoS ACAT2007 (2007)



M. Abdel-Bary et al.,
Eur.Phys.J A46(2010)



E. Eppe,
Diss. TUM (2014)

Transport Modell - UrQMD

Quantum Molecular Dynamics

Description of all
particle correlations

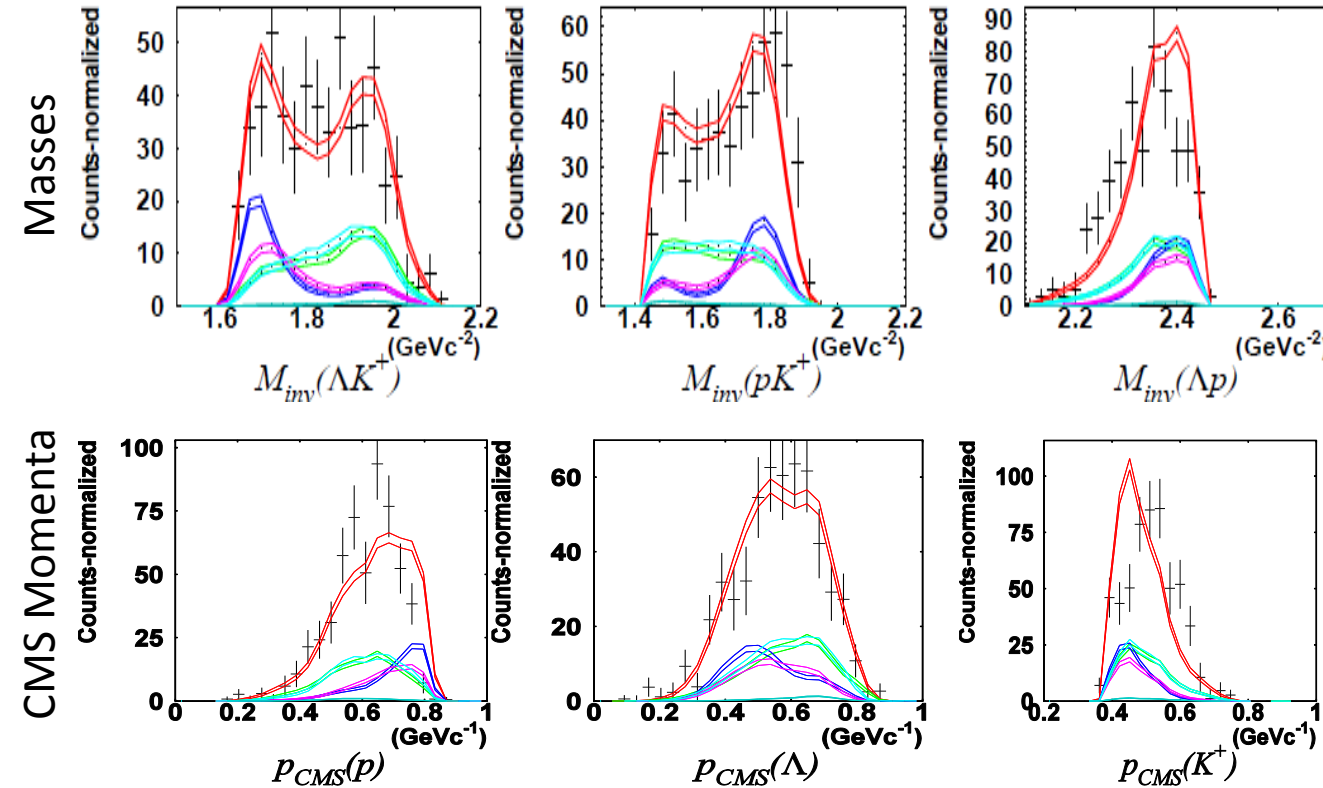
Production of p K⁺ Λ
via Resonances (N⁺*)

The UrQMD Model,
<http://urqmd.org/> 2013

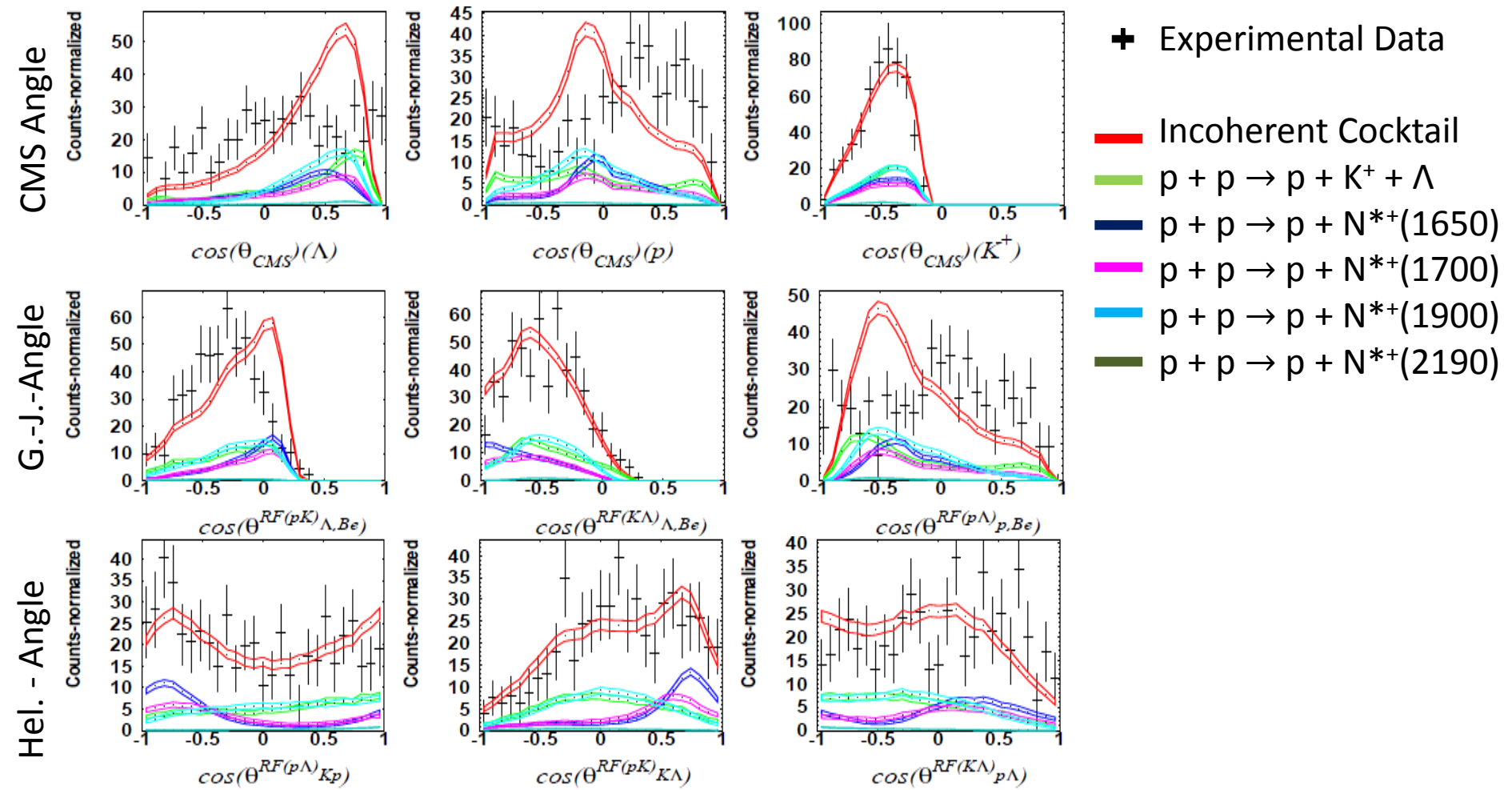
Phase Space Simulation

✚ Experimental Data

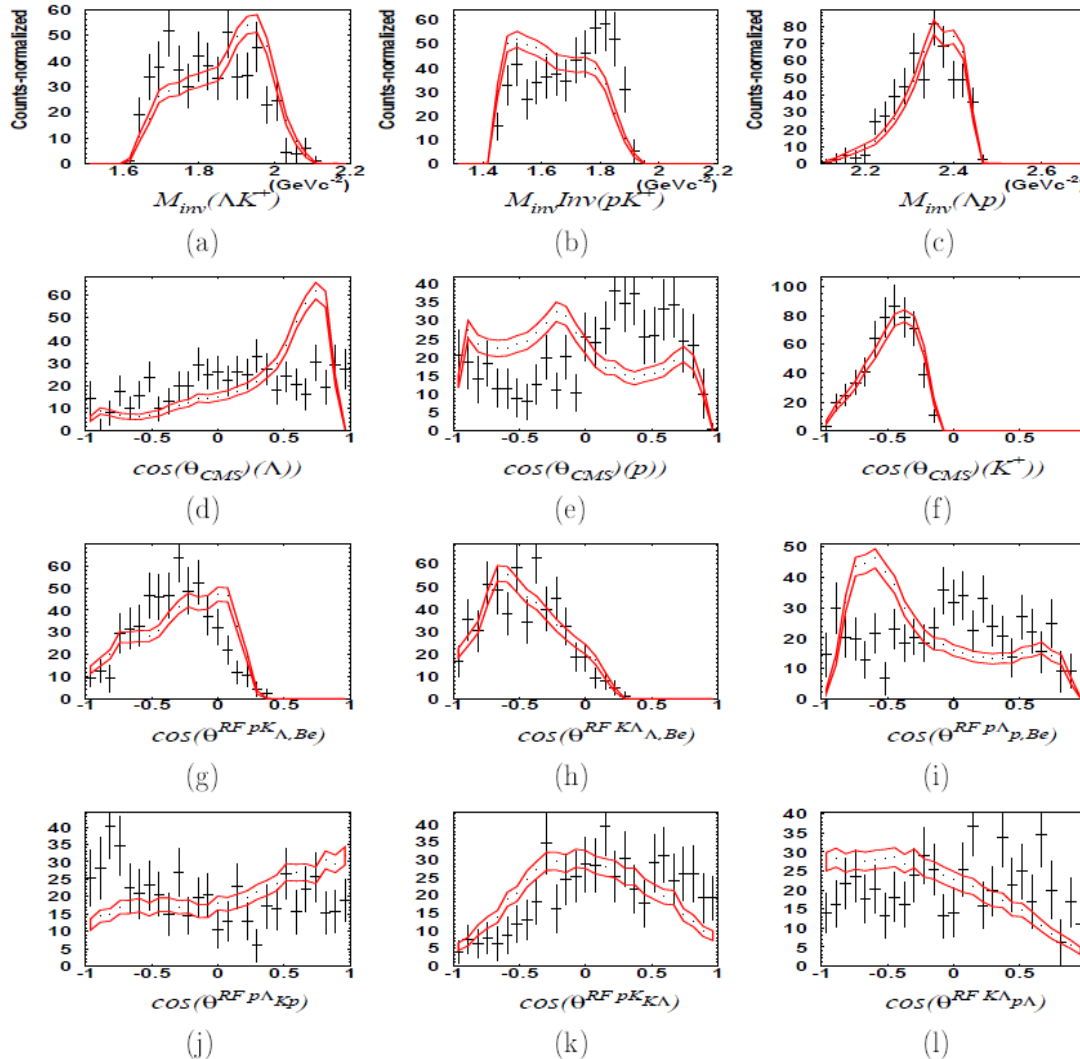
- Incoherent Cocktail
- $p + p \rightarrow p + K^+ + \Lambda$
- $p + p \rightarrow p + N^{*+}(1650)$
- $p + p \rightarrow p + N^{*+}(1700)$
- $p + p \rightarrow p + N^{*+}(1900)$
- $p + p \rightarrow p + N^{*+}(2190)$



Phase Space Simulation



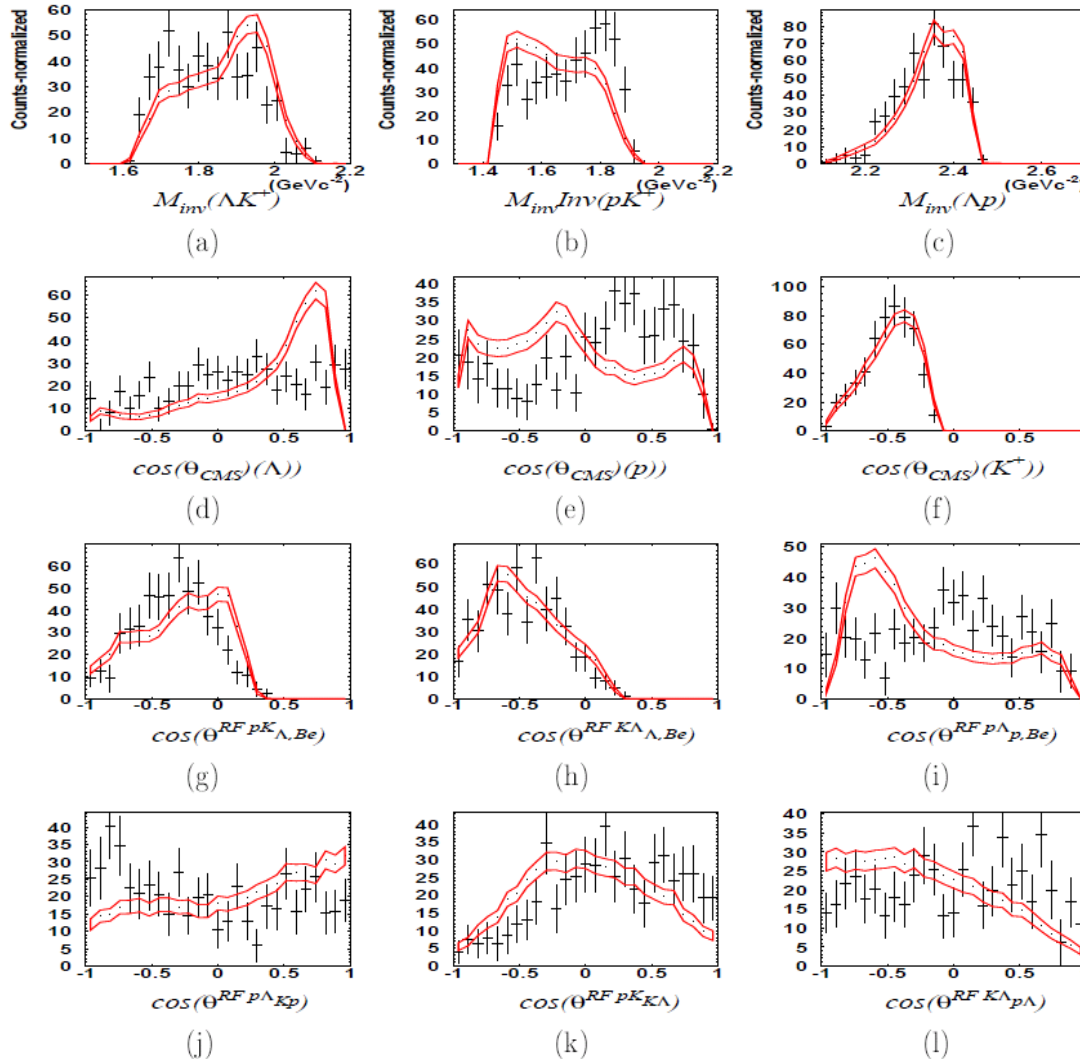
Phase Space Simulation



✚ Experimental Data

— pp \rightarrow p K^+ Λ Phase Space Simulation

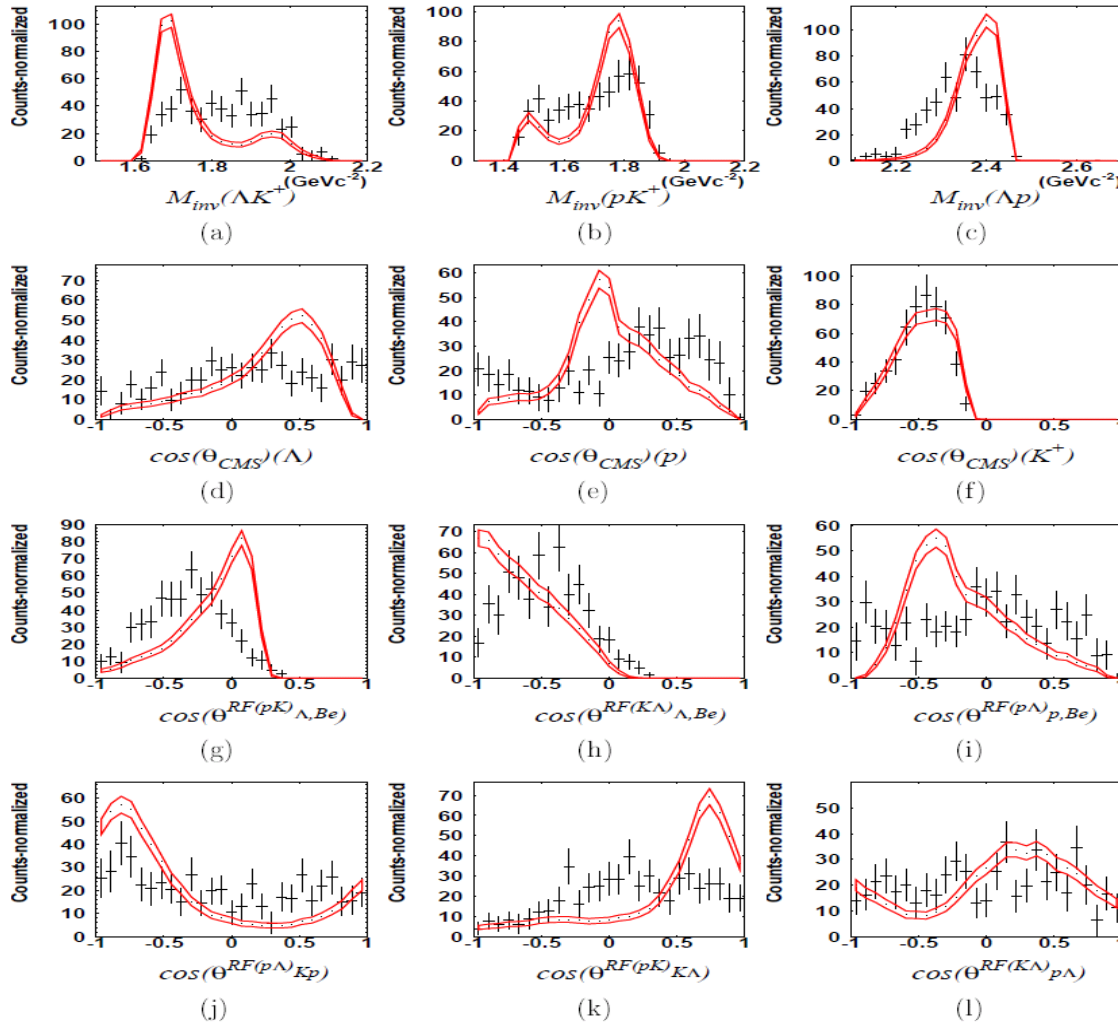
Phase Space Simulation



✚ Experimental Data

— pp \rightarrow p K^+ Λ Phase Space Simulation

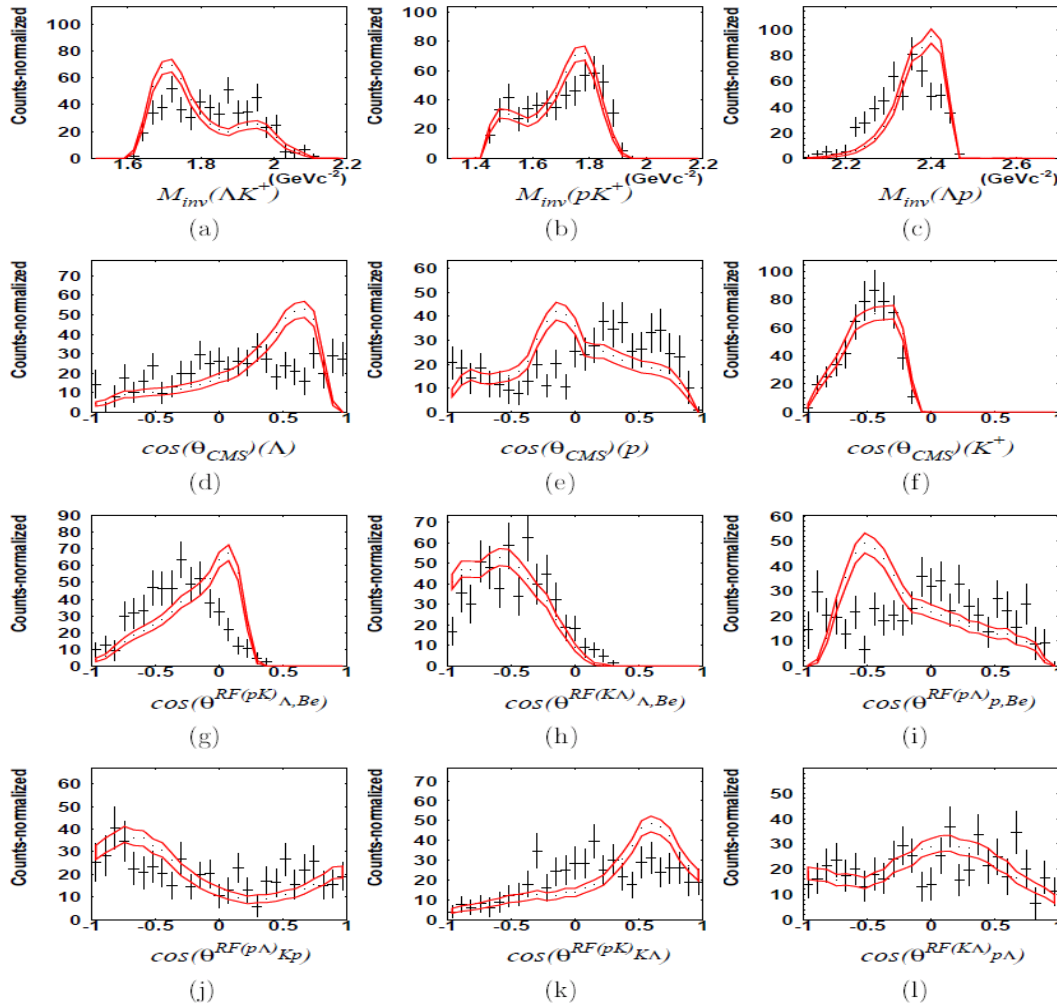
Phase Space Simulation



✚ Experimental Data

— pp \rightarrow p N $^{*+}(1650)$
Phase Space
Simulation

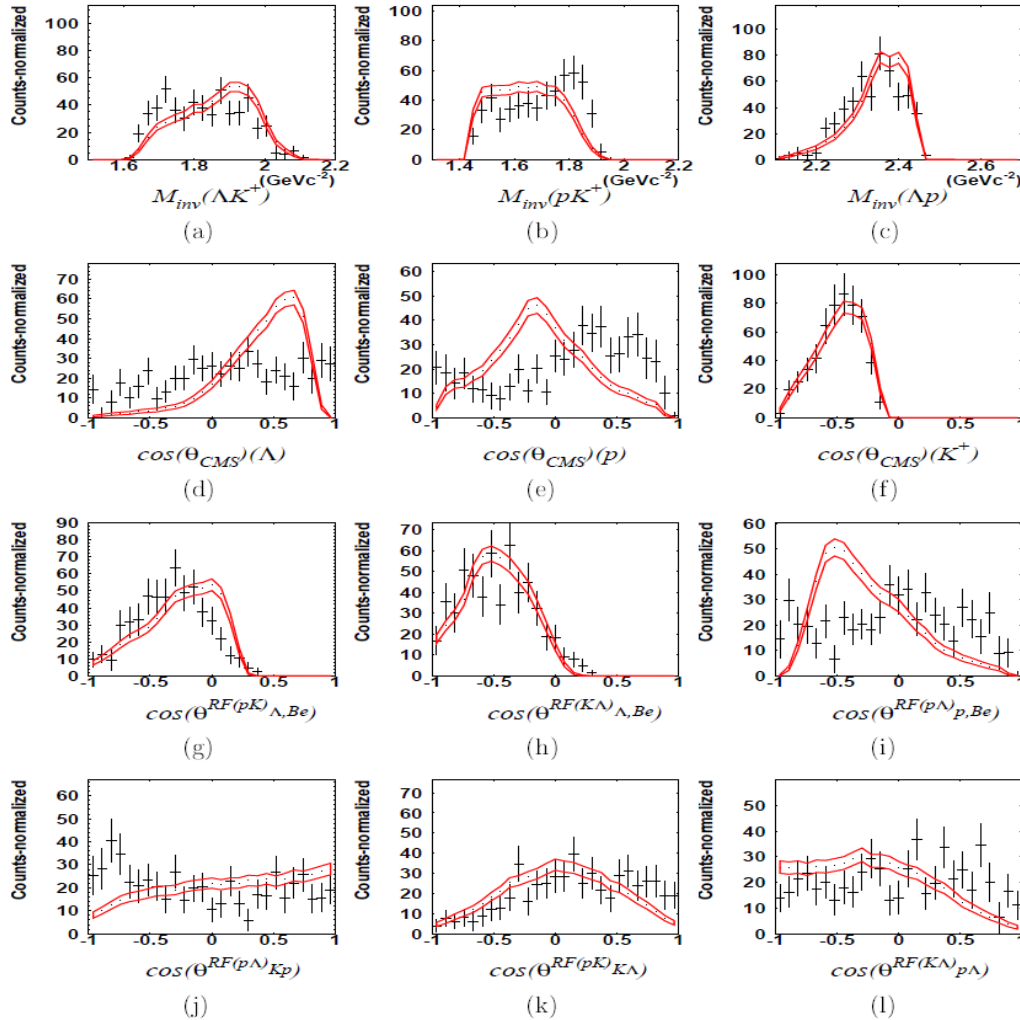
Phase Space Simulation



✚ Experimental Data

— $pp \rightarrow p N^{*+}(1700)$
Phase Space
Simulation

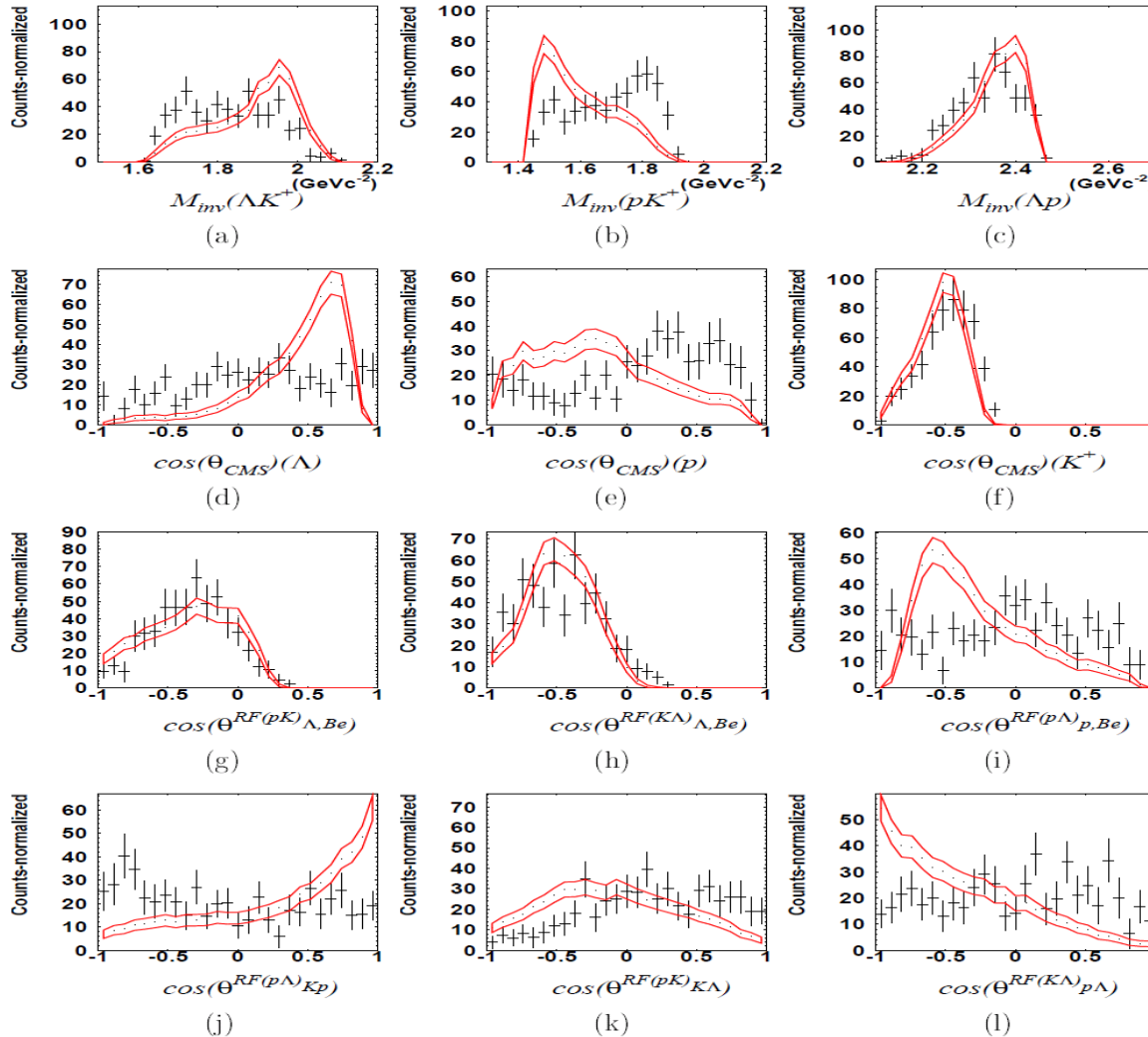
Phase Space Simulation



✚ Experimental Data

— pp \rightarrow p $N^{*+}(1900)$
Phase Space
Simulation

Phase Space Simulation



✚ Experimental Data

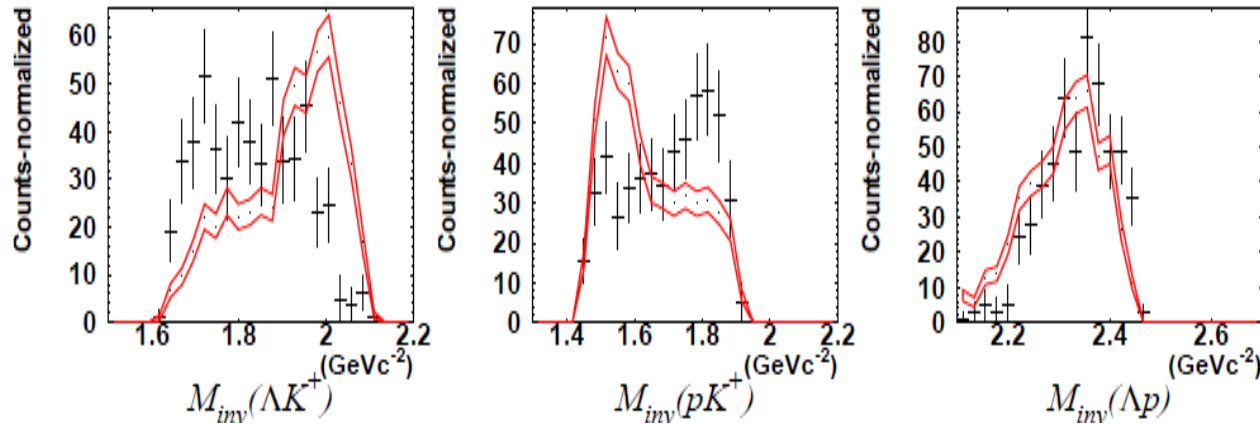
— $pp \rightarrow p N^{*+}(2190)$
Phase Space
Simulation

UrQMD Simulation

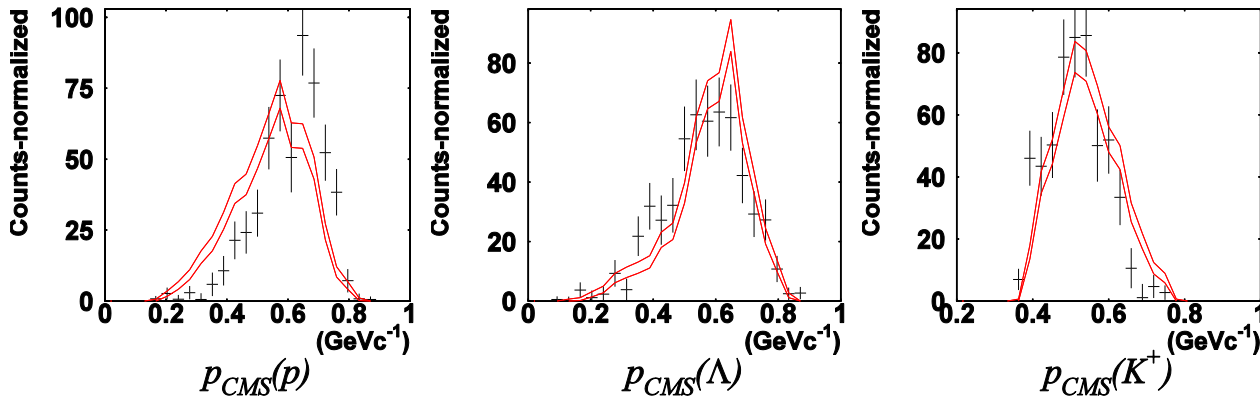
✚ Experimental Data

— UrQMD Simulations

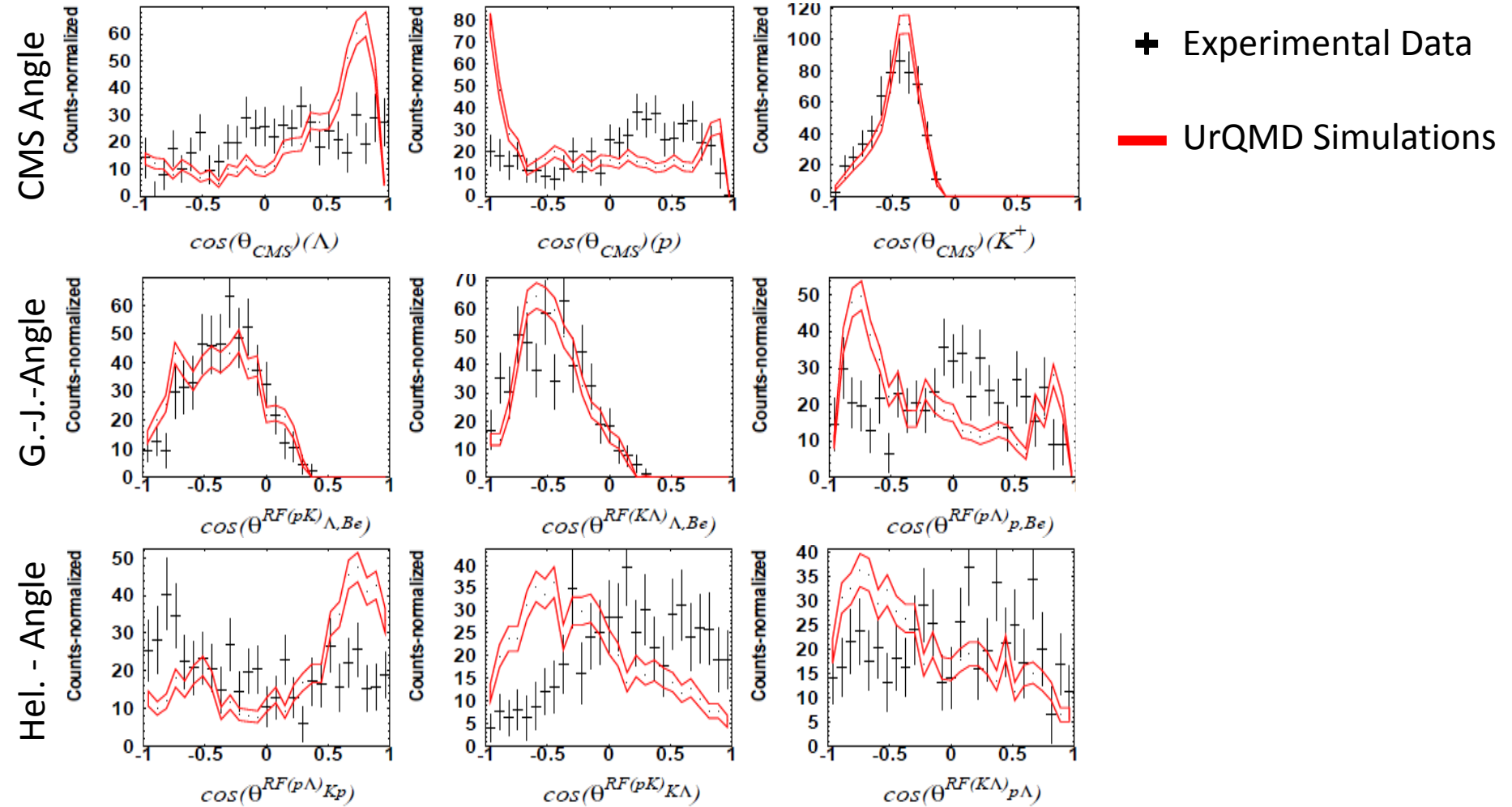
Masses



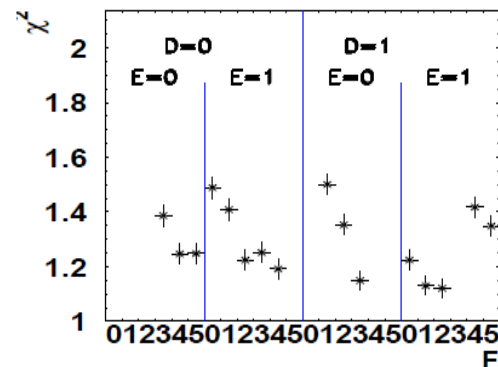
CMS Momenta



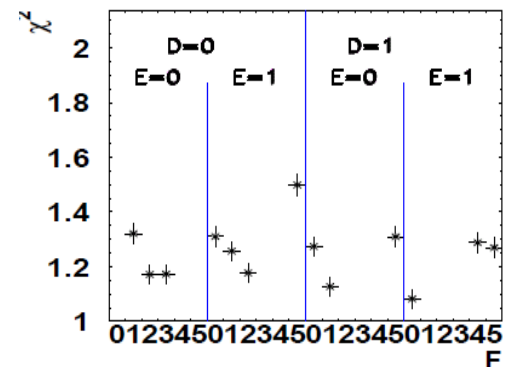
UrQMD Simulation



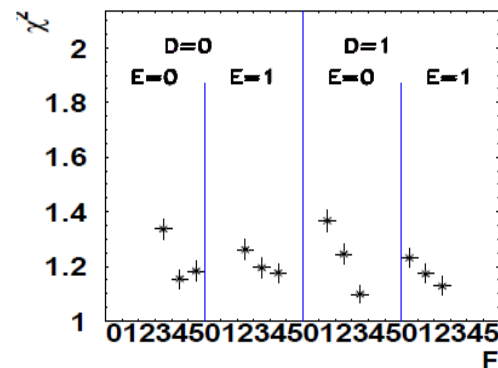
- $A =$ N^* (1875) waves enabled (1) / disabled (0)
 $B =$ N^* (1880) waves enabled (1) / disabled (0)
 $C =$ N^* (1895) waves enabled (1) / disabled (0)
 $D =$ N^* (1900) waves enabled (1) / disabled (0)
 $E =$ $pK^+\Lambda$ non resonant waves enabled (1) / disabled (0)
 $F = 5$ Initial proton states: $^1S_0, ^1D_2, ^3P_0, ^3P_1, ^3P_2, ^3F_3$
 $= 4$ Initial proton states: $^1S_0, ^1D_2, ^3P_0, ^3P_1, ^3P_2$
 $= 3$ Initial proton states: $^1S_0, ^1D_2, ^3P_0, ^3P_1$
 $= 2$ Initial proton states: $^1S_0, ^1D_2, ^3P_0$
 $= 1$ Initial proton states: $^1S_0, ^1D_2$
 $= 0$ Initial proton states: 1S_0



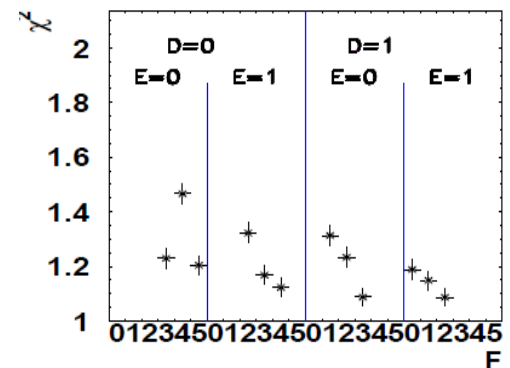
(a)



(b)

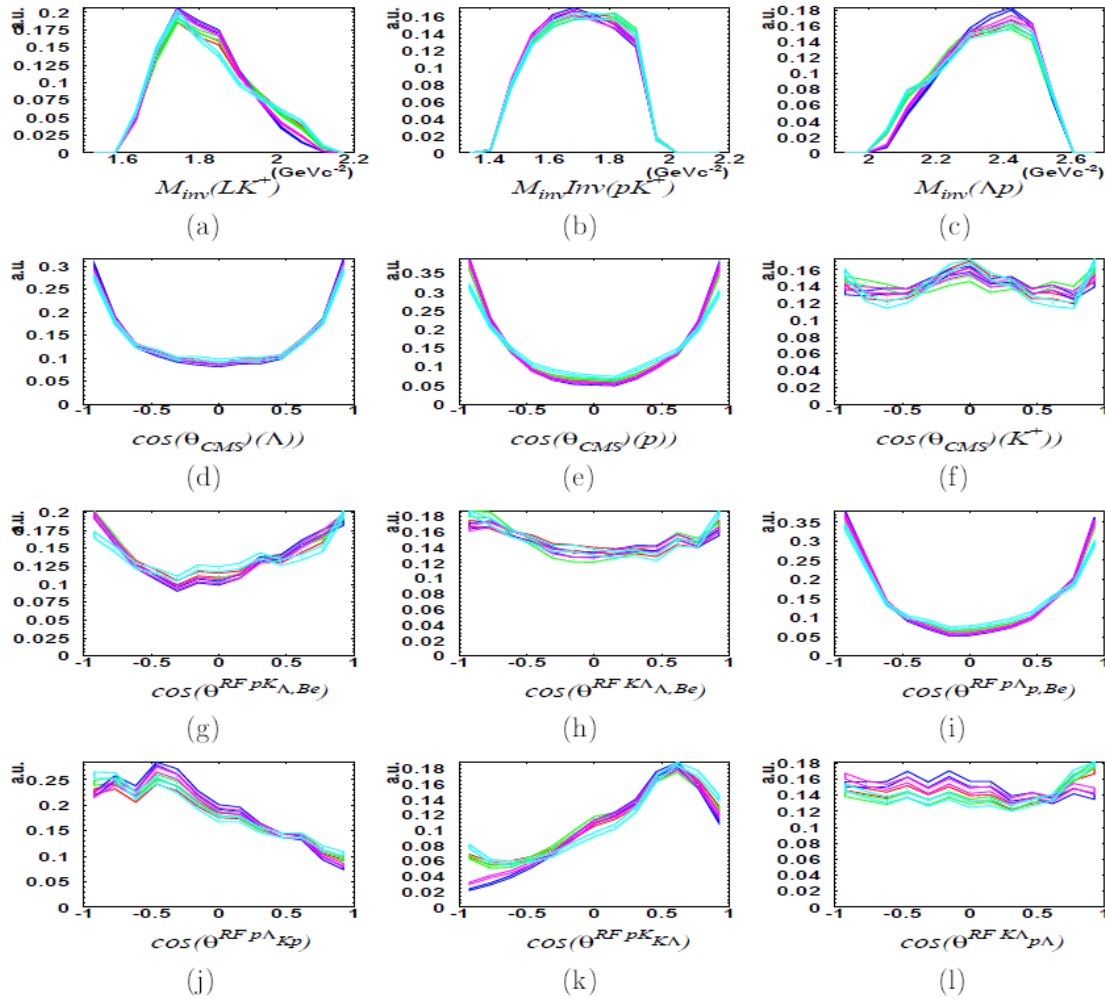


(c)



(d)

PWA Results in 4π



ppK⁻ Upper Limit Determination

Exclusion limit:

$$p_{\mu} > \alpha (1 - p_0)$$

$$p_{\mu} = \int_{\chi^2_{\text{signal}}}^{\infty} f_{\nu}(\chi^2) d\chi^2$$

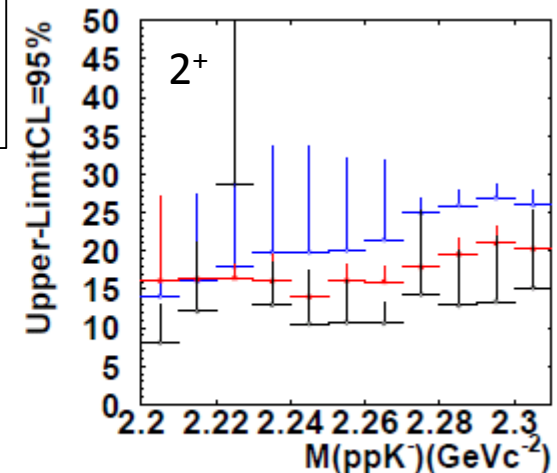
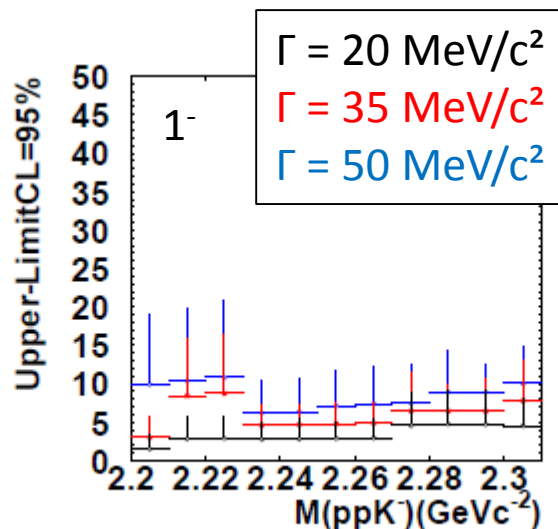
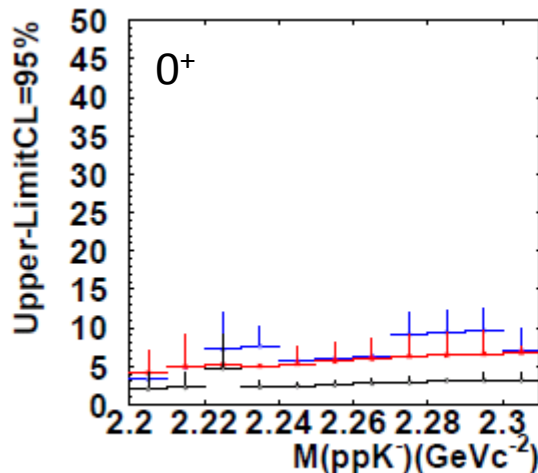
Scan of different mass and width

$$M(\text{ppK}^-) = 2.205\text{-}2.305 \text{ GeV}/c^2$$

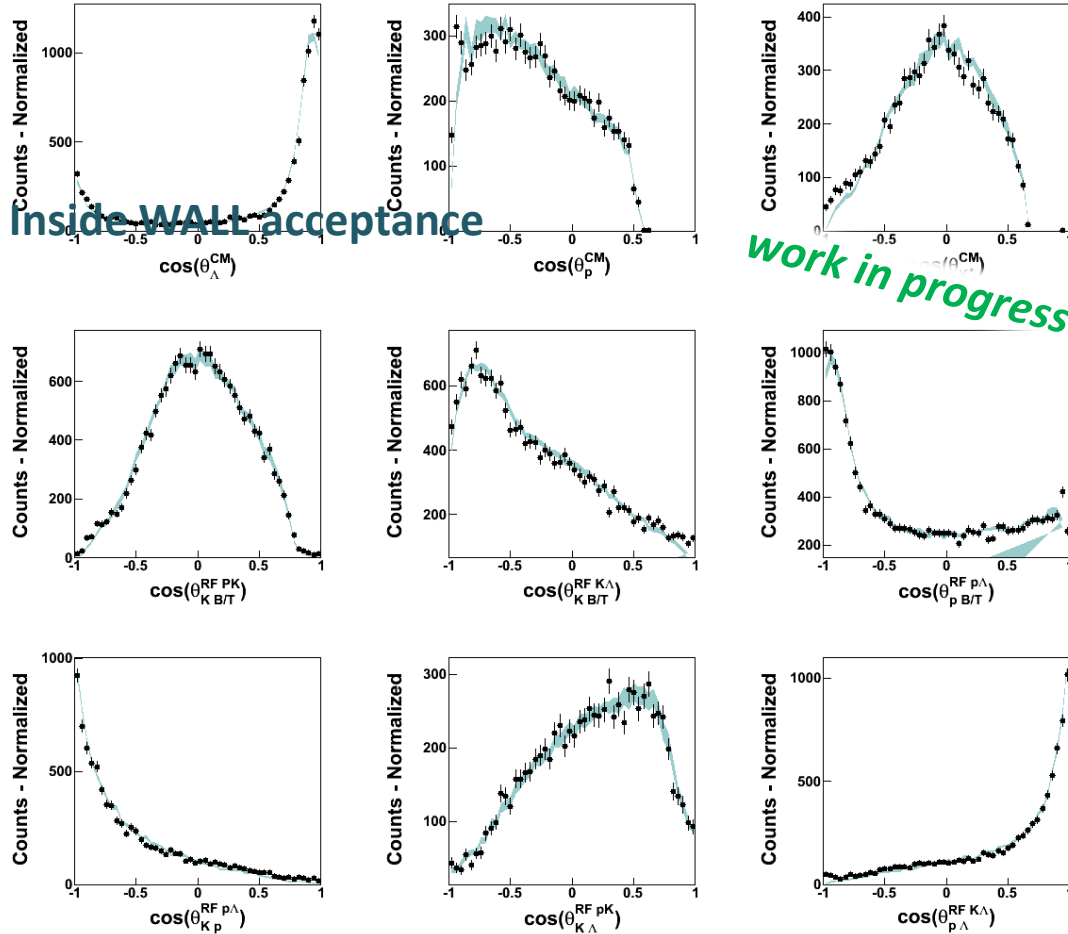
$$\Gamma(\text{ppK}^-) = 20\text{-}80 \text{ MeV}/c^2$$

And 5 best solution of PWA w/o ppK⁻

Background Solution: 000113



Hades Wall Data



Inside WALL acceptance

work in progress

Data
Systematic of
best PWA
solutions

Bonn-Gatchina PWA

Cross Section for the production of three particles out of a collision of two particle

$$d\sigma = \frac{(2\pi)^4 |A|^2}{4|k|\sqrt{s}} d\Phi_3(P, q_1, q_2, q_3), \quad P = k_1 + k_2$$

A - reaction amplitude

k – 3-momentum of the initial particle in the CM

s – $P^2 = (k_1 + k_2)^2$

$d\Phi_3(P, q_1, q_2, q_3)$ – invariant three-particles phase space

<http://pwa.hiskp.uni-bonn.de/>

A.V. Anisovich, V.V. Anisovich, E. Klempt,

V.A. Nikonov and A.V. Sarantsev

Eur. Phys. J. A 34, 129152 (2007)

The decomposition of the scattering amplitude into partial waves can be written as follows:

$$A = \sum A_{tr}^{\alpha}(s) Q_{\mu_1 \dots \mu_J}^{in}(SLJ) A_{2b}(i, S_2 L_2 J_2)(s_i) \times Q_{\mu_1 \dots \mu_J}^{fin}(i, S_2 L_2 J_2 S' L' J) . \quad (2)$$

S, L, J – spin, orbital mom. and total angular momentum of the pp system

S_2, L_2, J_2 – spin, orbital mom. and total angular momentum of the two particle system in fin. state

S', L' – spin, orbital mom. between the two particle system and the third particle with four mom. q_i

multiindex α – possible combinations of the $S, L, J, S_2, L_2, J_2, S', L'$ and i

$A_{tr}^{\alpha}(s)$ – transition Amplitude

$A_{2b}^{\alpha}(i, S_2, L_2, J_2)$ – rescattering process in the final two-particle channel (e.g. production of Δ)

Fitting Procedure

The transition Amplitude is parameterized as follows

$$A_{tr}^{\alpha}(s) = (a_1^{\alpha} + a_3^{\alpha} \sqrt{s}) e^{ia_2^{\alpha}}$$

This is a log-likelihood minimization on an event-by-event base

What we included to model the $PK^+\Lambda$ process:

N* Resonances in the PDG with measured decay into $K^+\Lambda$

Notation in PDG	Old notation	Mass [GeV/c ²]	Width [GeV/c ²]	$\Gamma_{\Lambda K}/\Gamma_{All}$ %
N(1650) $\frac{1}{2}^{-}$	N(1650)S ₁₁	1.655	0.150	3-11
N(1710) $\frac{1}{2}^{+}$	N(1710)P ₁₁	1.710	0.200	5-25
N(1720) $\frac{3}{2}^{+}$	N(1720)D ₁₃	1.720	0.250	1-15
N(1875) $\frac{3}{2}^{-}$	N(1875)D ₁₃	1.875	0.220	4 \pm 2
N(1880) $\frac{1}{2}^{+}$	N(1880)P ₁₁	1.870	0.235	2 \pm 1
N(1895) $\frac{1}{2}^{-}$	N(1895)S ₁₁	1.895	0.090	18 \pm 5
N(1900) $\frac{3}{2}^{+}$	N(1900)P ₁₃	1.900	0.250	0-10

And the production of $pK^+\Lambda$ via non resonant waves

Systematic

N* content

No.	Combination
0	N(1650), N(1710), N(1720)
1	N(1650), N(1710), N(1720), N(1900)
2	N(1650), N(1710), N(1720), N(1895)
3	N(1650), N(1710), N(1720), N(1880)
4	N(1650), N(1710), N(1720), N(1875)
5	N(1650), N(1710), N(1720), N(1900), N(1880)
6	N(1650), N(1710), N(1720), N(1900), N(1895)
7	N(1650), N(1710), N(1720), N(1900), N(1875)
8	N(1650), N(1710), N(1720), N(1895), N(1880)
9	N(1650), N(1710), N(1720), N(1895), N(1875)
10	N(1650), N(1710), N(1720), N(1880), N(1875)

non-resonant content

No.	Combination
0	no non-resonant waves
1	$(pL)(^1S_0) - K$
2	previous wave + $(pL)(^3S_1) - K$
3	previous waves + $(pL)(^1P_1) - K$
4	previous waves + $(pL)(^3P_0) - K$
5	previous waves + $(pL)(^3P_1) - K$
6	previous waves + $(pL)(^3P_2) - K$
7	previous waves + $(pL)(^1D_2) - K$
8	previous waves + $(pL)(^3D_1) - K$
9	previous waves + $(pL)(^3D_2) - K$

	No. of N* combination	No. of non-res. waves	Log-likelih.
Best Solutions	0	7	-2415.74
	1	8	-2708.49
	2	8	-2524.59
	3	8	-2712.49
	4	4	-2671.05
	5	8	-2310.4
	6	9	-2754.37
	7	8	-2657.77
	8	8	-2734.97
	9	6	-2698.86
	10	4	-2642.58

Solution inside WALL acceptance

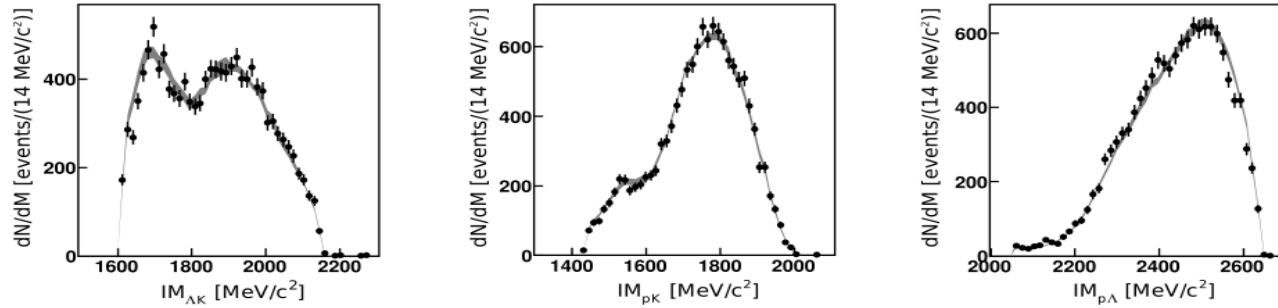


Figure 2.18: Two-particle masses for the **HADES data set** (black points) shown with the **four best PWA solutions** (gray band), obtained by a fit to the HADES and WALL data.

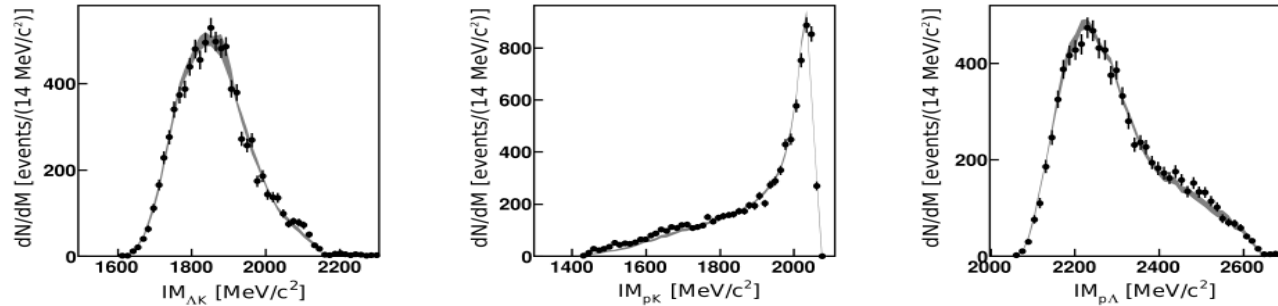
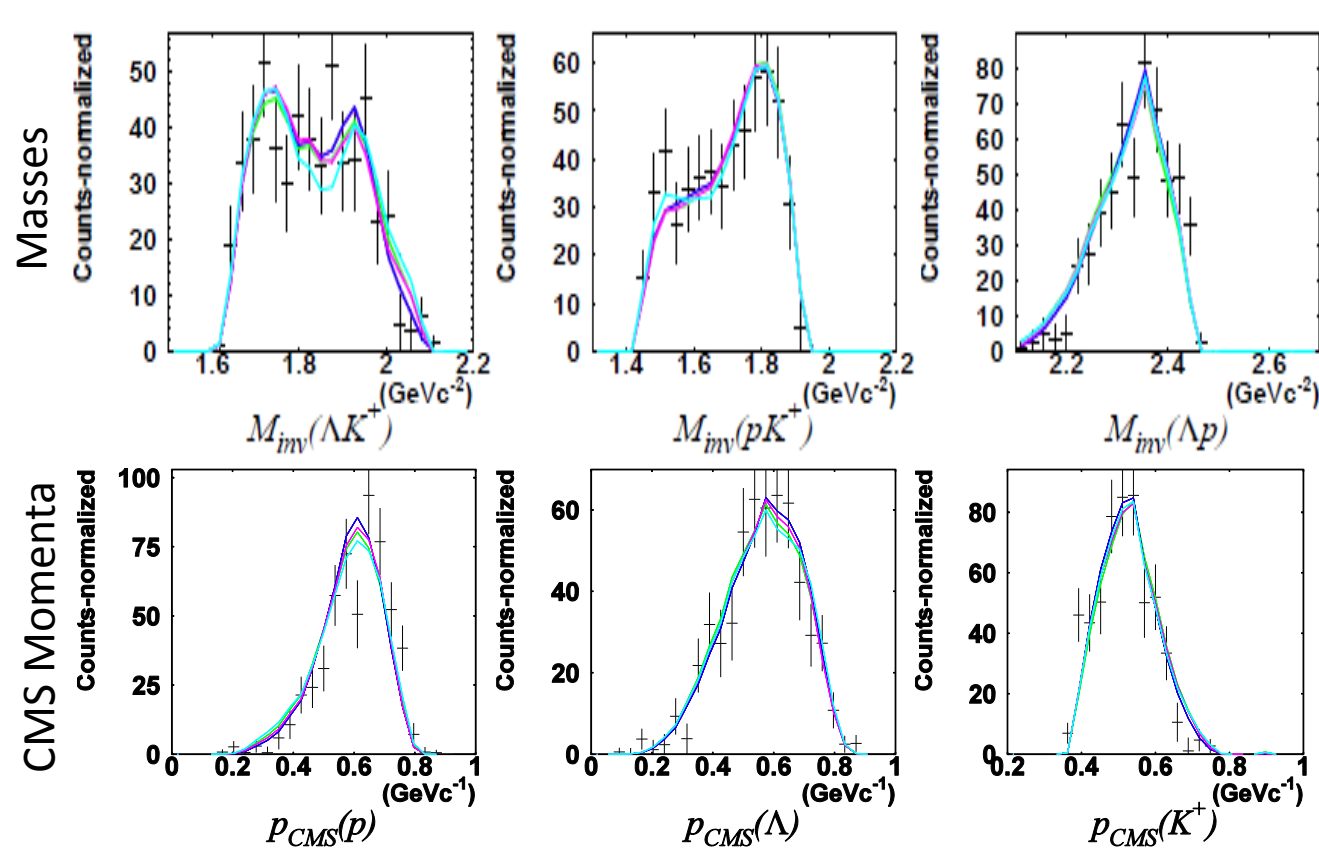


Figure 2.19: Two-particle masses for the **WALL data set** (black points) shown with the **four best PWA solutions** (gray band), obtained by a fit to the HADES and WALL data.

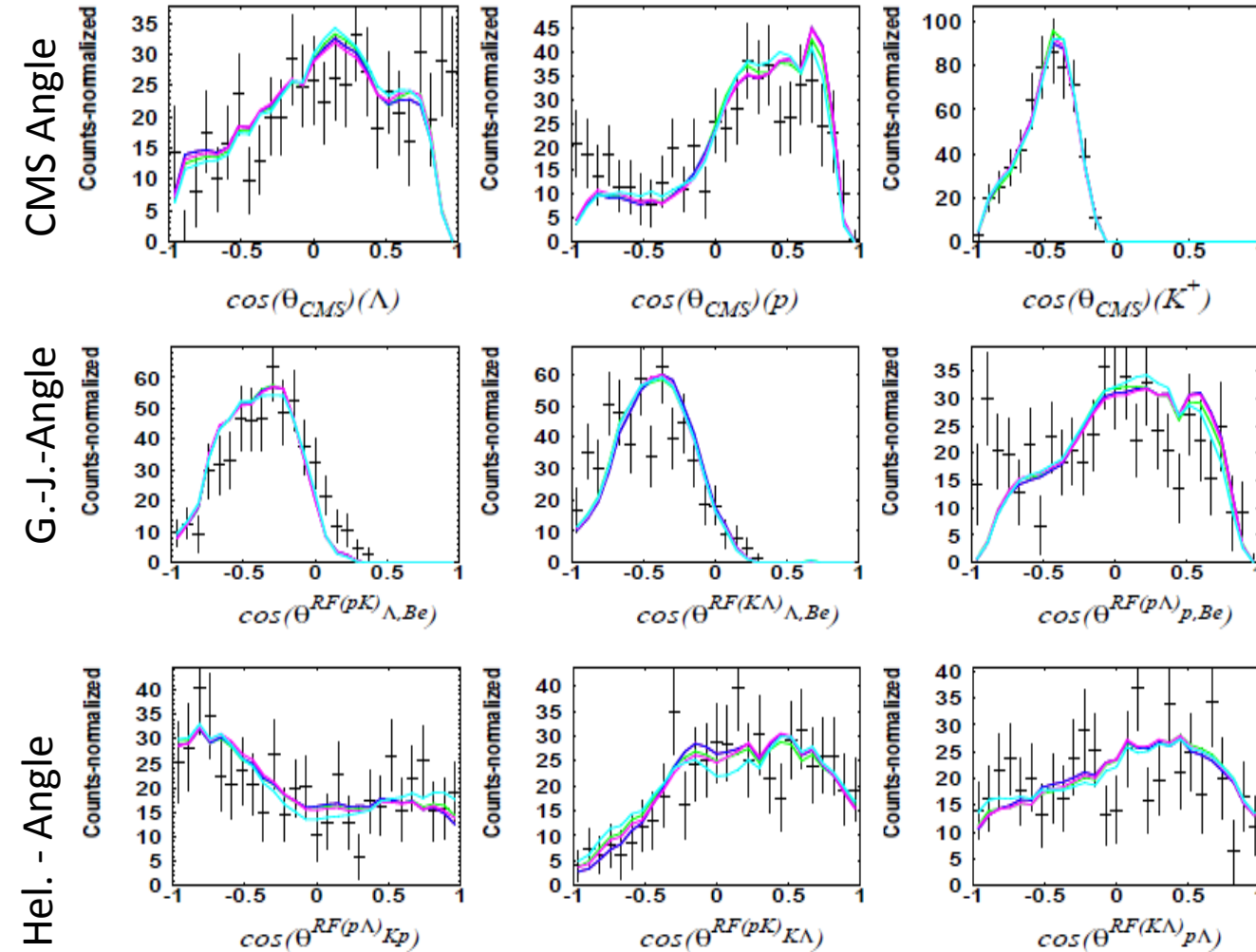
PWA Results



✚ Experimental Data

— Solution A
— Solution B
— Solution C
— Solution D
— Solution E

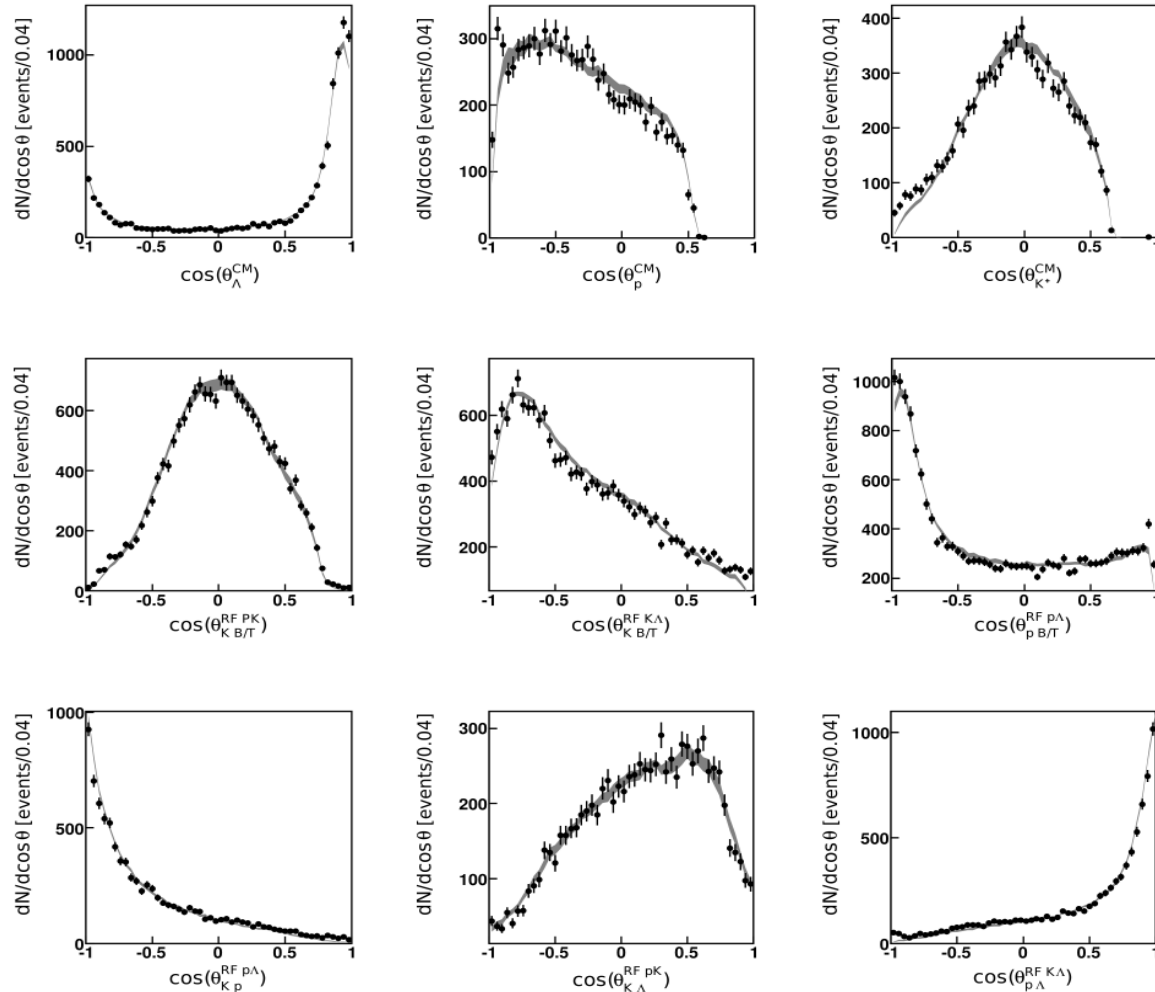
PWA Results



✦ Experimental Data

— Solution A
— Solution B
— Solution C
— Solution D
— Solution E

Solution inside WALL acceptance

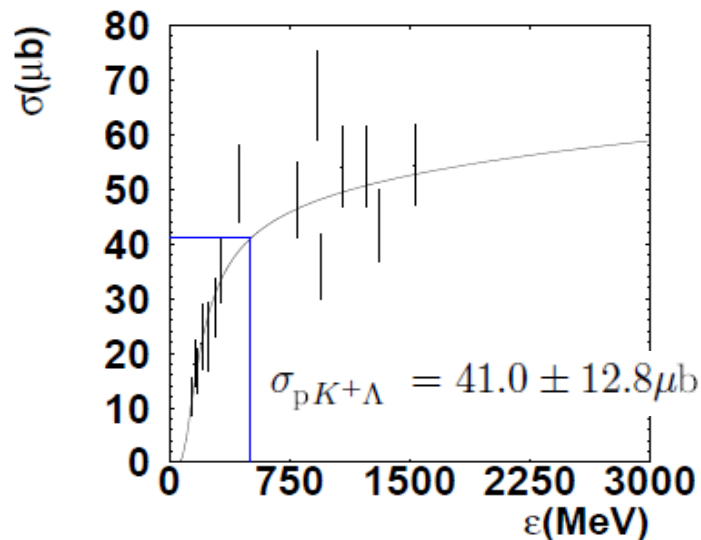


ppK⁻ Upper Limit

p + p → p + K⁺ + Λ
Total Cross Section

Upper Limit Cross Section

$$\sigma(\epsilon) = a \left(1 - \frac{s_0}{(\sqrt{s_0} + \epsilon)^2} \right)^b \left(\frac{s_0}{(\sqrt{s_0} + \epsilon)^2} \right)^c$$



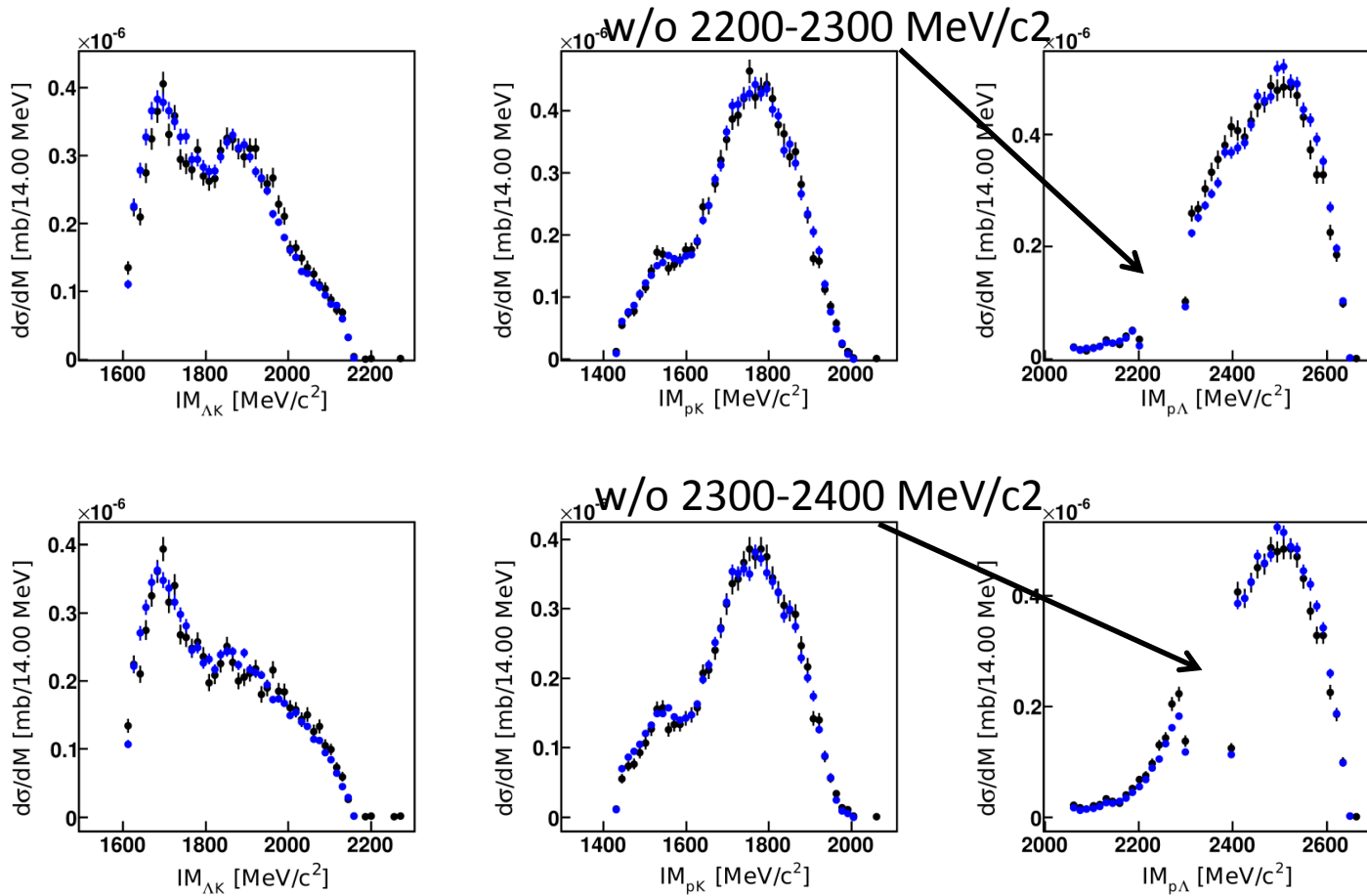
S. Abd El-Samad et al. Phys.Lett B688 (2010)
 S. Abd El-Samad et al. Phys.Lett B632 (2007)
 M. Abdel-Bary et al., Eur.Phys.J A46 (2010)
 S. Abd El-Samad et al., Eur.Phys.J A49 (2013)
 K.Fuchs et al., Springer Verlag 1985

Γ (MeVc ⁻²)	Cross Section (μb)
20	$7.6 \pm 1.2^{-3.5} - 22.4 \pm 3.6^{-10.7}$
35	$6.3 \pm 1.7^{-0.6} - 9.5 \pm 2.6^{-0.9}$
50	$10.2 \pm 1.8^{-4.5} - 11.6 \pm 3.4^{-0.6}$
60	$11.2 \pm 1.9^{-5.0} - 33.8 \pm 5.2^{-16.9}$
80	$11.4 \pm 2.7^{-3.8} - 35.9 \pm 5.7^{-17.4}$

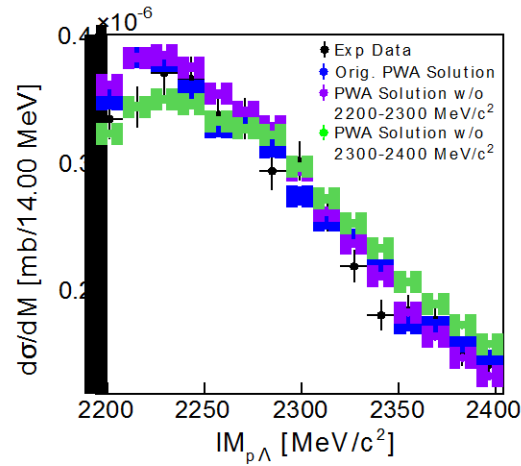
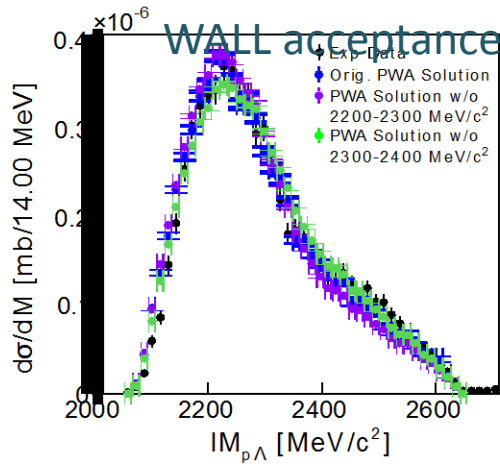
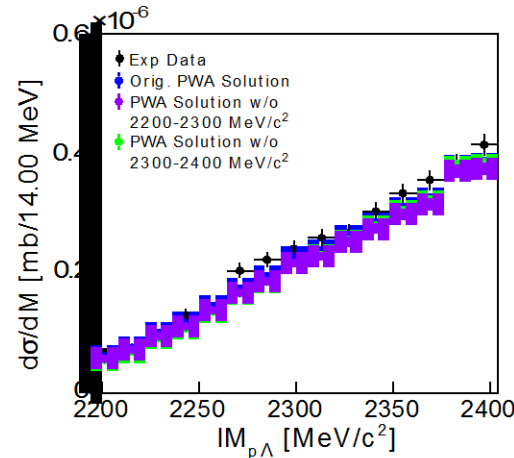
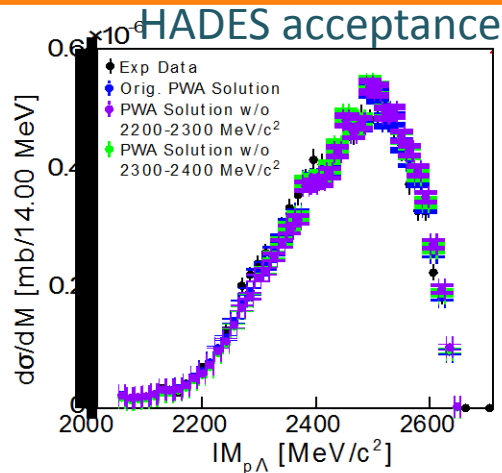
High production cross section
even though no peak is visible

Peak structure suppressed
due to interference

Cross Check

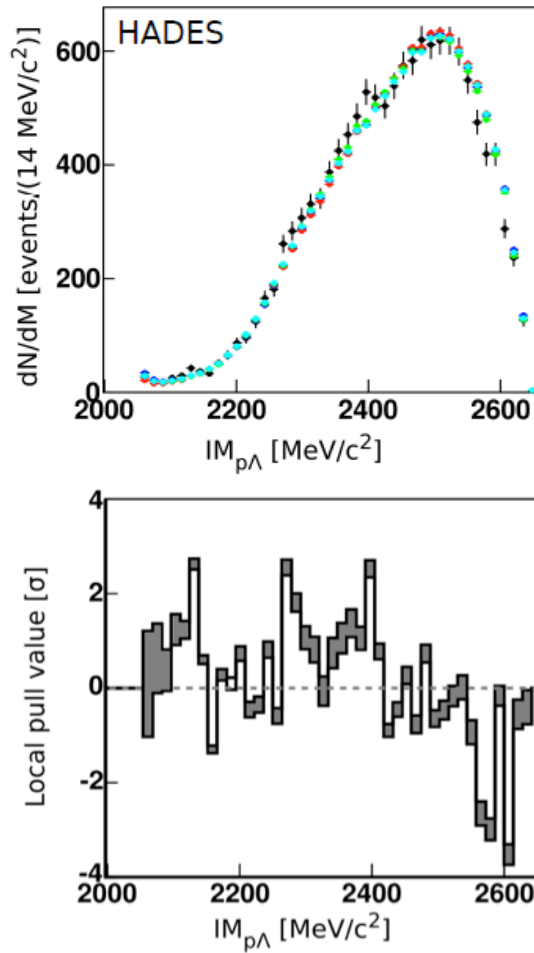


Cross Check



Good consistency among the results.
The solution is not biased by a possible signal in the excluded mass range

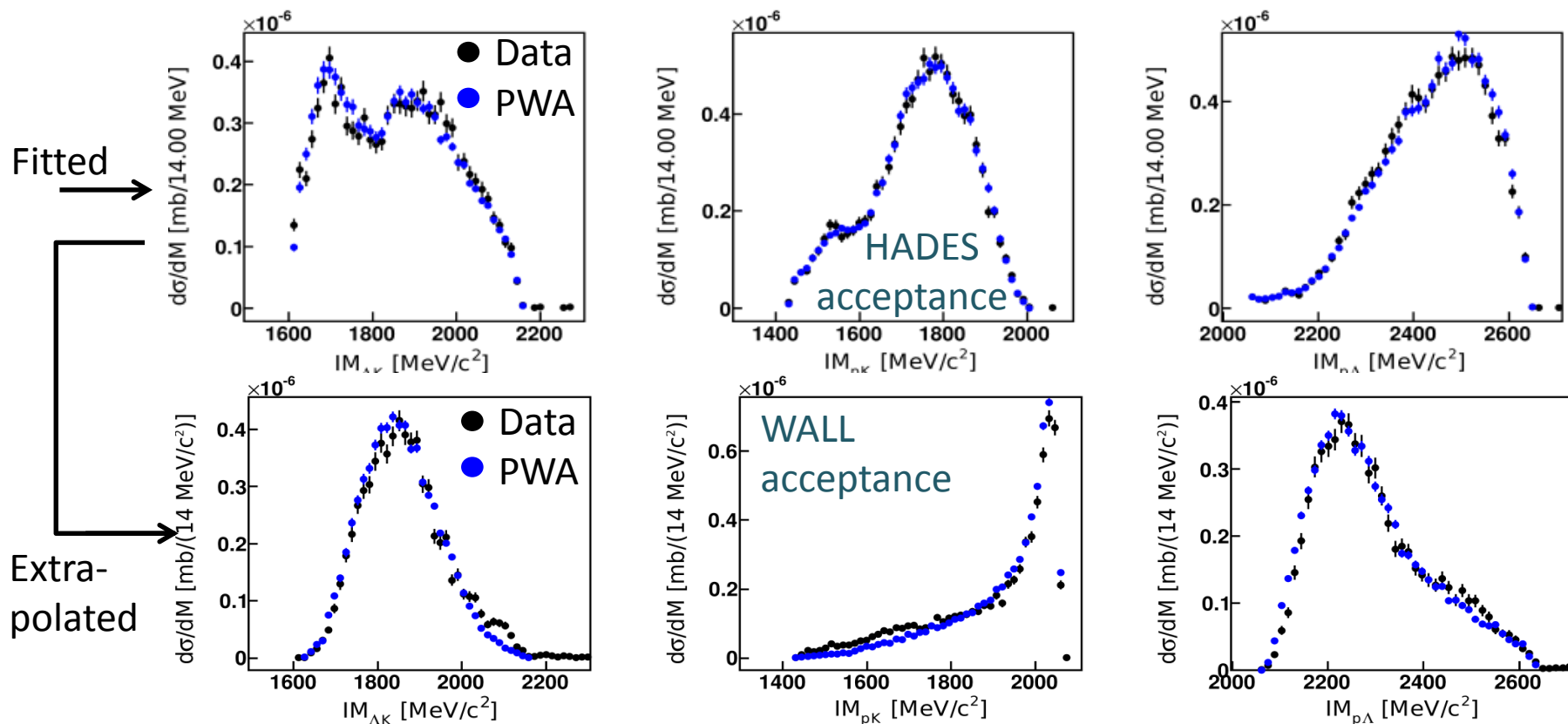
Result



$$pull = \sum_{i=1}^{N_b} \frac{(m_i - \lambda_i)}{\lambda_i}$$

m_i are the number of measured events in the bin i
 λ_i number of expected events in the bin according to the model
 N_b is the number of bins

The best solution



Included resonances:

Non-resonant waves:

$N(1650)$, $N(1710)$, $N(1720)$, $N(1900)$, $N(1895)$

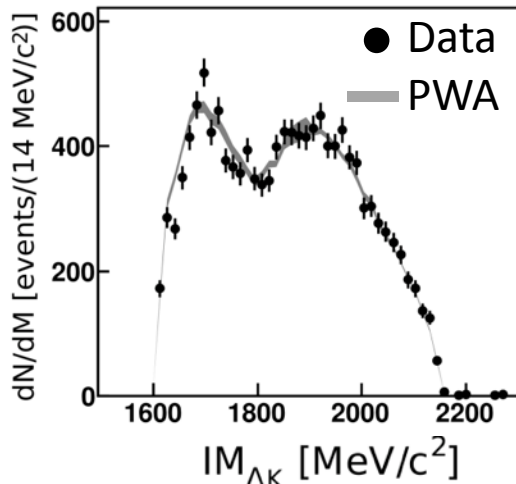
$(pL)(^1S_0) - K$ $(pL)(^3S_1) - K$ $(pL)(^1P_1) - K$

$(pL)(^3P_0) - K$ $(pL)(^3P_2) - K$ $(pL)(^3P_1) - K$

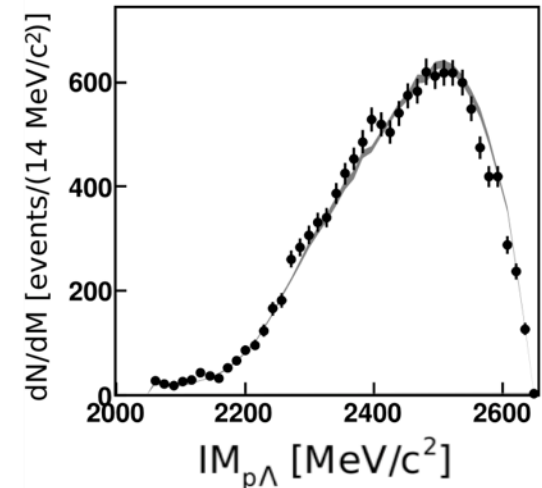
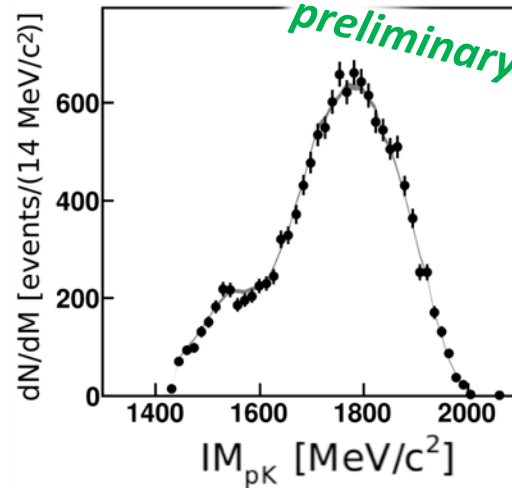
$(pL)(^3D_1) - K$ $(pL)(^1D_2) - K$ $(pL)(^3D_2) - K$

Four Best PWA Solutions

Inside HADES acceptance



Measured data
PWA solutions

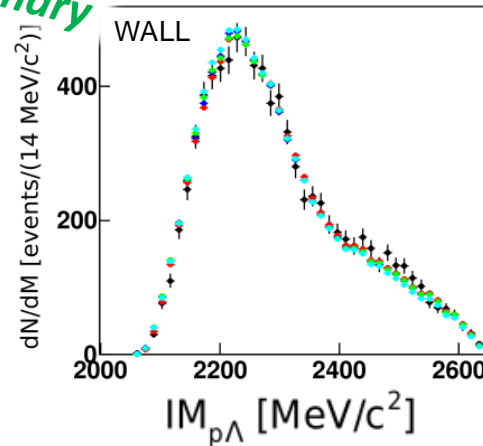
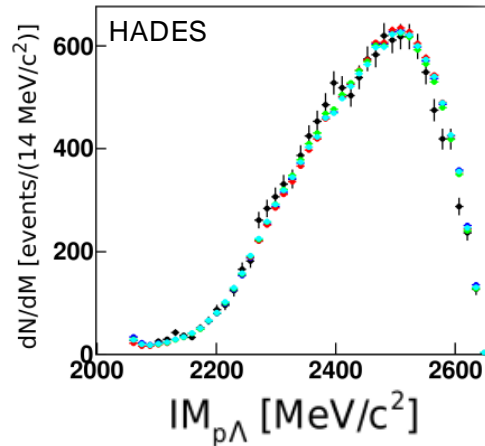


Name	N* combination
1/8	N(1650), N(1710), N(1720), N(1900)
3/8	N(1650), N(1710), N(1720), N(1880)
6/9	N(1650), N(1710), N(1720), N(1900), N(1895)
8/8	N(1650), N(1710), N(1720), N(1895), N(1880)

Test of the Null Hypothesis

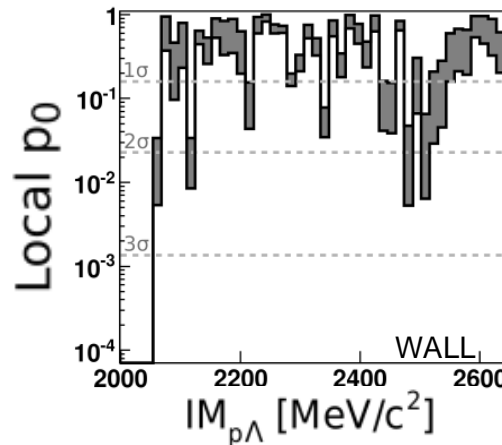
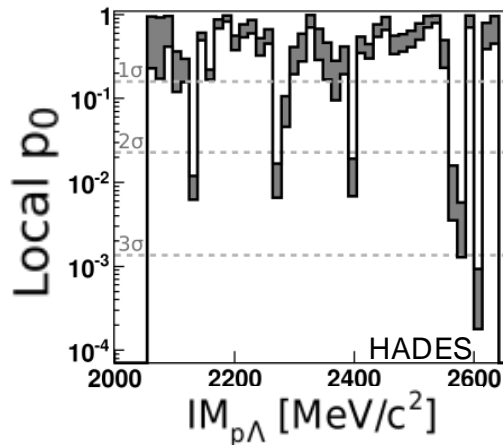
Test of the Null Hypothesis

preliminary



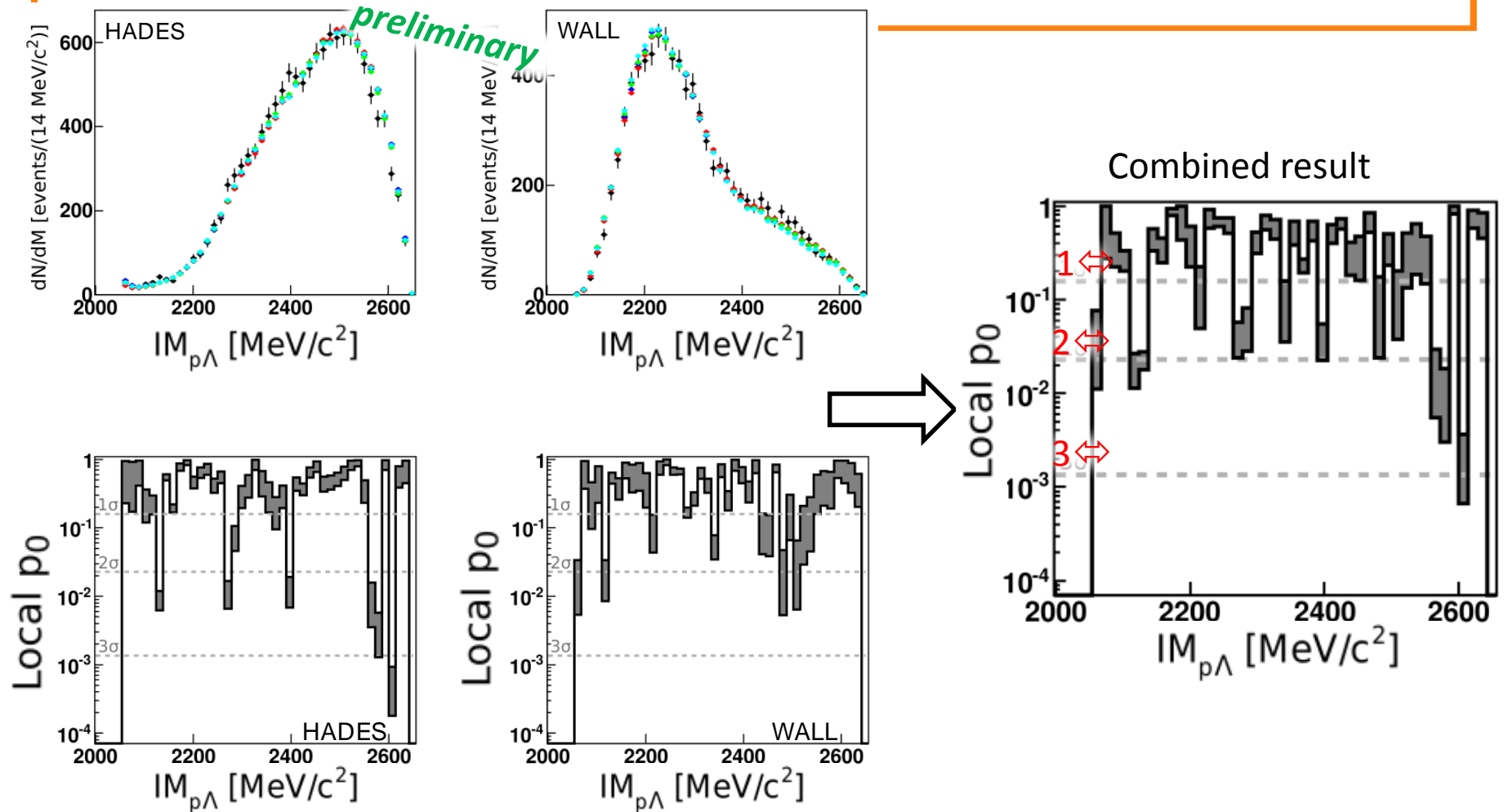
$$\chi_P^2 = \frac{(m_i - \lambda_i)^2}{\lambda_i}$$

$$p - value = \int_{\chi_{P,d}^2}^{\infty} P(\chi^2, Ndf) d\chi^2$$

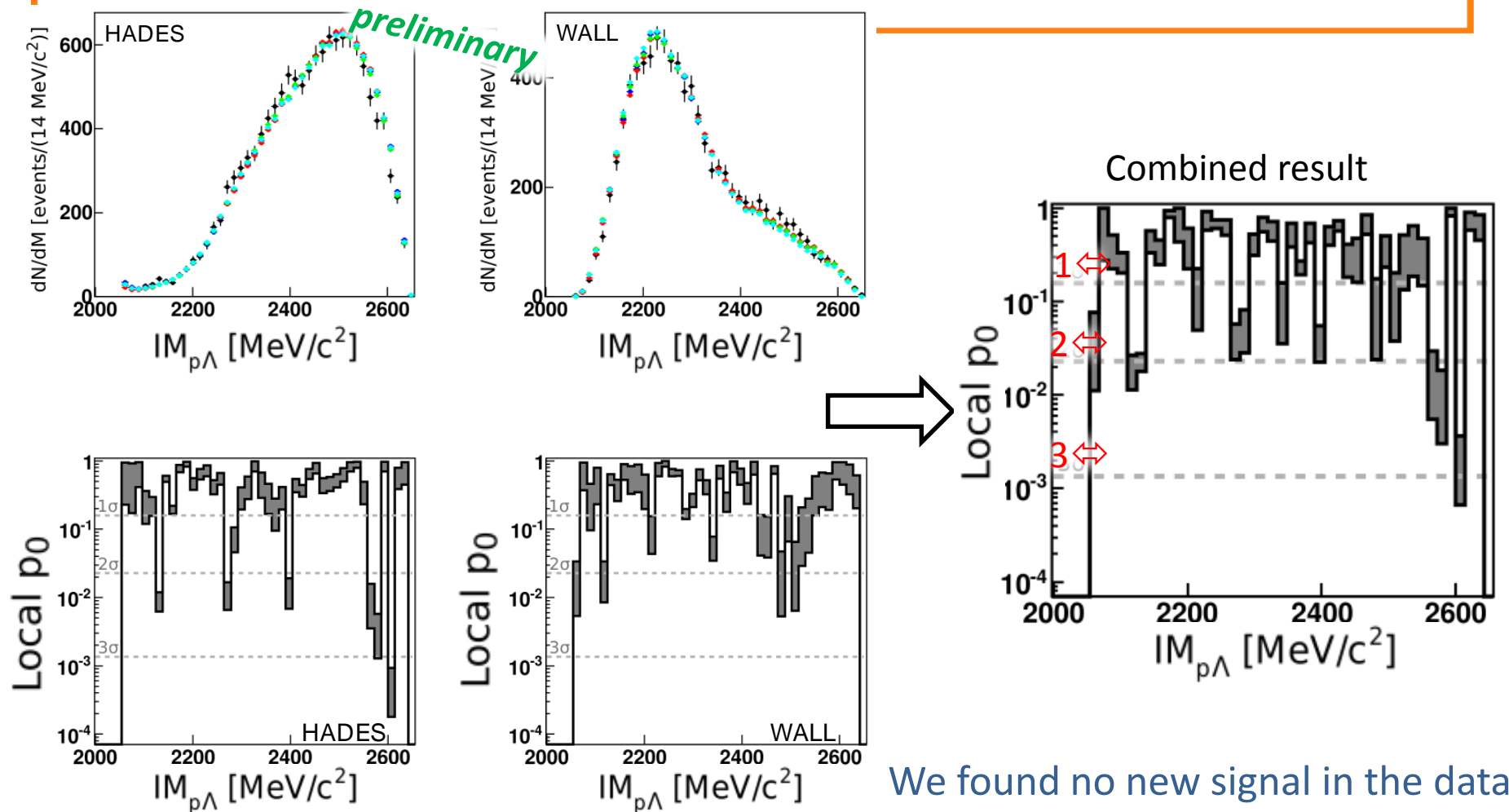


m_i measured events in bin i
 λ_i expected events in bin i
 according to the model

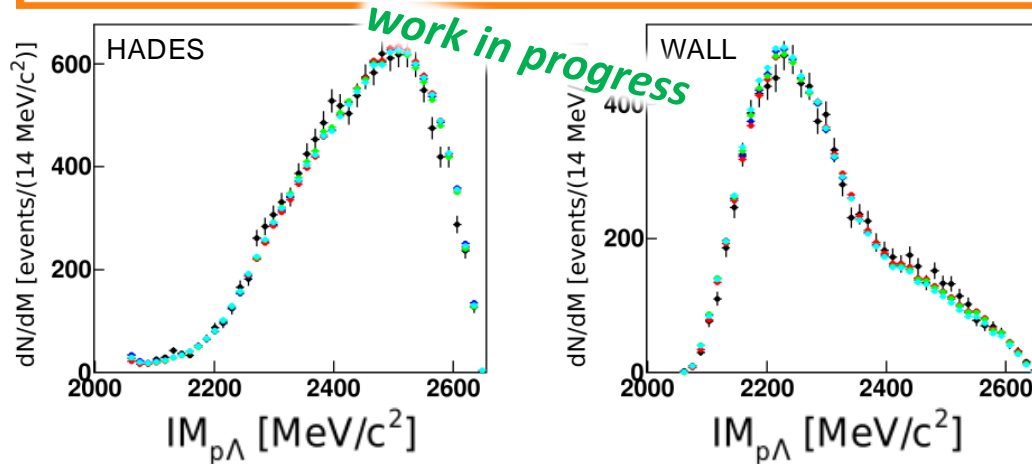
Test of the Null Hypothesis



• Test of the Null Hypothesis

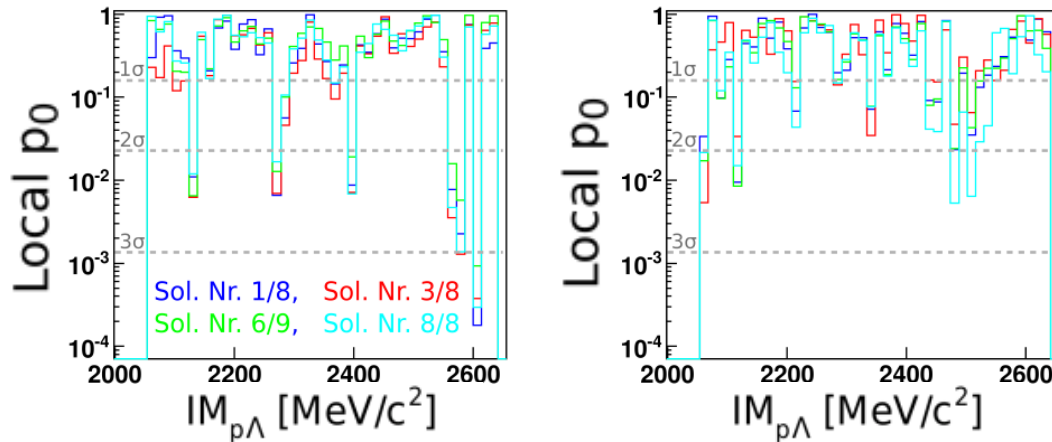


Test of the Null Hypothesis



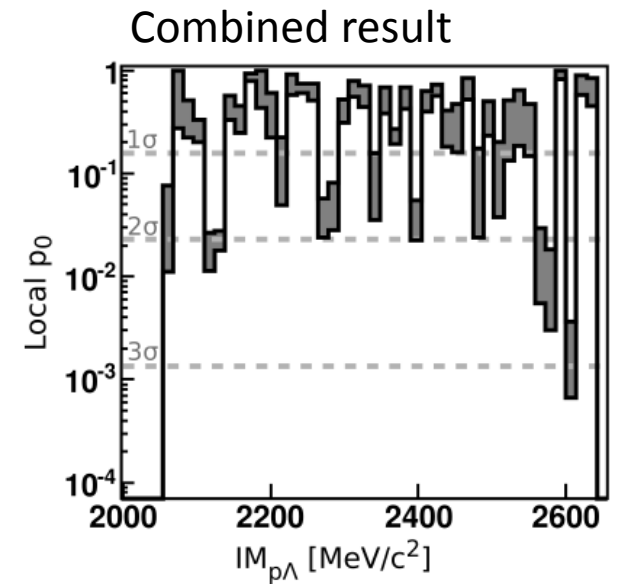
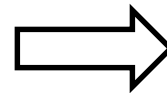
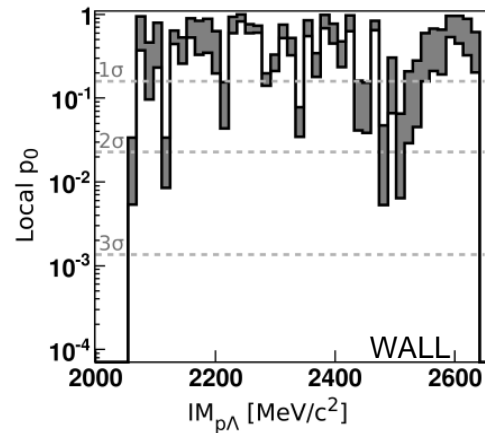
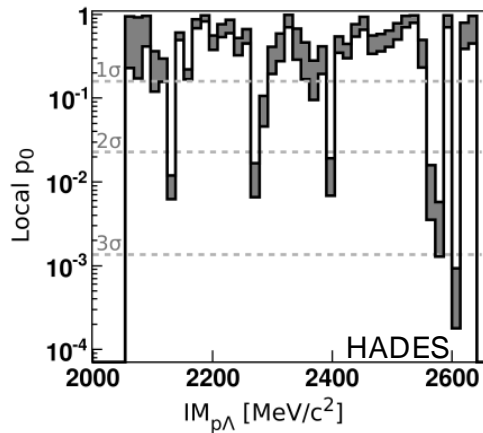
$$\chi_P^2 = \frac{(m - \lambda)^2}{\lambda}$$

$$p - value = \int_{\chi_{P,d}^2}^{\infty} P(\chi^2, Ndf) d\chi^2$$



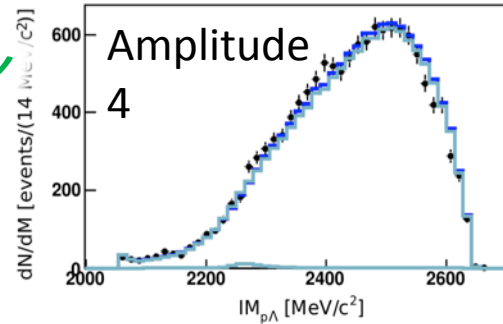
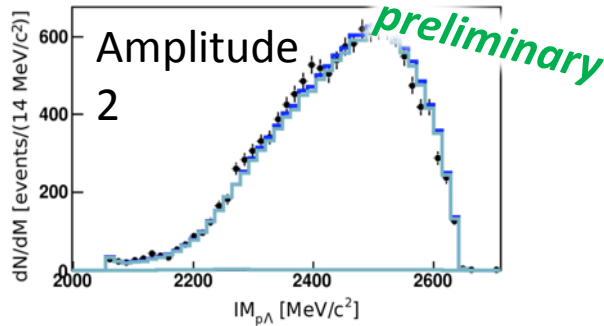
m_i measured events in bin i
 λ_i expected events in bin i
 according to the model

$$\chi_P^2 = \frac{(m - \lambda)^2}{\lambda} \Rightarrow \chi_P^2 = \sum_{i=1}^{N_b} \frac{(m_i - \lambda_i)^2}{\lambda_i}$$

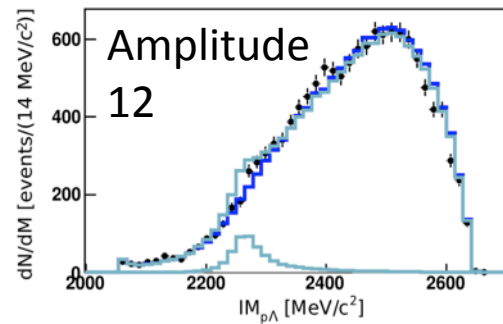
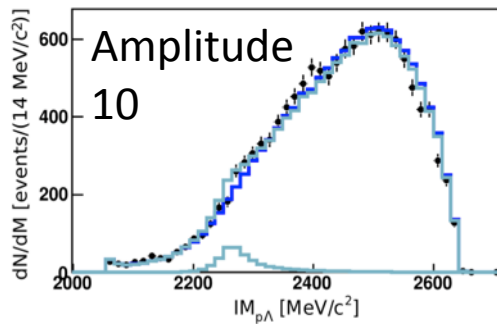
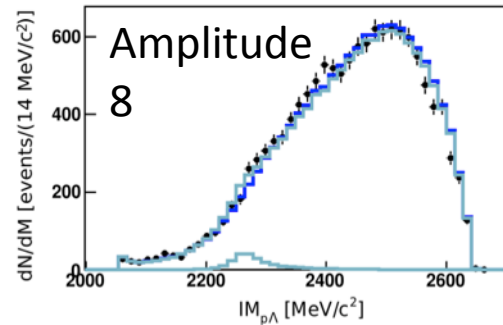
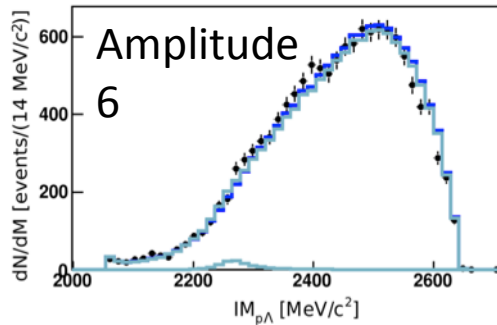


Test of the Signal Hypothesis

Inclusion of a new State

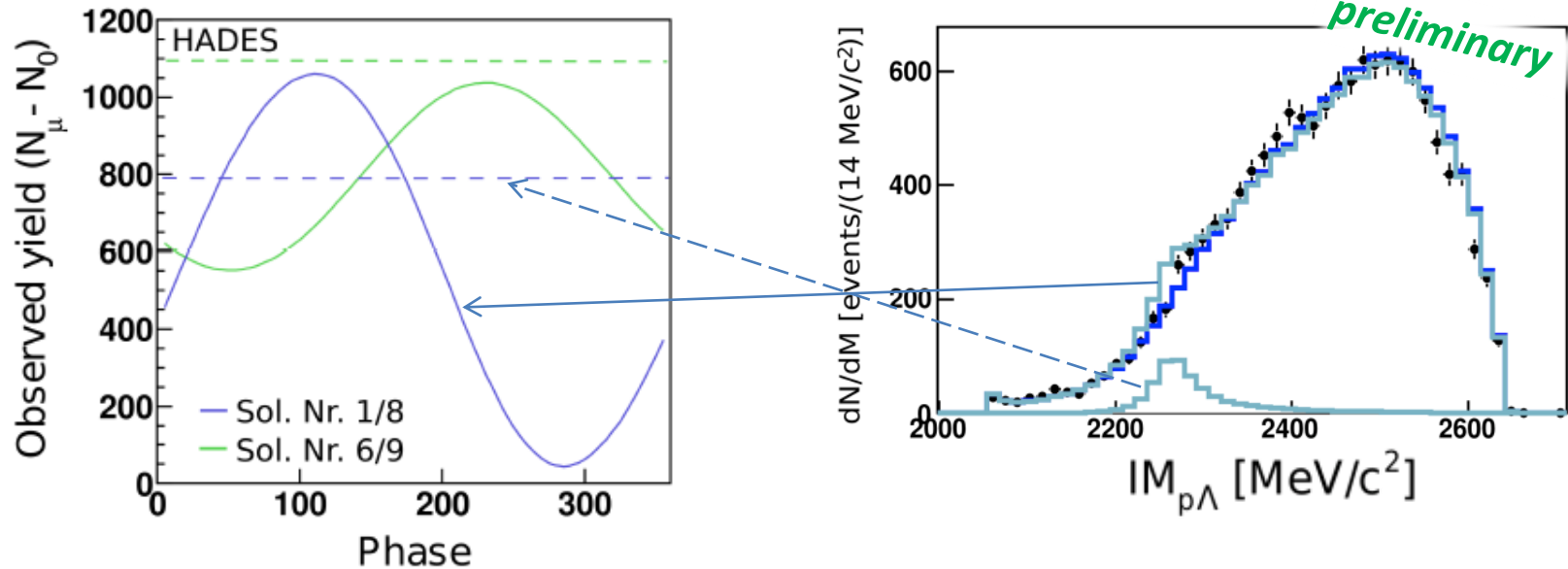


Data Points
Null Hypothesis
Hypothesis with ppK-



Feature of a PWA

... Interferences



The minimum has to be found
by the fit

Upper limit at CL_s 95%

These waves are included into the four best solutions of the PWA

$$^{2S+1}L$$

$$\text{WaveA: } 'p + p' \ ^1S_0 \rightarrow 'ppK(2250) - K' \ ^1S_0$$

$$\text{WaveB: } 'p + p' \ ^3P_1 \rightarrow 'ppK(2250) - K' \ ^1P_1$$

$$\text{WaveC: } 'p + p' \ ^1D_2 \rightarrow 'ppK(2250) - K' \ ^1D_2$$

Scanned masses:

2220 – 2370 MeV/c² (in steps of 10 MeV/c²)

Scanned widths:

30 MeV, 50 MeV, and 70 MeV

Thanks to the HADES Collaboration

Jörn Adamczewski-Musch, Geydar Agakishiev, Claudia Behnke, Alexander Belyaev, **Jia-Chii Berger-Chen**, Alberto Blanco, Christoph Blume, Michael Böhmer, Pablo Cabanelas, Nuno Carolino, Sergey Chernenko, Jose Díaz, Adrian Dybczak, **Eliane Eppe**, **Laura Fabbietti**, Oleg Fateev, Paulo Fonte, Jürgen Friese, Ingo Fröhlich, Tetyana Galatyuk, Juan A. Garzón, Roman Gernhäuser, Alejandro Gil, Marina Golubeva, Fedor Guber, Malgorzata Gumberidze, Szymon Harabasz, Klaus Heidelberg, Thorsten Heinz, Thierry Hennino, Romain Holzmann, Jochen Hutsch, Claudia Höhne, Alexander Ierusalimov, Alexander Ivashkin, Burkhard Kämpfer, Marcin Kajetanowicz, Tatiana Karavicheva, Vladimir Khomyakov, Ilse Koenig, Wolfgang Koenig, Burkhard W. Kolb, Vladimir Kolganov, Grzegorz Korcyl, Georgy Kornakov, Roland Kotte, Erik Krebs, Hubert Kuc, Wolfgang Kühn, Andrej Kugler, Alexei Kurepin, Alexei Kurilkin, Pavel Kurilkin, Vladimir Ladygin, **Rafal Lalik**, **Kirill Lapidus**, Alexander Lebedev, Ming Liu, Luís Lopes, Manuel Lorenz, Gennady Lykasov, Ludwig Maier, Alexander Malakhov, Alessio Mangiarotti, Jochen Markert, Volker Metag, Jan Michel, Christian Müntz, **Robert Münzer**, Lothar Naumann, Marek Palka, Vladimir Pechenov, Olga Pechenova, Americo Pereira, Jerzy Pietraszko, Witold Przygoda, Nicolay Rabin, Béatrice Ramstein, Andrei Reshetin, Laura Rehnisch, Philippe Rosier, Anar Rustamov, Alexander Sadovsky, Piotr Salabura, Timo Scheib, Alexander Schmah, Heidi Schuldes, Erwin Schwab, **Johannes Siebenson**, Vladimir Smolyankin, Manfred Sobiella, Yuri Sobolev, Stefano Spataro, Herbert Ströbele, Joachim Stroth, Christian Sturm, Khaled Teilab, Vladimir Tiflov, Pavel Tlusty, Michael Traxler, Alexander Troyan, Haralabos Tsertos, Evgeny Usenko, Taras Vasiliev, Vladimir Wagner, Christian Wendisch, Jörn Wüstenfeld, Yuri Zanevsky



References for the Calculations

- [AY02] Yoshinori Akaishi and Toshimitsu Yamazaki. Nuclear anti-K bound states in light nuclei. *Phys.Rev.*, C65:044005, 2002.
- [BGL12] N. Barnea, A. Gal, and E.Z. Liverts. Realistic calculations of $\bar{K}NN$, $\bar{K}NNN$, and $\bar{K}\bar{K}NN$ quasibound states. *Phys.Lett.*, B712:132–137, 2012.
- [BO12a] M. Bayar and E. Oset. $\bar{K}NN$ Absorption within the Framework of the Fixed Center Approximation to Faddeev equations. 2012.
- [BO12b] M. Bayar and E. Oset. Improved Fixed Center Approximation of the Faddeev equations for the $\bar{K}NN$ system with $S=0$. *Nucl.Phys.*, A883:57–68, 2012.
- [DHW08] Akinobu Dote, Tetsuo Hyodo, and Wolfram Weise. K^-pp system with chiral SU(3) effective interaction. *Nucl.Phys.*, A804:197–206, 2008.
- [DHW09] Akinobu Dote, Tetsuo Hyodo, and Wolfram Weise. Variational calculation of the ppK^- system based on chiral SU(3) dynamics. *Phys.Rev.*, C79:014003, 2009.
- [FIK⁺11] M. Faber, A.N. Ivanov, P. Kienle, J. Marton, and M. Pitschmann. Molecule model for kaonic nuclear cluster $\bar{K}NN$. *Int.J.Mod.Phys.*, E20:1477–1490, 2011.
- [IKS10] Yoichi Ikeda, Hiroyuki Kamano, and Toru Sato. Energy dependence of $\bar{K}N$ interactions and resonance pole of strange dibaryons. *Prog.Theor.Phys.*, 124:533–539, 2010.
- [IS07] Y. Ikeda and T. Sato. Strange dibaryon resonance in the $\bar{K}NN - \pi YN$ system. *Phys.Rev.*, C76:035203, 2007.
- [IS09] Yoichi Ikeda and Toru Sato. On the resonance energy of the $\bar{K}NN - \pi YN$ system. *Phys.Rev.*, C79:035201, 2009.
- [RS14] J. Revai and N.V. Shevchenko. Faddeev calculations of the $\bar{K}NN$ system with chirally-motivated $\bar{K}N$ interaction. II. The K^-pp quasi-bound state. 2014.
- [SGM07] N.V. Shevchenko, A. Gal, and J. Mares. Faddeev calculation of a K^-pp quasi-bound state. *Phys.Rev.Lett.*, 98:082301, 2007.
- [SGMR07] N.V. Shevchenko, A. Gal, J. Mares, and J. Revai. $\bar{K}NN$ quasi-bound state and the $\bar{K}N$ interaction: Coupled-channel Faddeev calculations of the $\bar{K}NN-\pi\Sigma N$ system. *Phys.Rev.*, C76:044004, 2007.
- [WG09] S. Wycech and A. M. Green. Variational calculations for \bar{K} -few-nucleon systems. *Phys. Rev. C*, 79:014001, 2009.
- [YA02] T. Yamazaki and Y. Akaishi. (K^-, π^-) production of nuclear \bar{K} bound states in proton-rich systems via Λ^* doorways. *Phys.Lett.*, B535:70–76, 2002.

N* resonances

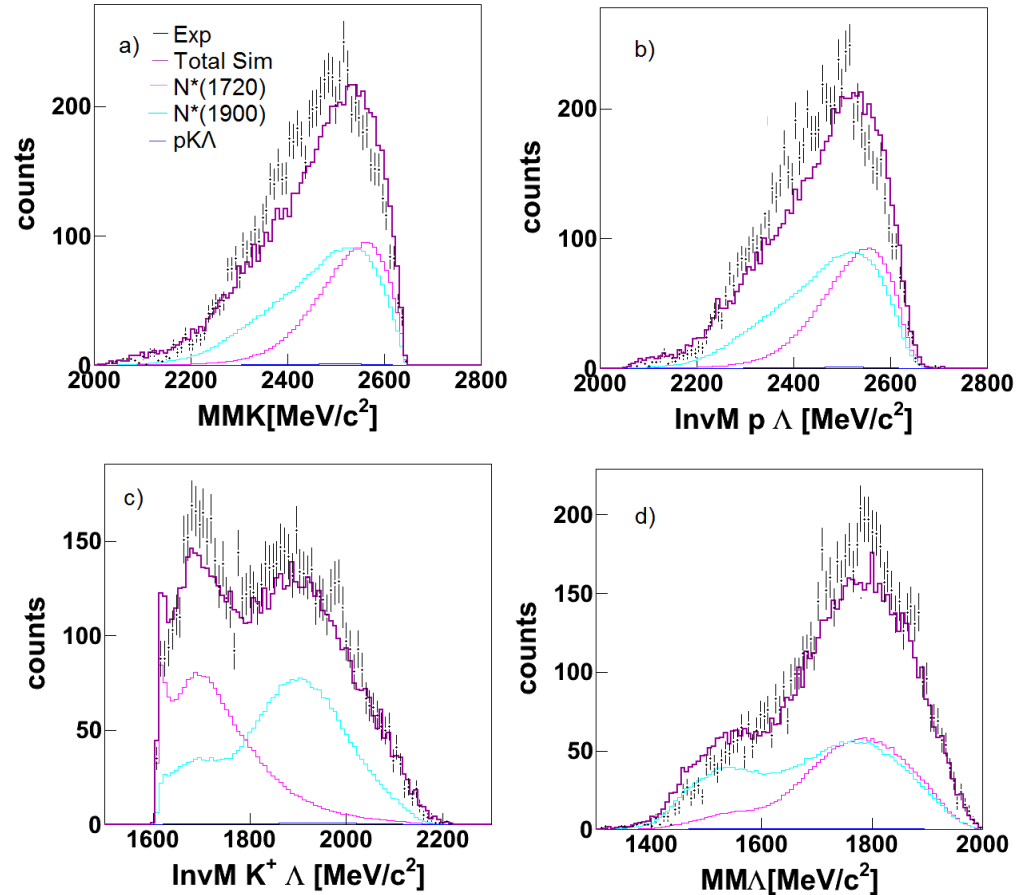
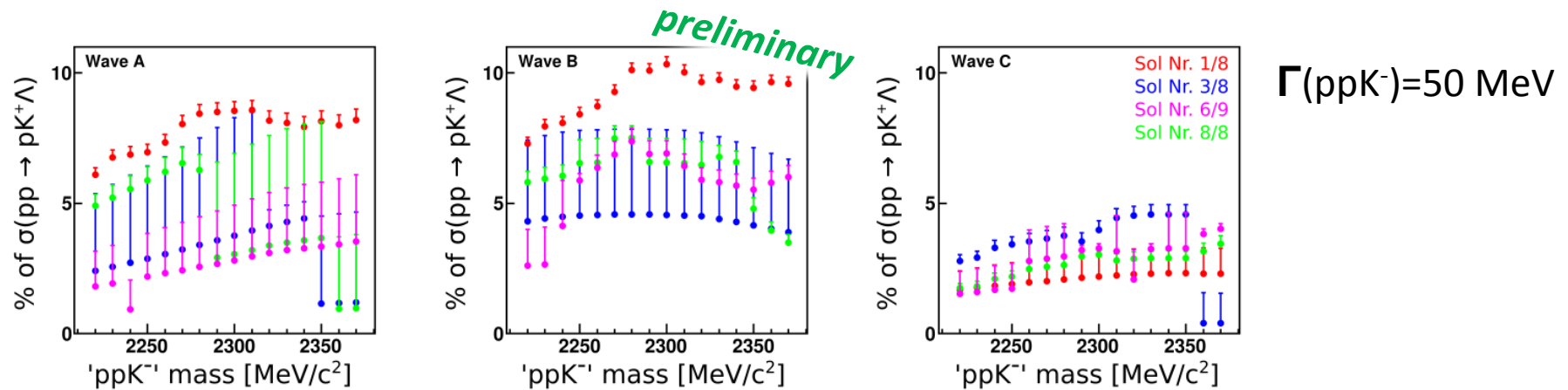


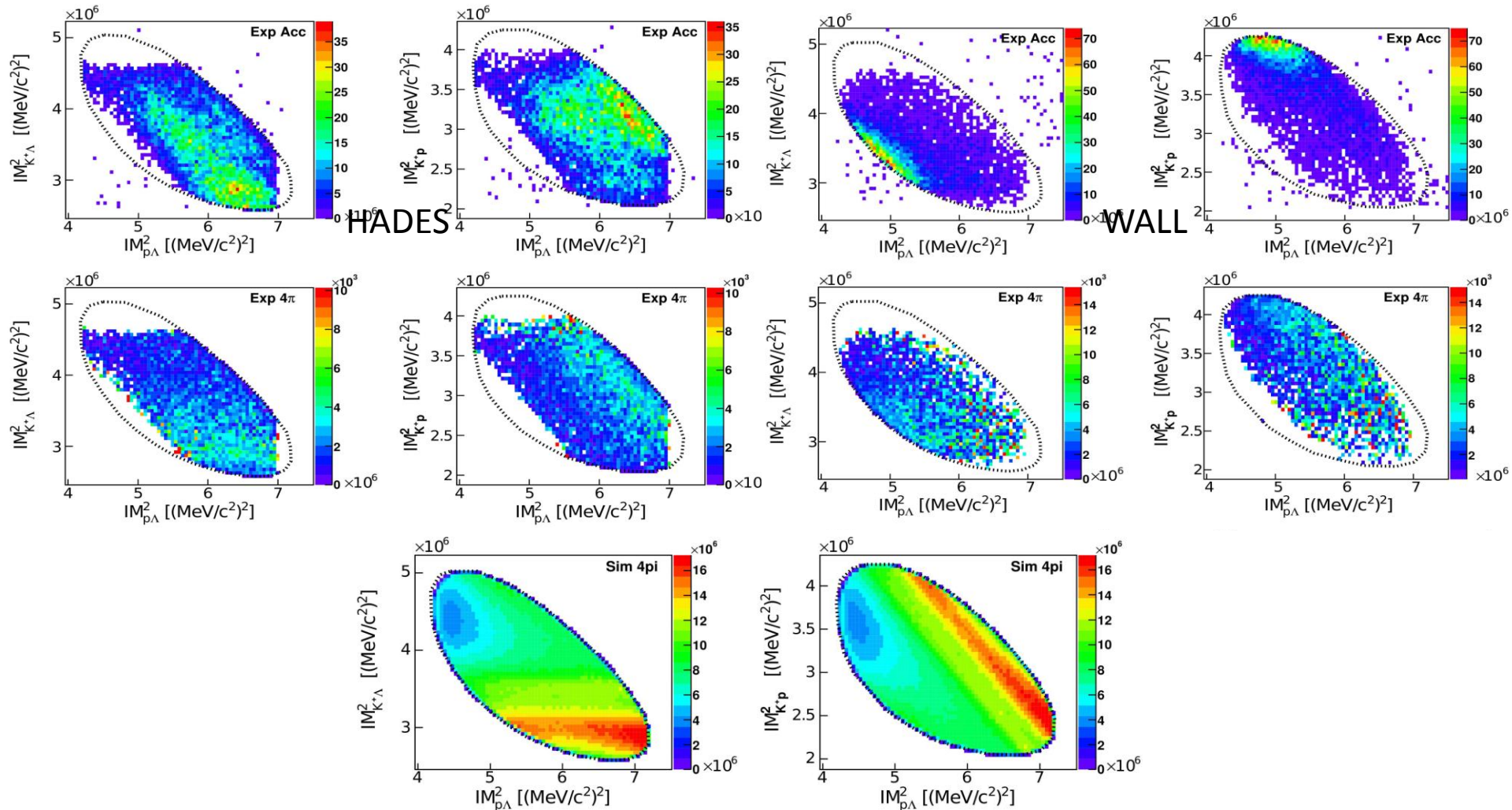
Figure 6.10: a) $IM_{K^+\Lambda}$, b) $IM_{p\Lambda}$, c) $MM_{K^+\Lambda}$ and d) MM_{Λ} fitted with the sum of the four N^{*+} -resonances from table 6.2 and the simulation of a direct $pK^+\Lambda$ production.

Master Thesis A. Solaguren-Beascoa Negre

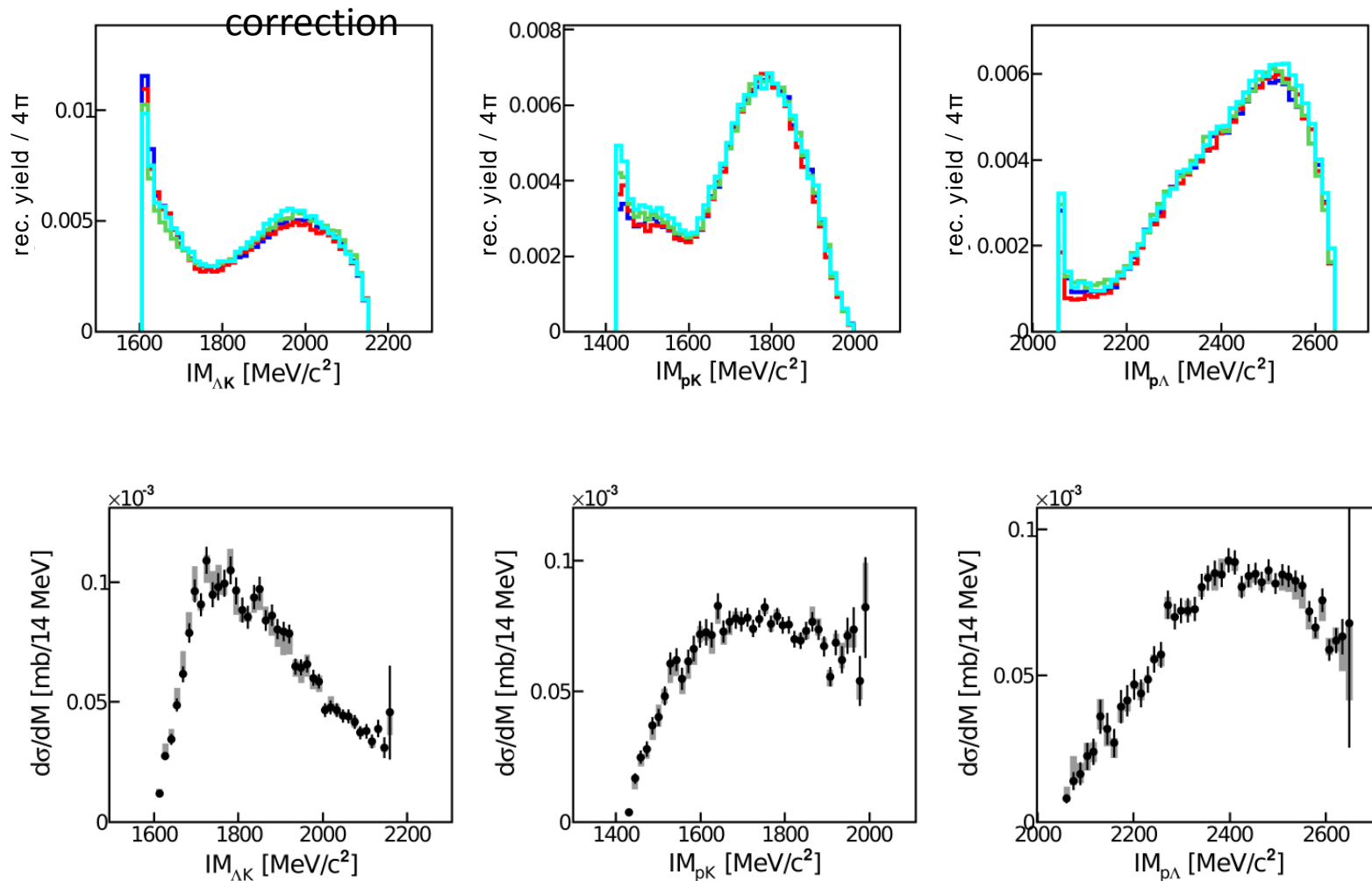
Upper Limit

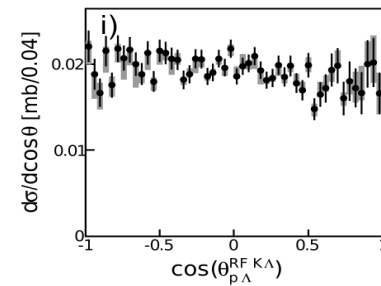
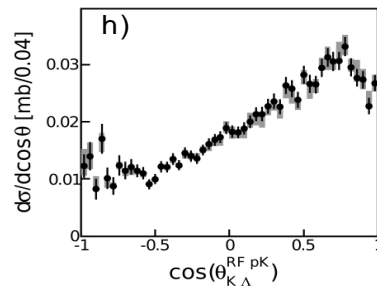
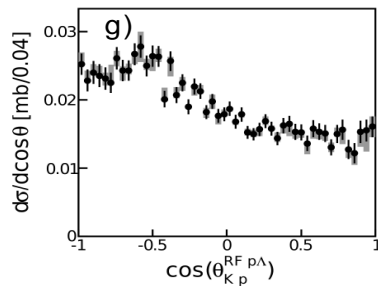
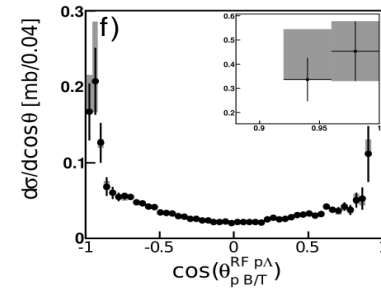
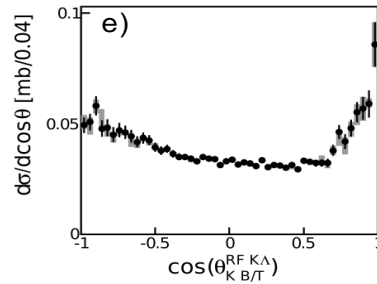
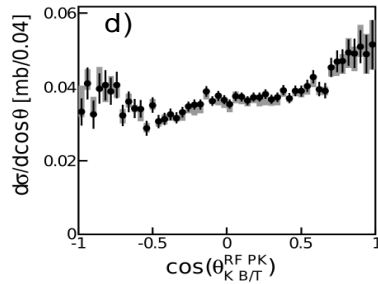
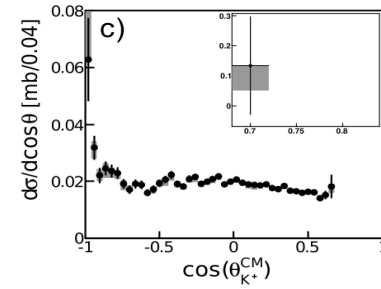
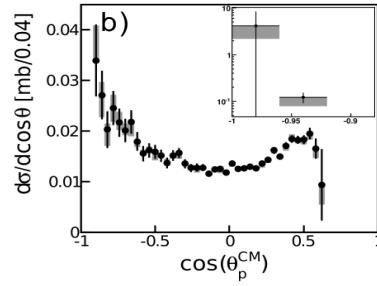
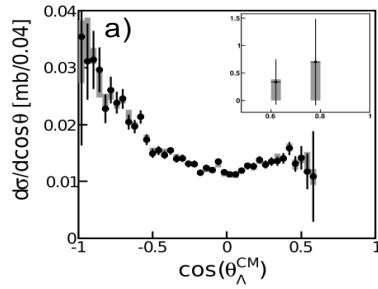


Dalitz Plots



Cross Section





Multi PWA

Combined Analysis of HADES and FOPI

4 Best HADES Solutions

HADES-only

1_8 ($s = -0.27 \cdot 10^4$)

8_8 ($s = -0.27 \cdot 10^4$)

3_8 ($s = -0.27 \cdot 10^4$)

6_9 ($s = -0.27 \cdot 10^4$)



4 Best HADES Solutions

HADES+FOPI

1_8 ($s = -0.83 \cdot 10^5$)

8_8 ($s = -0.82 \cdot 10^5$)

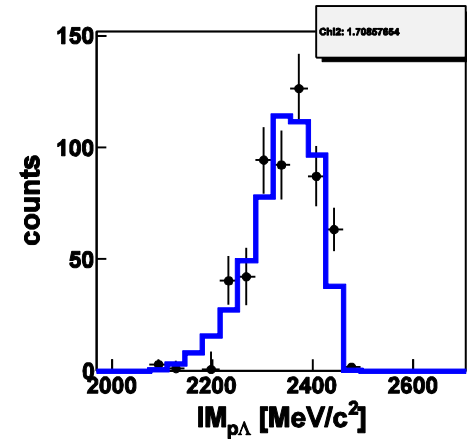
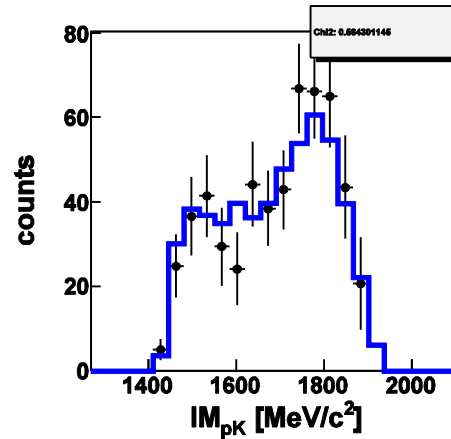
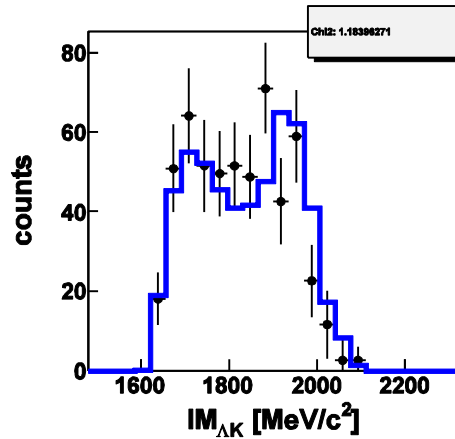
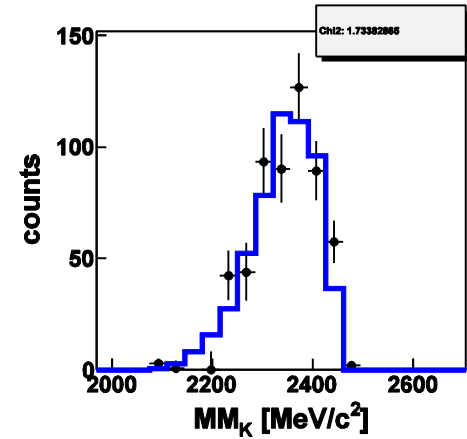
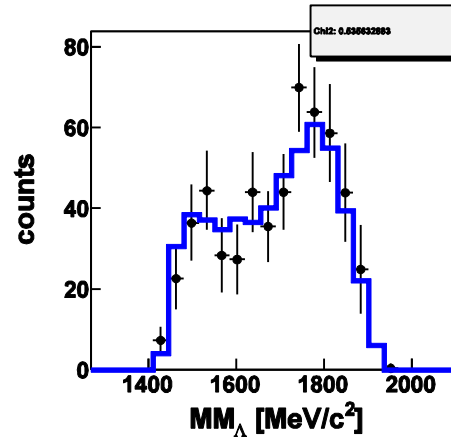
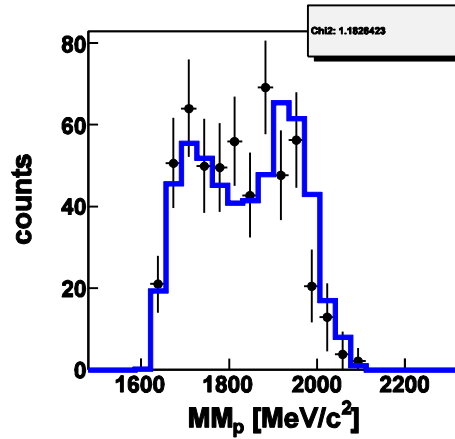
3_8 ($s = -0.98 \cdot 10^5$)

6_9 ($s = -0.78 \cdot 10^5$)

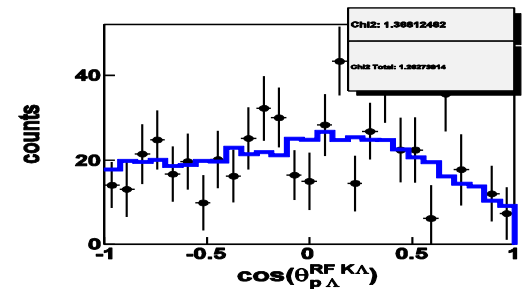
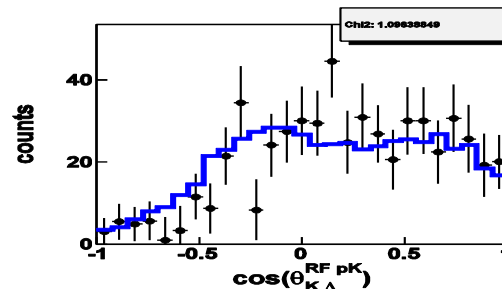
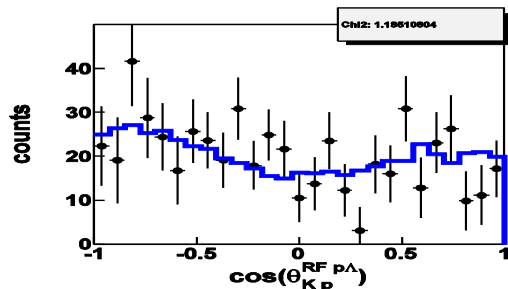
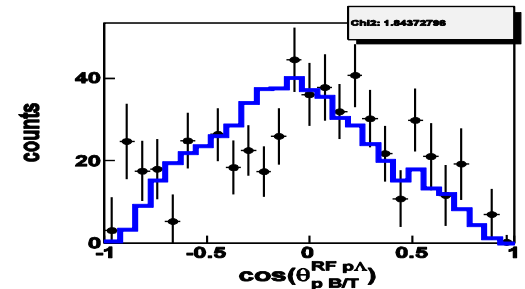
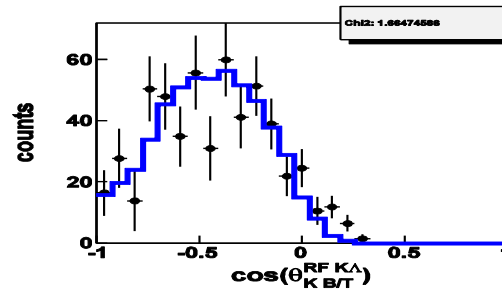
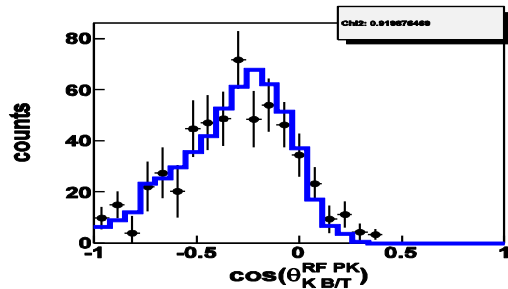
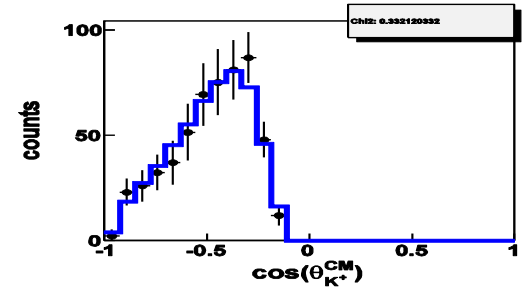
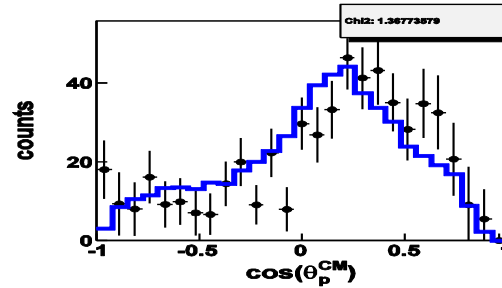
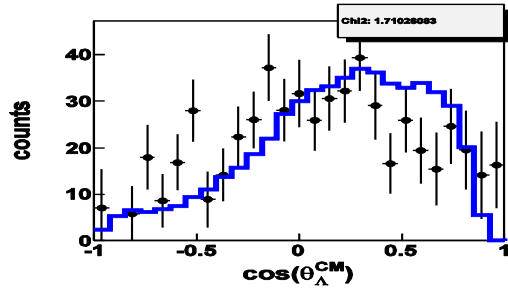
s : - (Log Likely hood) of PWA

Energy dependent coefficient =0

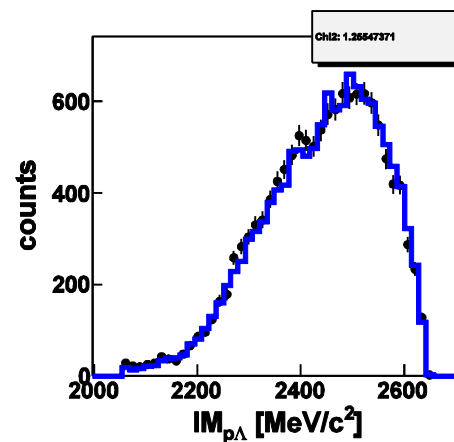
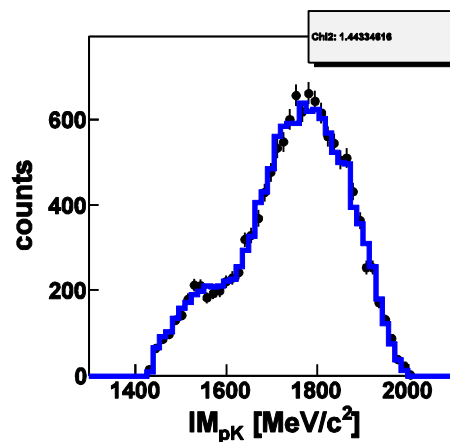
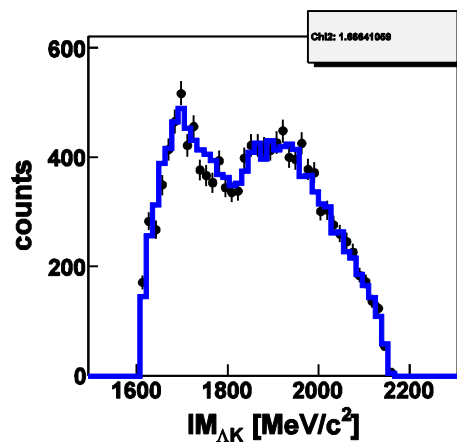
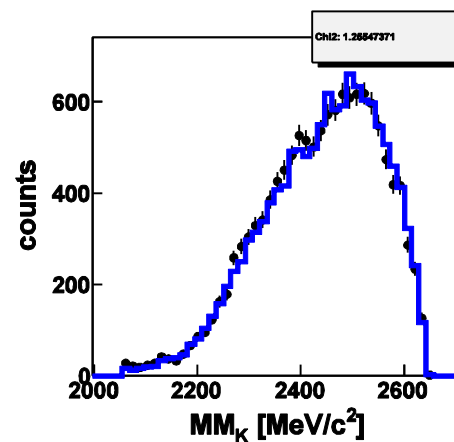
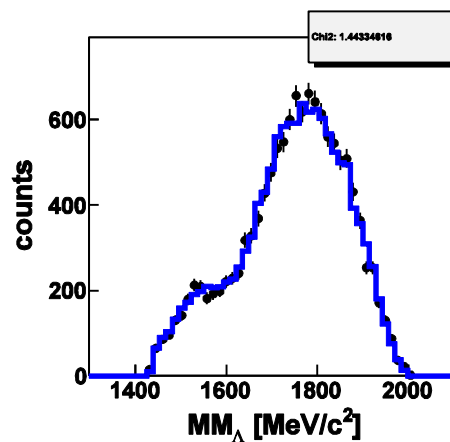
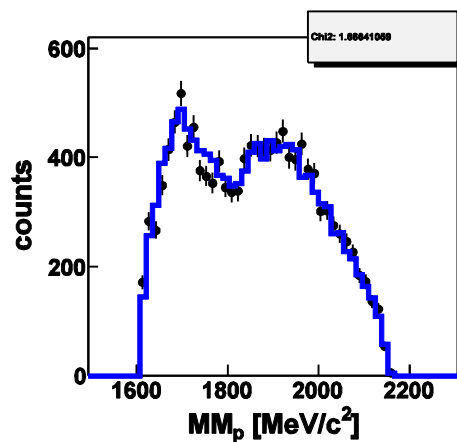
Results of 3_8



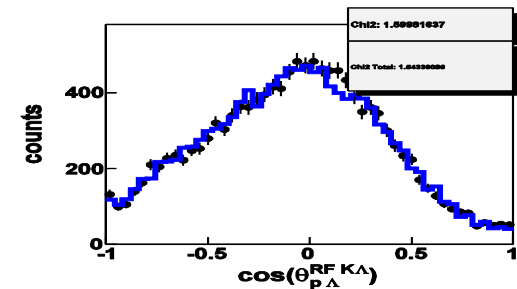
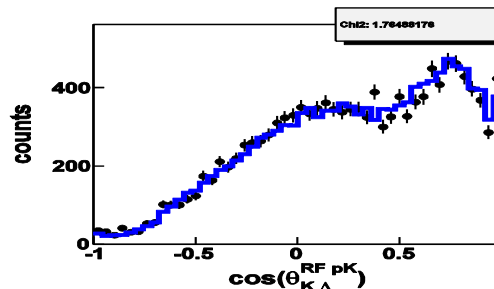
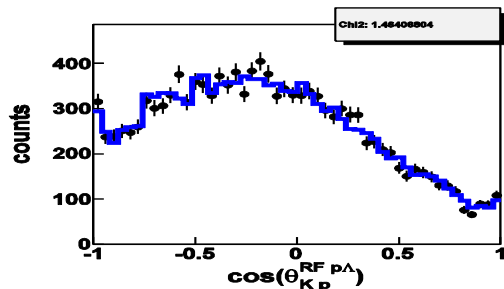
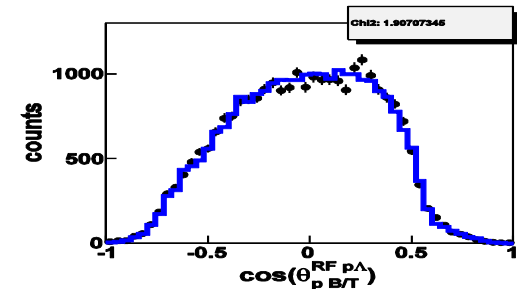
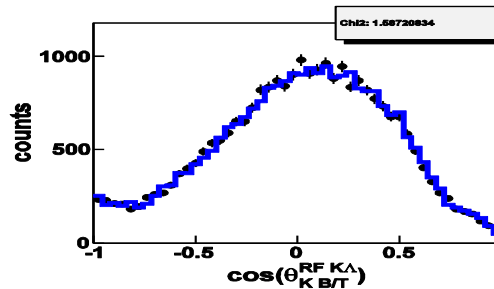
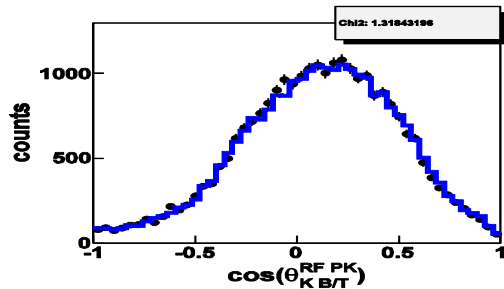
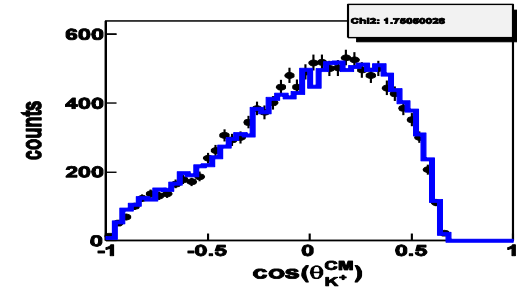
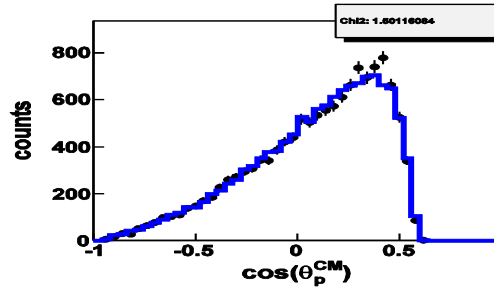
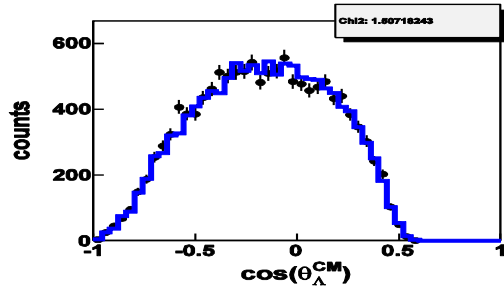
Results of 3_8



Results of 3_8



Results of 3_8



Combined Analysis of HADES and FOPI

4 Best HADES Solutions

HADES-FOPI (ene-fix)

1_8 ($s = -0.83 \cdot 10^5$)

8_8 ($s = -0.82 \cdot 10^5$)

3_8 ($s = -0.98 \cdot 10^5$)

6_9 ($s = -0.78 \cdot 10^5$)



4 Best HADES Solutions

HADES+FOPI (ene_dep)

1_8 ($s = -0.73 \cdot 10^5$)

8_8 ($s = -0.76 \cdot 10^5$)

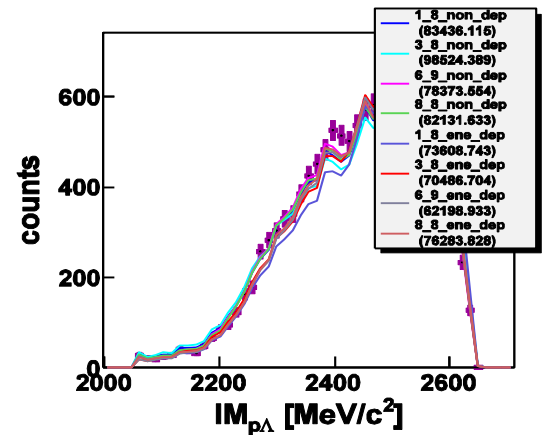
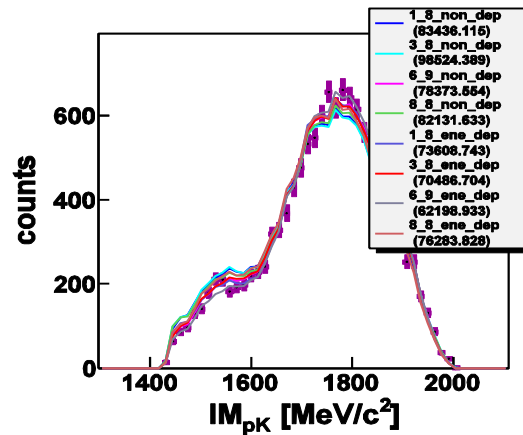
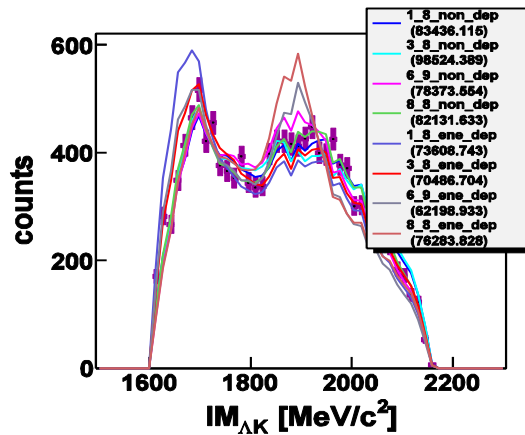
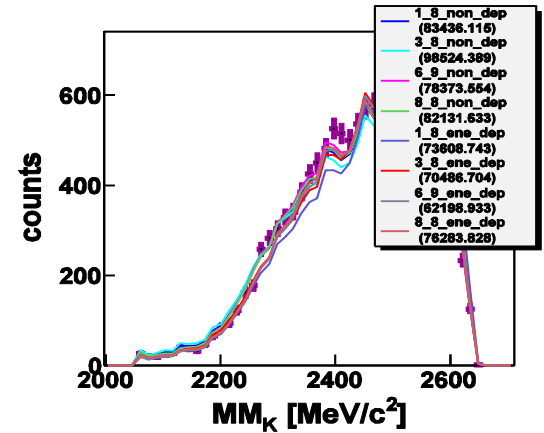
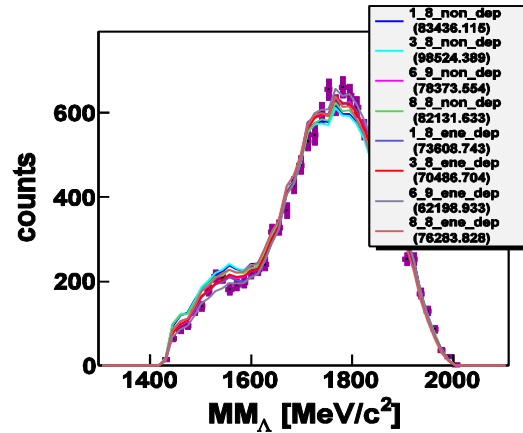
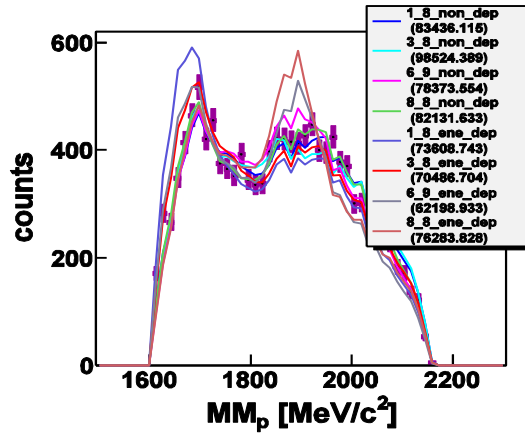
3_8 ($s = -0.70 \cdot 10^5$)

6_9 ($s = -0.62 \cdot 10^5$)

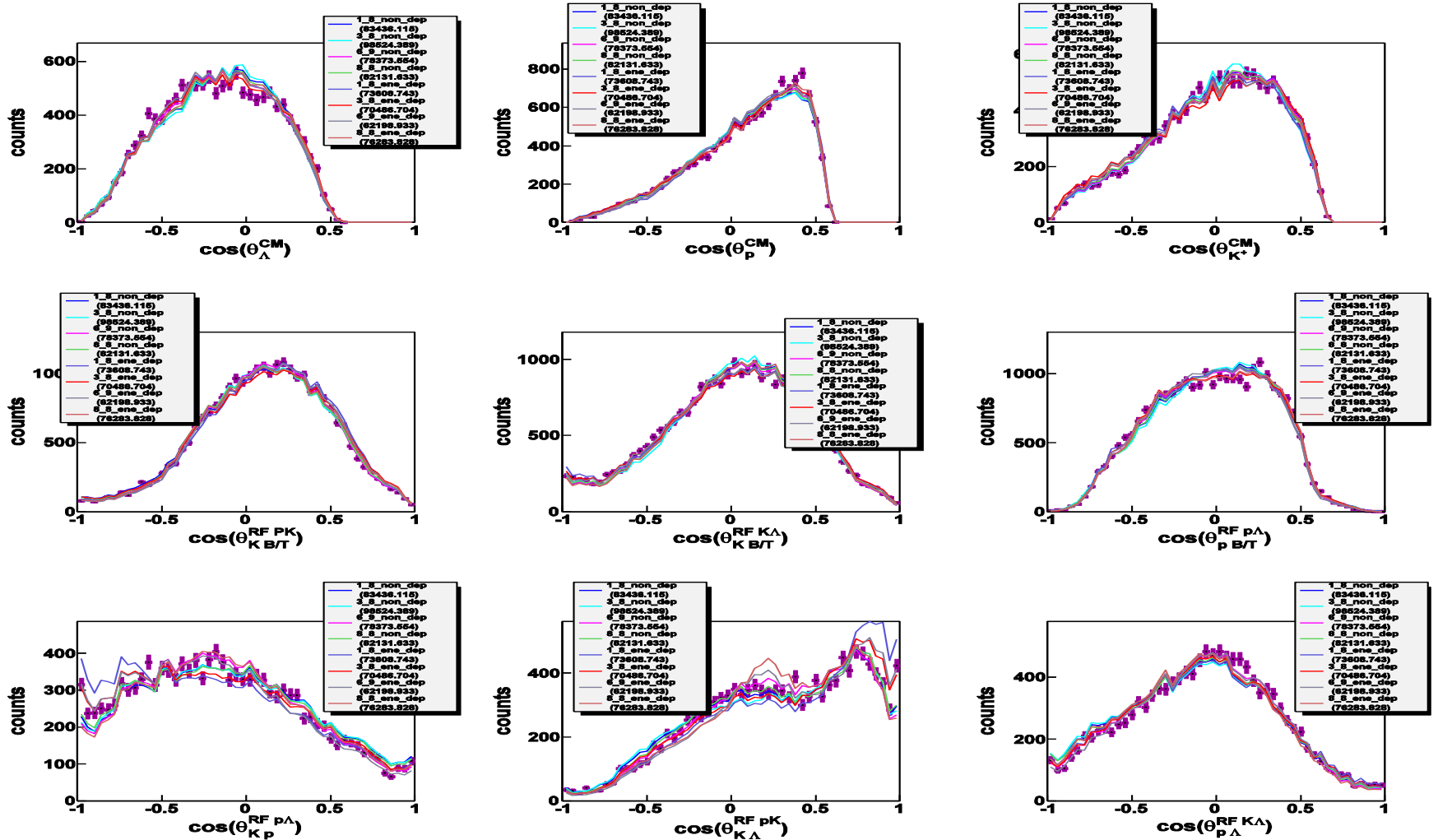
s : - (Log Likely hood) of PWA

Energy dependent coefficient fitted

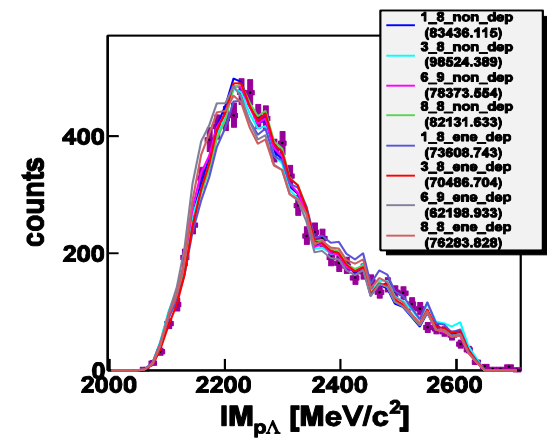
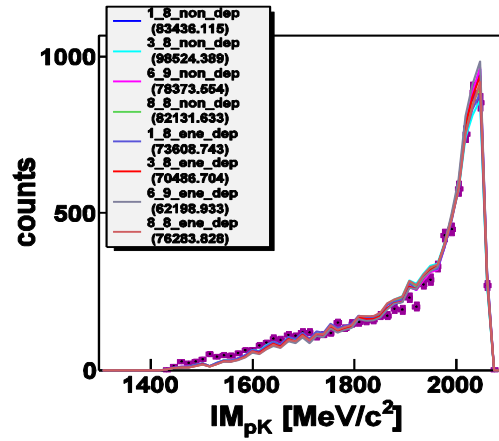
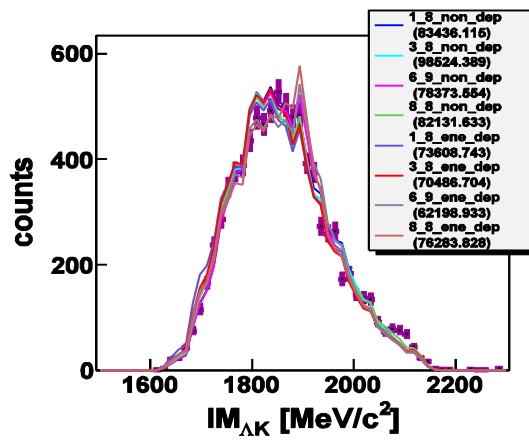
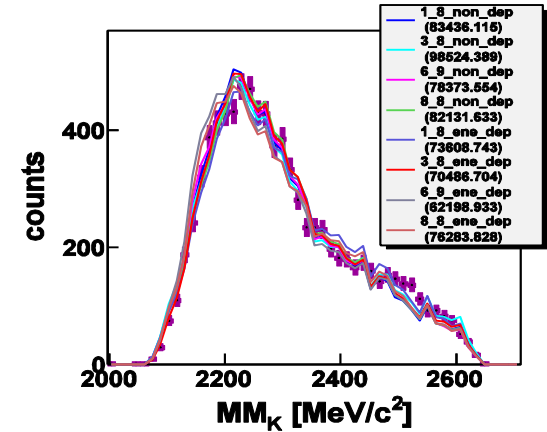
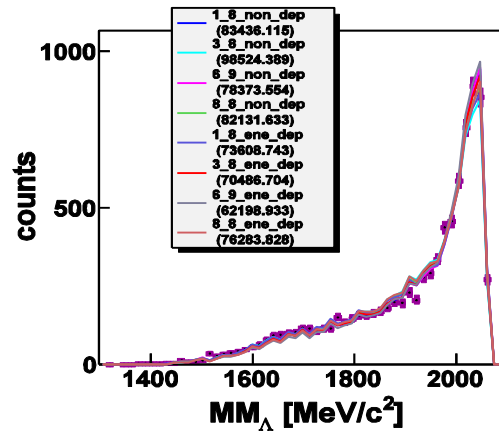
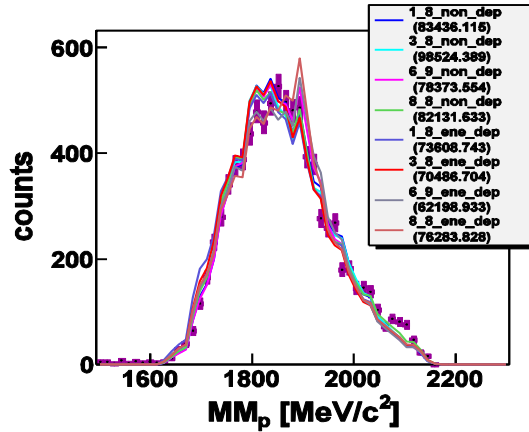
Results HADES



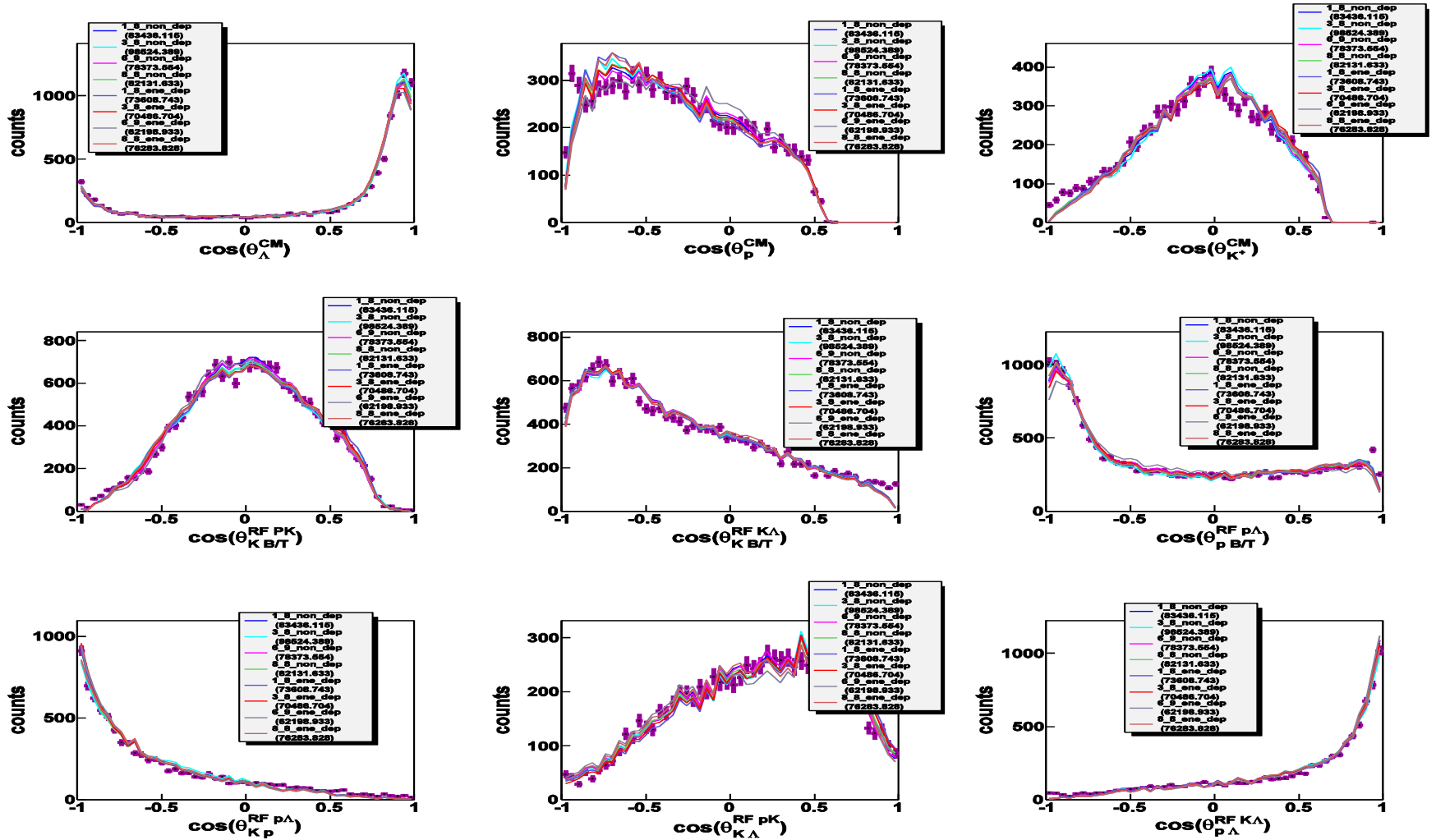
Results HADES



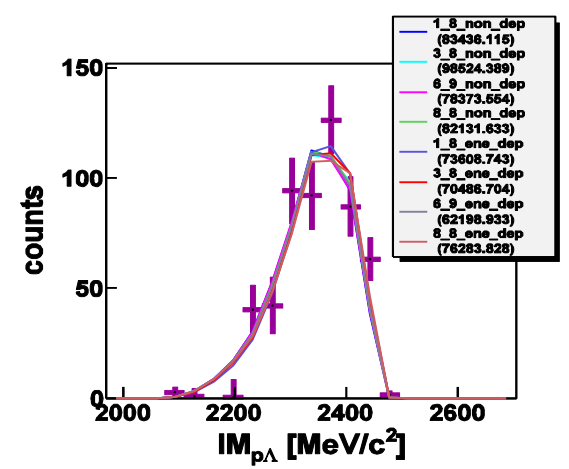
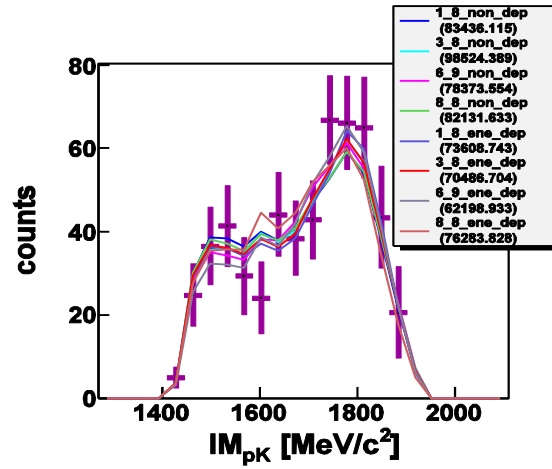
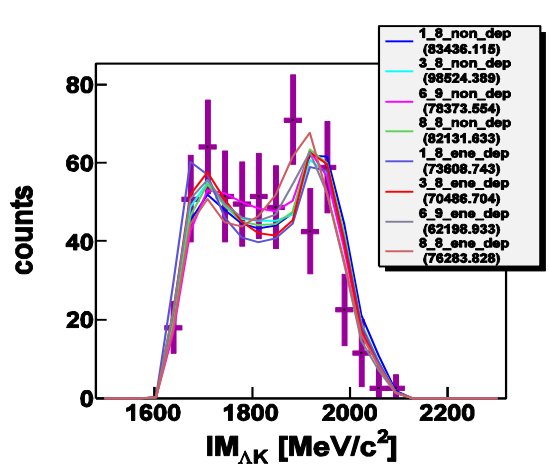
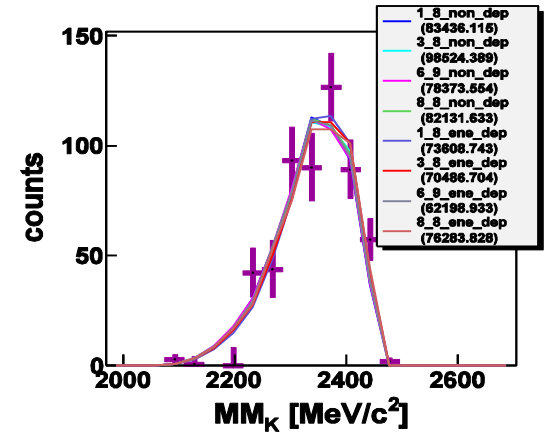
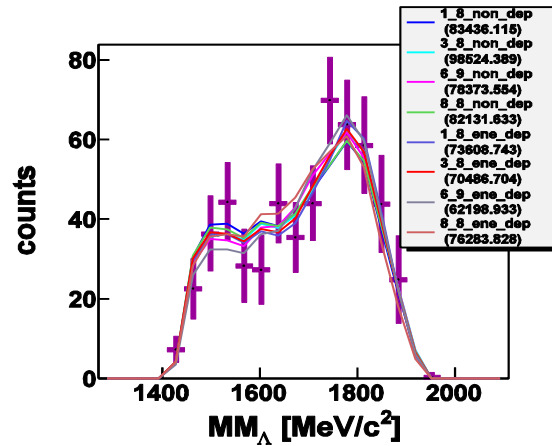
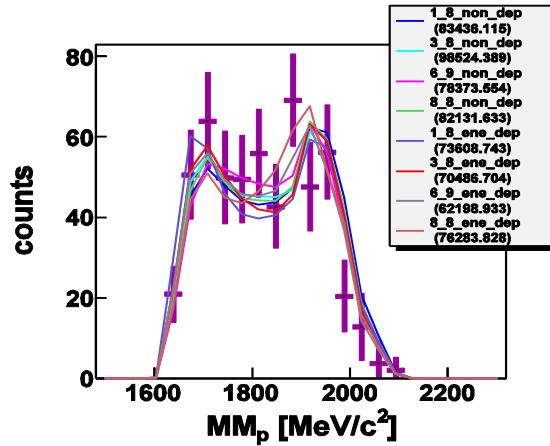
Results WALL



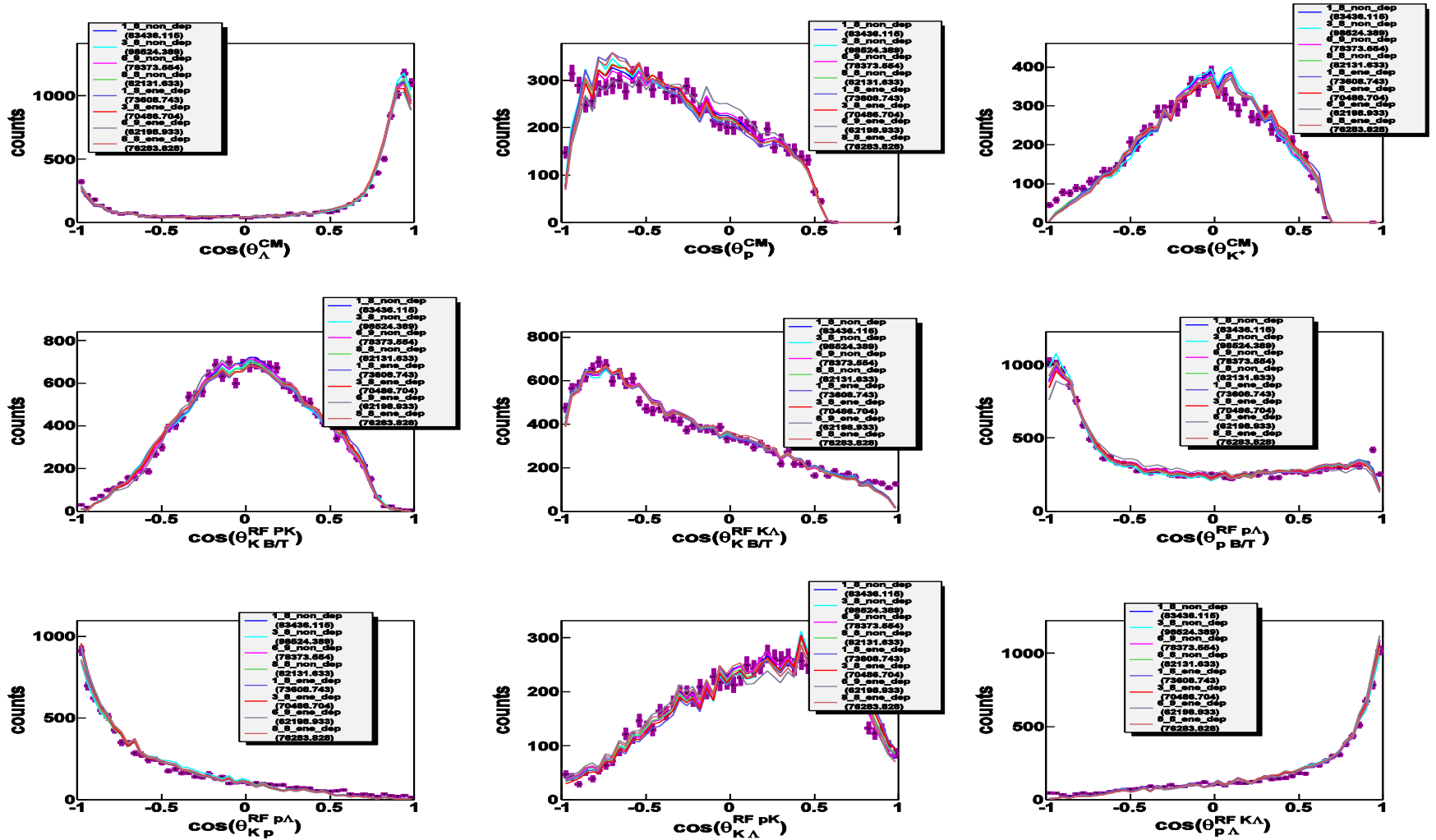
Results WALL



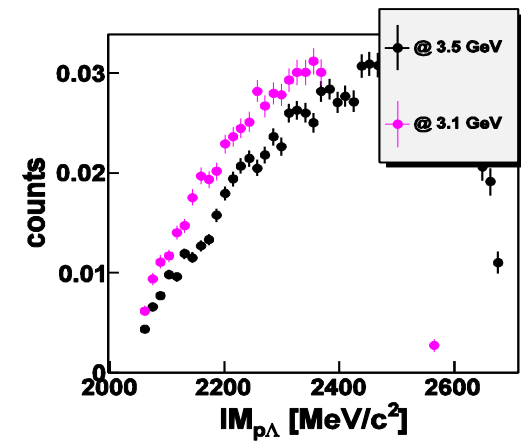
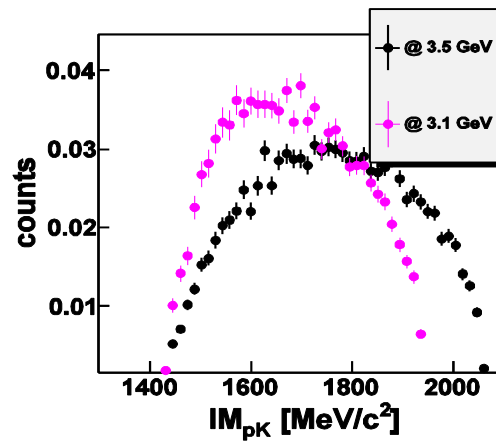
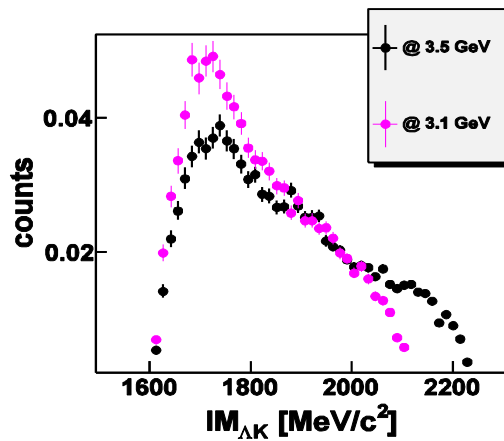
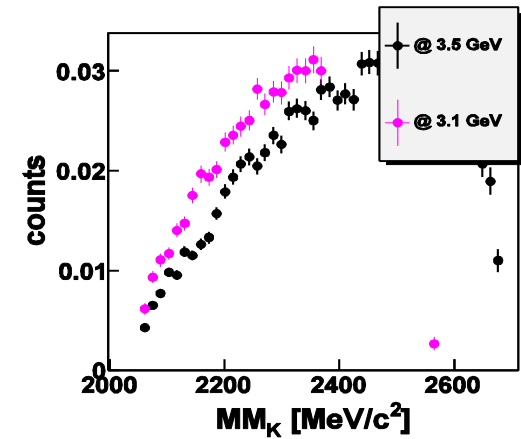
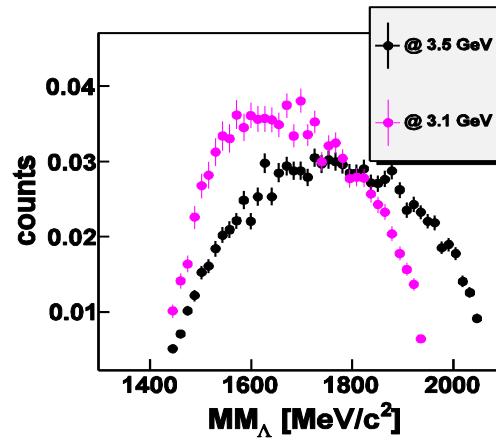
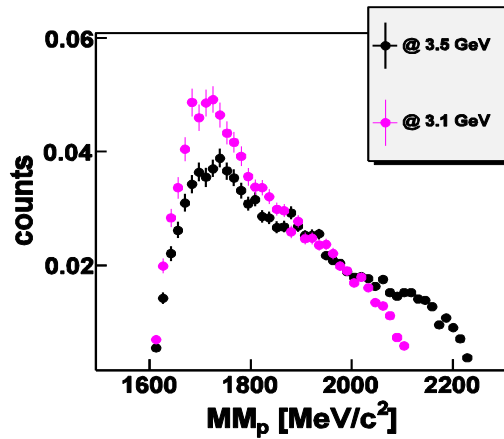
Results FOPI



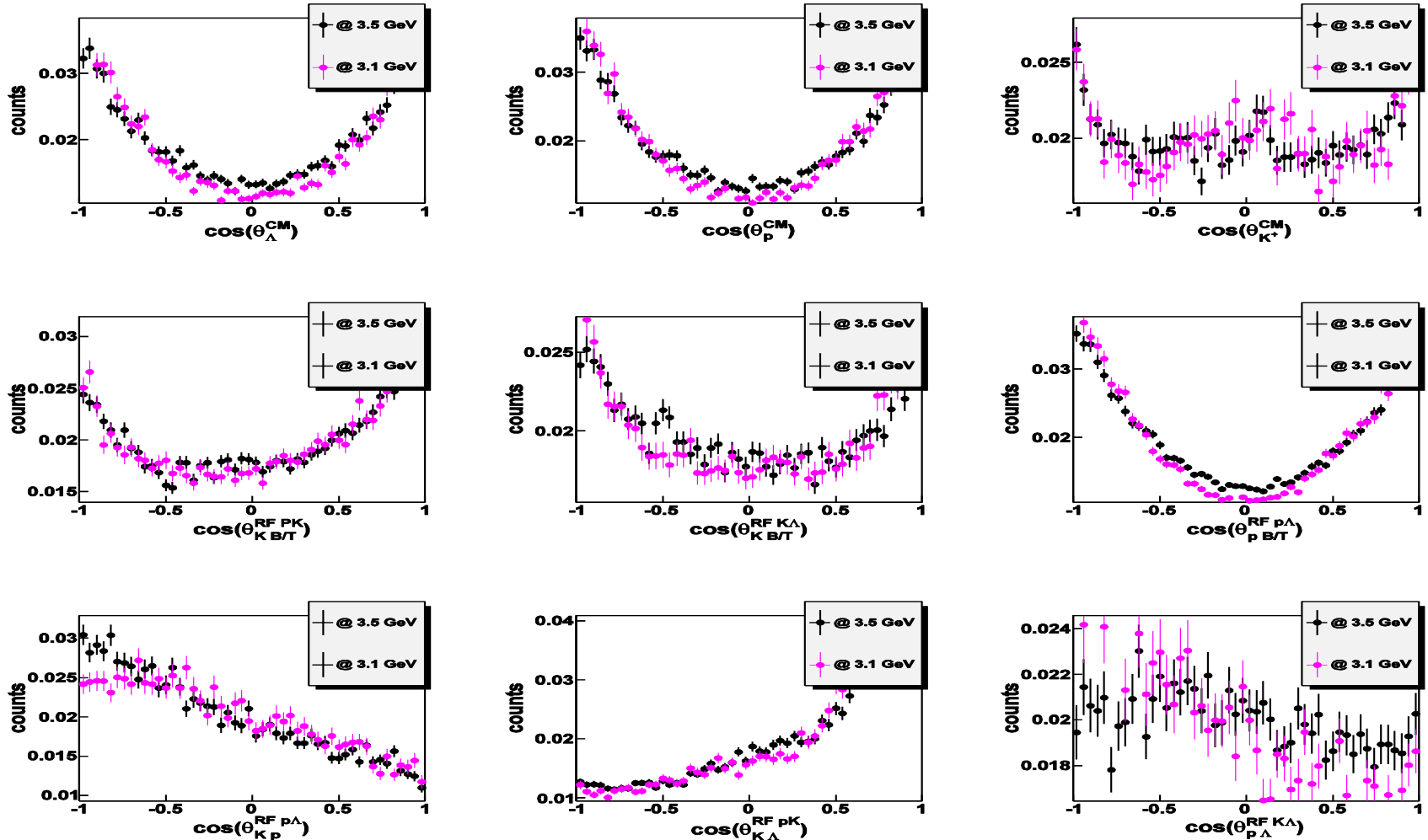
Results FOPI



4 PI – param_3_8_ene_dep

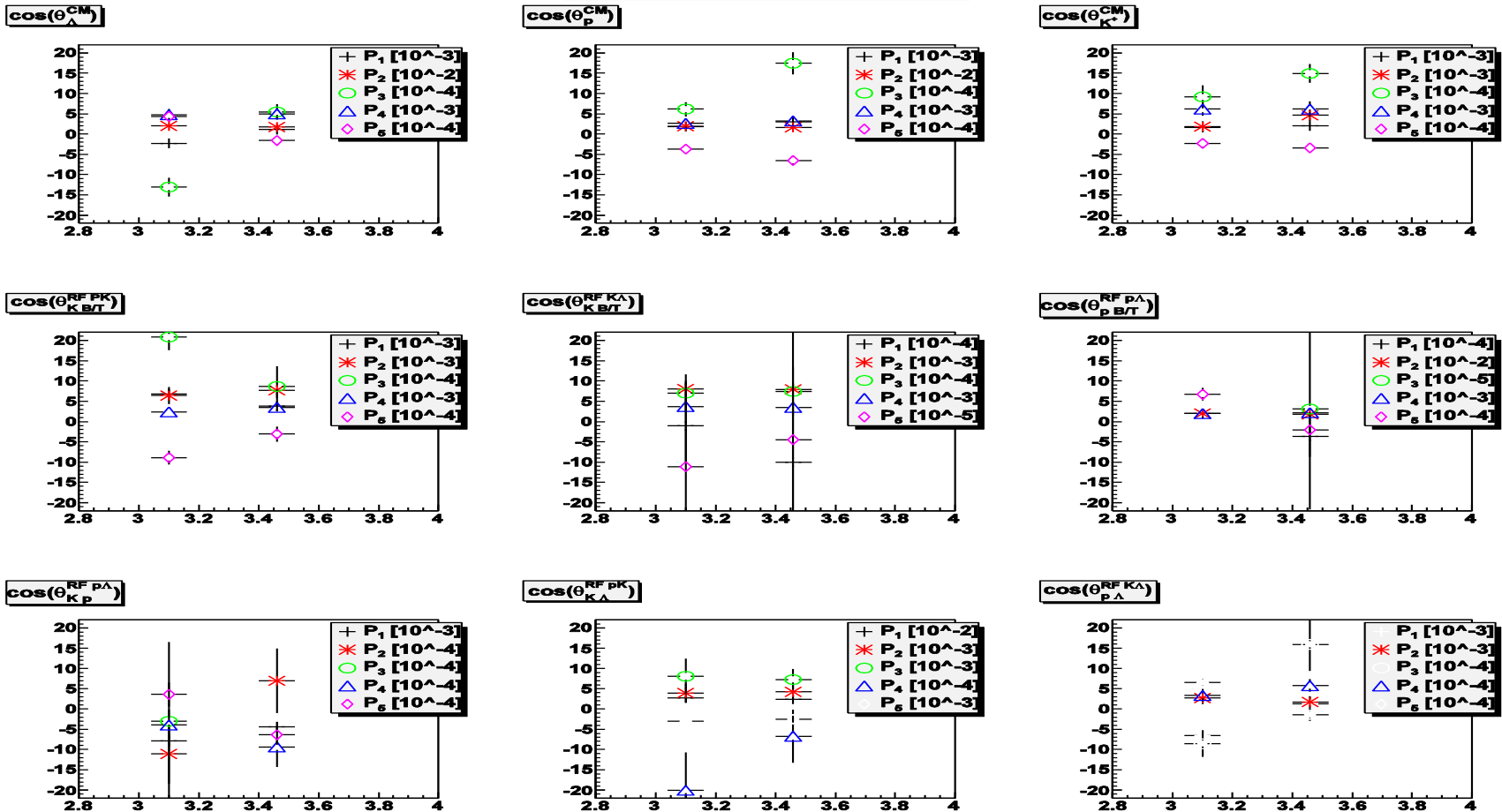


4 PI - param_3_8_ene_dep

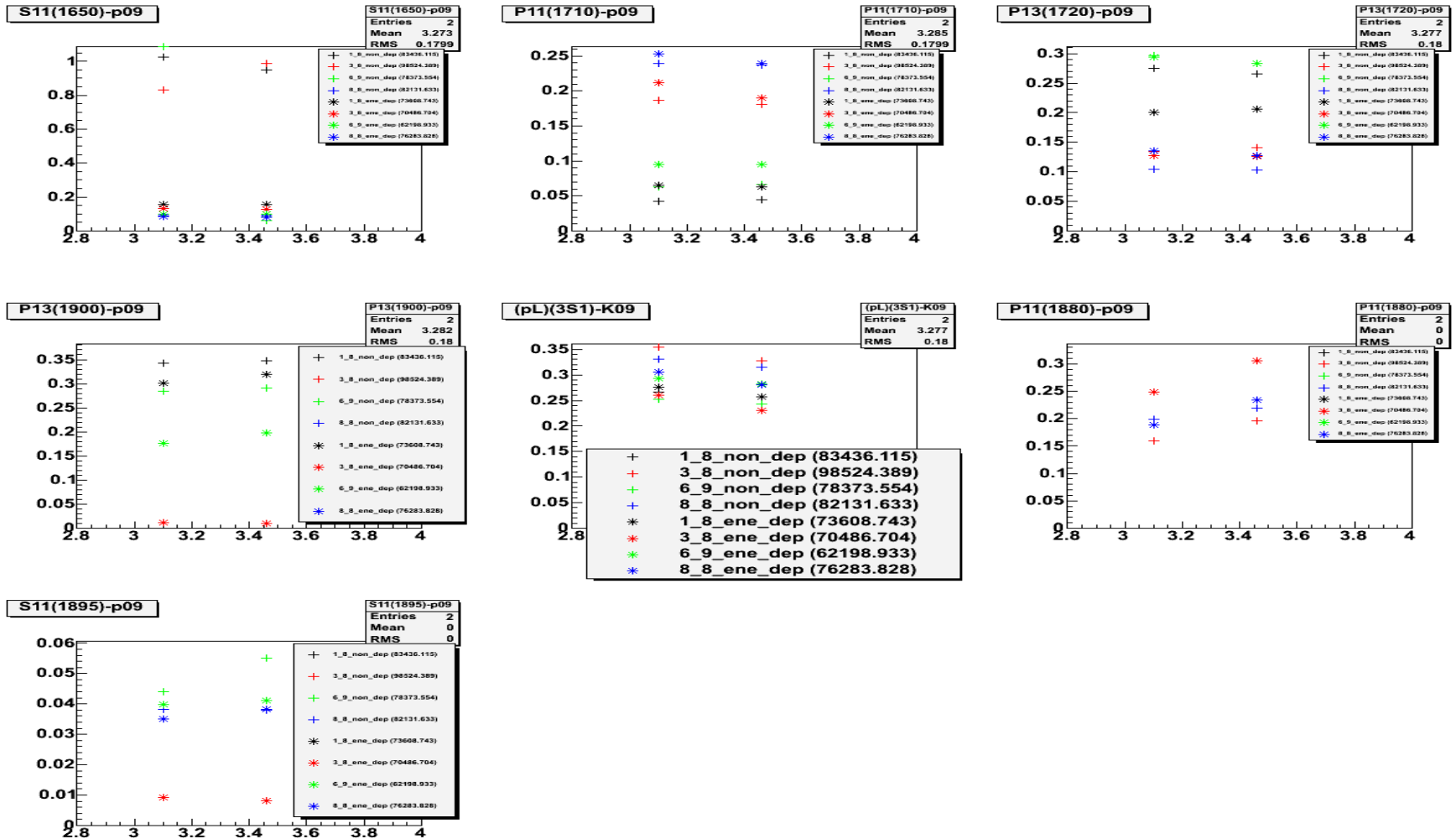


Legendre Fits

Mean of all solutions



Contributions



PWA without Interference

Combined Analysis of HADES and FOPI

With Interference:

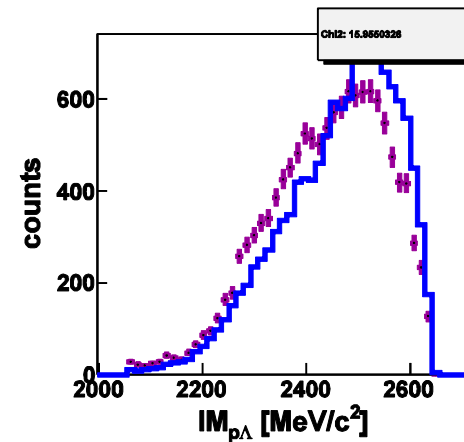
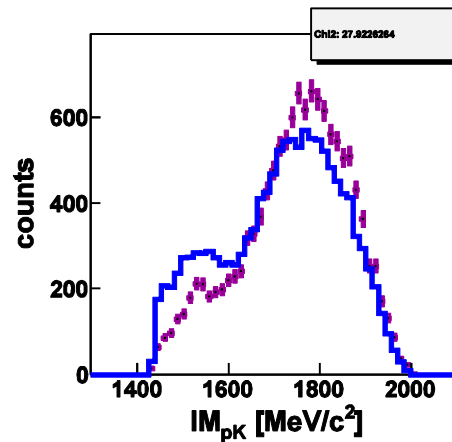
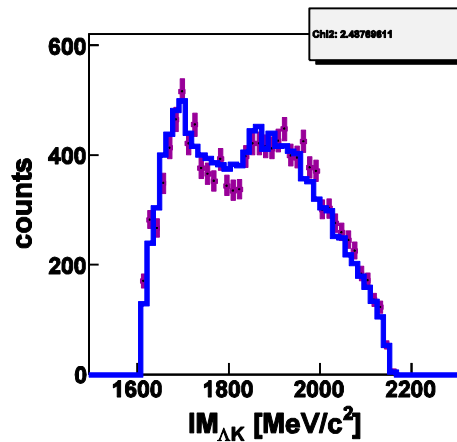
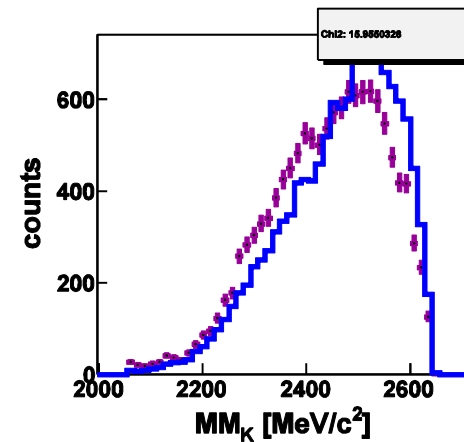
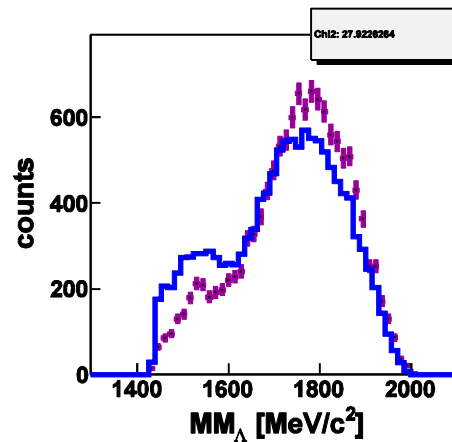
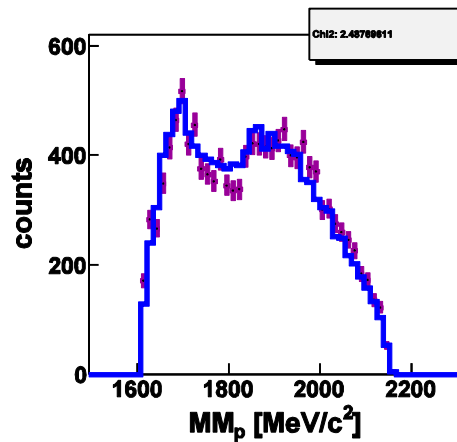
1. $\text{cfgg} = \sum \text{cp} * \text{tensor}$
2. Cross section = $\sum \text{cfgg} * \text{cfgg}^+$



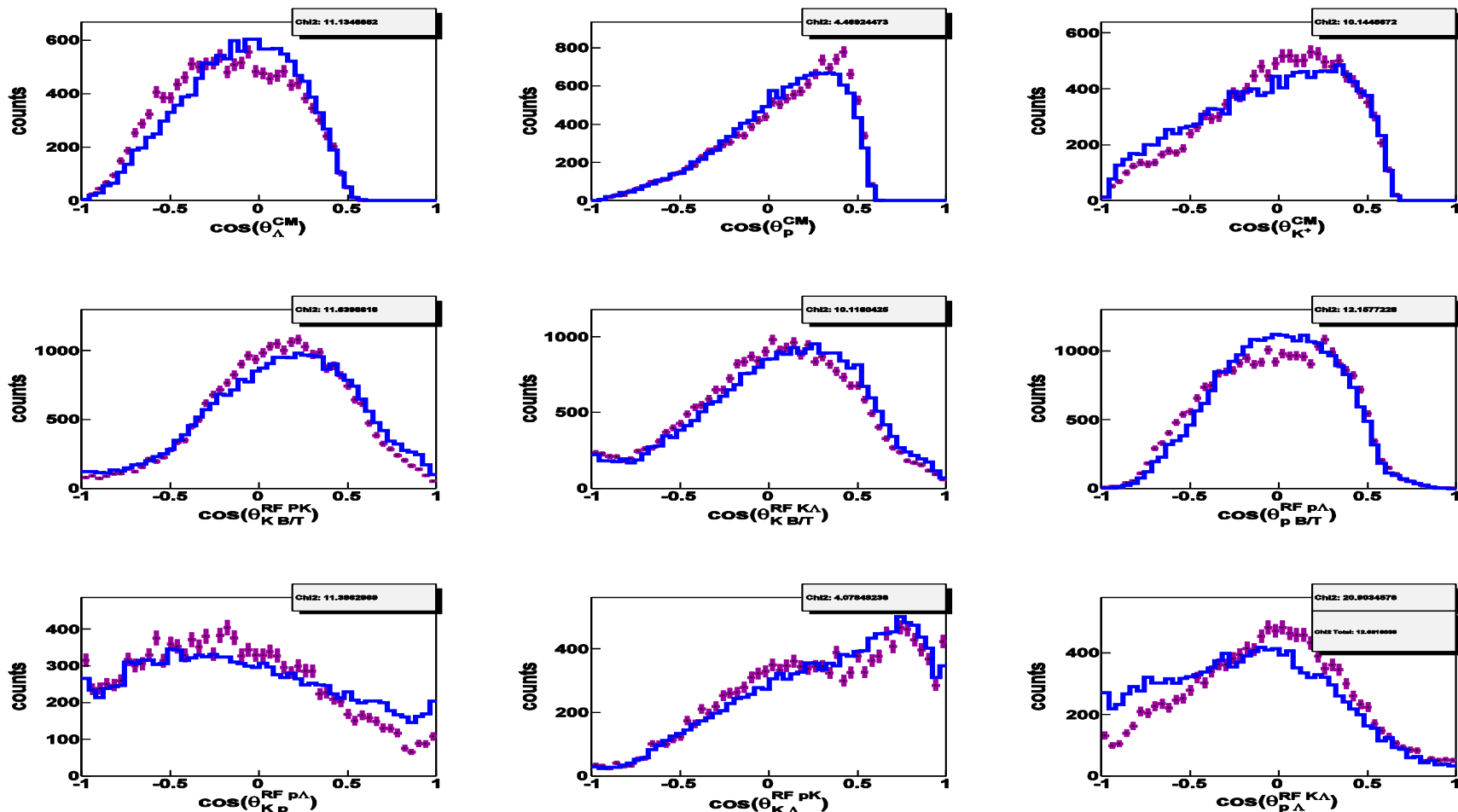
Without Interference:

1. $\text{cfgg} = \sum (\text{cp} * \text{tensor}) * (\text{cp} * \text{tensor})^+$
2. Cross section = $\sum \text{cfgg}$

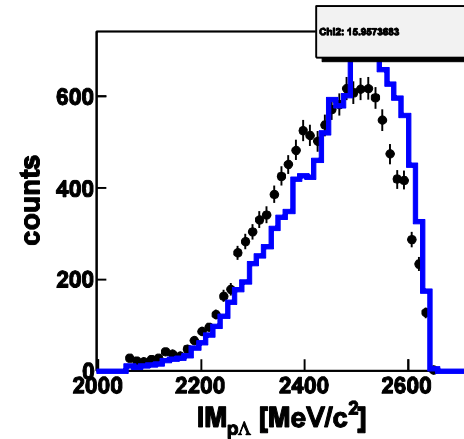
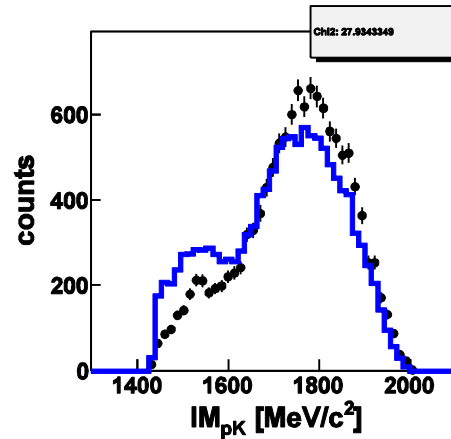
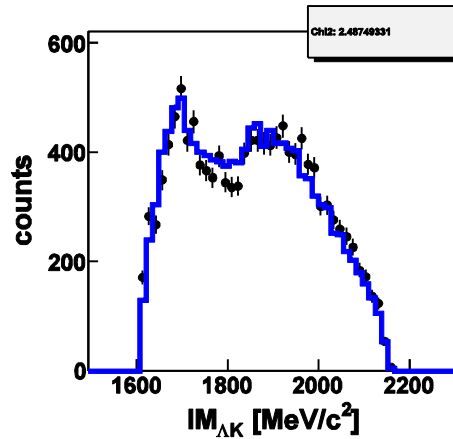
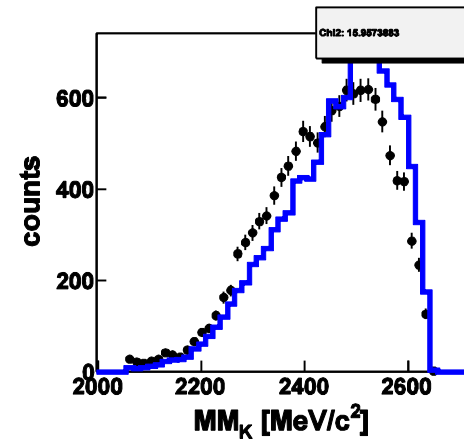
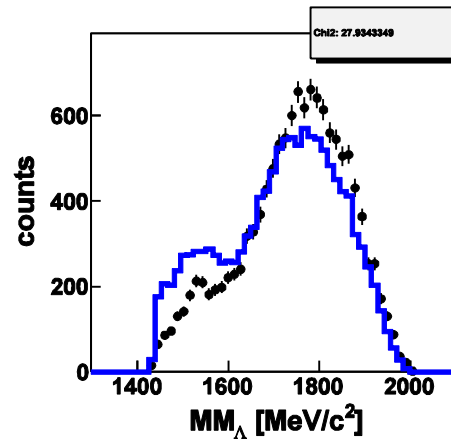
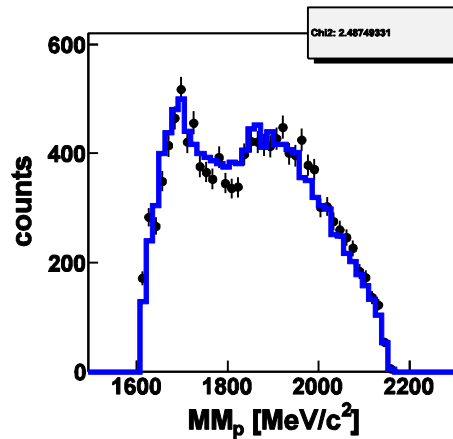
Results of 3_8_wo_int (not fitted)



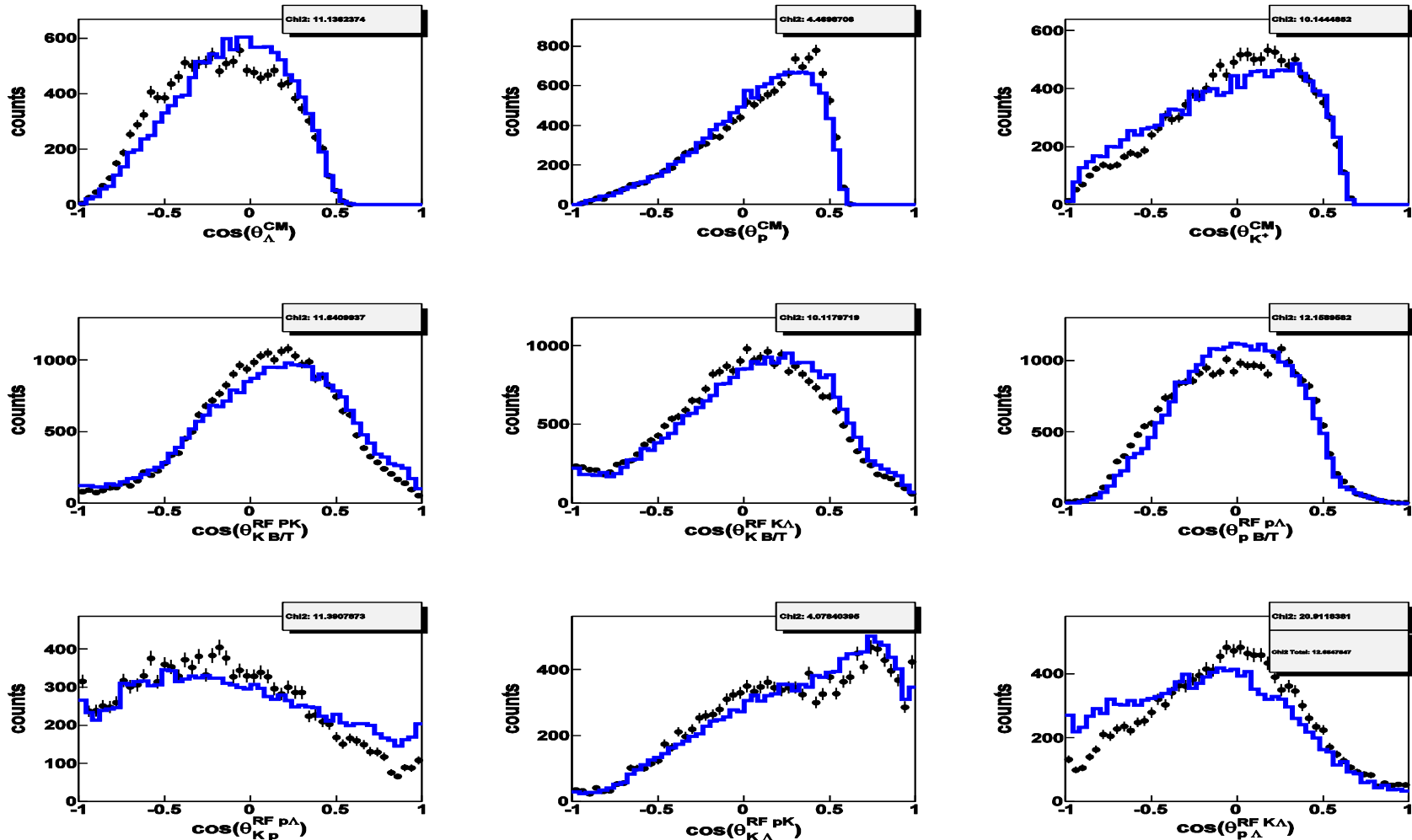
Results of 3_8_wo_int (not fitted)



Results of 3_8_wo_int (100 iter)



Results of 3_8_wo_int (100 iter)



Contribution of Production Channels

PWA Results – Relative Contribution

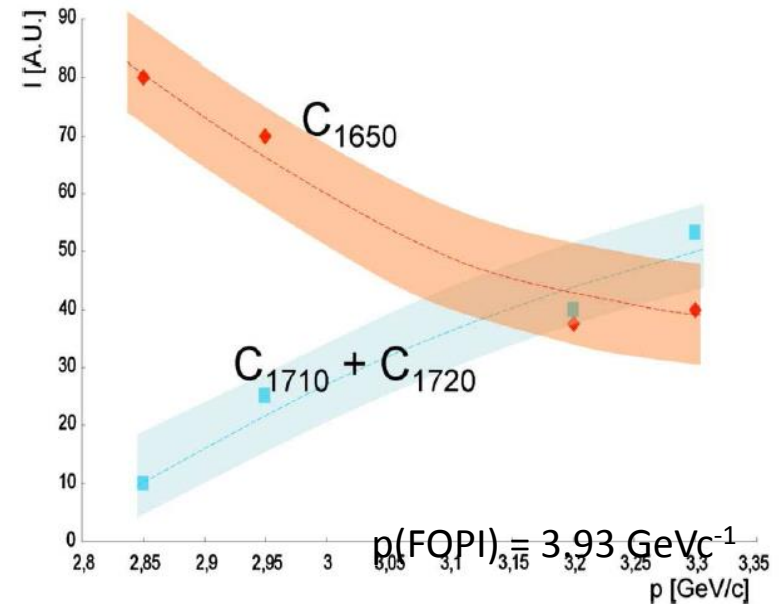
Sol.	χ^2 / ndf	Direct $pK^+\Lambda$	N^{*+} (1650)	N^{*+} (1710)	N^{*+} (1720)	N^{*+} (1875)	N^{*+} (1880)	N^{*+} (1895)	N^{*+} (1900)
A	1.09	0 %	11.3 %	52.4 %	11.8 %	6.3 %	10.9 %	0 %	7.3 %
B	1.09	16.6 %	9.4 %	42.3 %	14.1 %	0 %	9.7 %	0 %	7.9 %
C	1.10	0 %	11.1 %	49.5 %	7.5 %	0 %	14.1 %	9.3 %	8.5 %
D	1.12	13.9 %	6.8 %	43.8 %	11.9 %	5.3 %	9.4 %	0 %	8.9 %
E	1.15	21.1 %	8.6 %	41.9 %	17.6 %	0 %	0 %	0 %	10.8 %

PWA Results – Relative Contribution

Sol.	χ^2 / ndf	Direct $pK^+\Lambda$	N^{*+} (1650)	N^{*+} (1710)	N^{*+} (1720)	N^{*+} (1875)	N^{*+} (1880)	N^{*+} (1895)	N^{*+} (1900)
A	1.09	0 %	11.3 %	52.4 %	11.8 %	6.3 %	10.9 %	0 %	7.3 %
B	1.09	16.6 %	9.4 %	42.3 %	14.1 %	0 %	9.7 %	0 %	7.9 %
C	1.10	0 %	11.1 %	49.5 %	7.5 %	0 %	14.1 %	9.3 %	8.5 %
D	1.12	13.9 %	6.8 %	43.8 %	11.9 %	5.3 %	9.4 %	0 %	8.9 %
E	1.15	21.1 %	8.6 %	41.9 %	17.6 %	0 %	0 %	0 %	10.8 %

PWA Results – Relative Contribution

Sol.	χ^2 / ndf	Direct $pK^+\Lambda$	N^{*+} (1650)	N^{*+} (1710)	N^{*+} (1720)	N^{*+} (1875)	N^{*+} (1880)	N^{*+} (1895)	N^{*+} (1900)
A	1.09	0 %	11.3 %	52.4 %	11.8 %	6.3 %	10.9 %	0 %	7.3 %
B	1.09	16.6 %	9.4 %	42.3 %	14.1 %				
C	1.10	0 %	11.1 %	49.5 %	7.5 %				
D	1.12	13.9 %	6.8 %	43.8 %	11.9 %				
E	1.15	21.1 %	8.6 %	41.9 %	17.6 %				



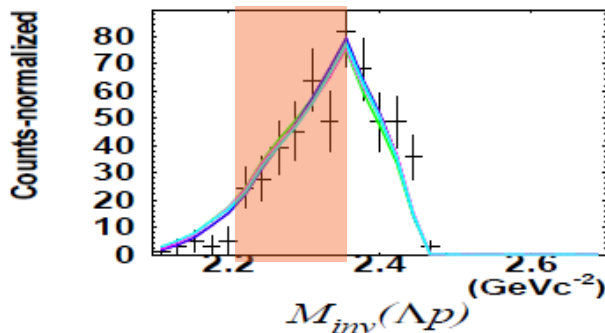
S. Abd El-Samad et al.
Phys.Lett B688 (2010)

PWA Results – Relative Contribution

Sol.	χ^2 / ndf	Direct $pK^+\Lambda$	N^{*+} (1650)	N^{*+} (1710)	N^{*+} (1720)	N^{*+} (1875)	N^{*+} (1880)	N^{*+} (1895)	N^{*+} (1900)
A	1.09	0 %	11.3 %	52.4 %	11.8 %	6.3 %	10.9 %	0 %	7.3 %
B	1.09	16.6 %	9.4 %	42.3 %	14.1 %	0 %	9.7 %	0 %	7.9 %
C	1.10	0 %	11.1 %	49.5 %	7.5 %	0 %	14.1 %	9.3 %	8.5 %
D	1.12	13.9 %	6.8 %	43.8 %	11.9 %	5.3 %	9.4 %	0 %	8.9 %
E	1.15	21.1 %	8.6 %	41.9 %	17.6 %	0 %	0 %	0 %	10.8 %

PWA Results – Relative Contribution

Sol.	χ^2 / ndf	Direct $pK^+\Lambda$	N^{*+} (1650)	N^{*+} (1710)	N^{*+} (1720)	N^{*+} (1875)	N^{*+} (1880)	N^{*+} (1895)	N^{*+} (1900)
A	1.09	0 %	11.3 %	52.4 %	11.8 %	6.3 %	10.9 %	0 %	7.3 %
B	1.09	16.6 %	9.4 %	42.3 %	14.1 %	0 %	9.7 %	0 %	7.9 %
C	1.10	0 %	11.1 %	49.5 %	7.5 %	0 %	14.1 %	9.3 %	8.5 %
D	1.12	13.9 %	6.8 %	43.8 %	11.9 %	5.3 %	9.4 %	0 %	8.9 %
E	1.15	21.1 %	8.6 %	41.9 %	17.6 %	0 %	0 %	0 %	10.8 %



Experimental Data can be described
by known sources